BOUND STATE SOLUTIONS OF THE SCHRÖDINGER EQUATION FOR POTENTIALS WITH DIRAC DELTA FUNCTIONS

by

Haydar Uncu

BC. in Physics, Ege University, 1998,

MSc. in Physics, Ege University, 2001

Submitted to the Institute for Graduate Studies in
Science and Engineering in partial fulfillment of
the requirements for the degree of
Doctor of Philosophy

Graduate Program in

Boğaziçi University

2007

BOUND STATE SOLUTIONS OF THE SCHRÖDINGER EQUATION FOR POTENTIALS WITH DIRAC DELTA FUNCTIONS

APPROVED BY:

Prof. Ersan Demiralp (Thesis Supervisor)	.....
Prof. Metin Arık	.....
Prof. Ömer Faruk Dayı	.....
Assoc. Prof. Nihat Sadık Değer	.....
Prof. Osman Teoman Turgut	.....

DATE OF APPROVAL: 12.06.2007

PREFACE

To Late Ali Ayan

ACKNOWLEDGEMENTS

In the first place, I would like to thank my thesis supervisor Prof. Ersan Demiralp for all his encouragement, foresight and relieving guidance throughout my Ph.D. thesis study, creating a productive and cooperative atmosphere for research.

I would like to express my gratitude to Prof. Haluk Beker for his guide and contributions to this thesis. I have furthermore to thank the Faculty members for the exciting and instructive courses.

Our collaborators Assoc. Prof. Özgür Müstecaplıoğlu from Koç University and Devrim Tarhan from Harran University made important contributions to this thesis. I gratefully acknowledge these contributions.

Love and affection to my wife Güzide for the enormous sacrifice she has made. My deepest appreciation to my father, mother and sister for their mental support.

Special thank to my friends Fatih Erman and Dr. Ahmet Baykal for the endless, inspiring and interesting conversations on Physics and Mathematics. In addition, I gratefully acknowledge Hakan Erkol, Azmi Ali Altıntaş and Mehmet Erkol for helpful discussions and for their assistance when i was writing my thesis.

My gratitude to the librarians Oya Özdoğan and Mustafa Cevizbaş for their smiling faces and assistance using the library.

I could dedicate my thesis to all those people above I mentioned. However, without the guidance of Ali Ayan, for me, it was impossible to pass successfully the courses I have taken and to write this thesis. When, I came to Boğaziçi University, he opened a new world to me. Thanks from the bottom of my heart.

ABSTRACT

BOUND STATE SOLUTIONS OF THE SCHRÖDINGER EQUATION FOR POTENTIALS WITH DIRAC DELTA FUNCTIONS

A general method for the bound state solutions of the Schrödinger equation for analytically solvable potentials with any finite number of Dirac delta functions is introduced for n-dimensional systems. Then, the potentials with Dirac delta functions are used to model some physical systems. The eigenvalue equations for harmonic and linear potentials with a finite number of Dirac delta functions located randomly are derived for one dimensional systems. For the latter potential, the behavior of the eigenvalues of the ground and the first excited states for various strengths and locations of Dirac delta functions is investigated. The eigenvalues and the number of bound states for a $\mathcal{PT}$-symmetric system with two Dirac delta functions are studied. In case of a contact interaction, to get the changes from a liner potential, the changes in the masses of s states for charmonium is presented. It is also shown that the Fermi energy of a triangular well changes if there is an impurity in the well. By describing a dimple potential with a Dirac delta function, it is shown that tight and deep dimple potentials can increase the condensate fraction and critical temperature of a Bose-Einstein condensate. We conclude that addition of the point interactions which can be modelled by Dirac delta functions changes the properties of the physical systems considerably.

ÖZET

DİRAC DELTA FONKSİYONLARI İÇEREN POTANSİYELLER İÇİN SCHRÖDINGER DENKLEMİNİN ÇÖZÜMLERİ

Sonlu sayıda nokta etkileşim içeren, analitik olarak çözülebilir potansiyellerin bağlı durumlarının n-boyutta Schrödinger denklemi çözümü için genel bir yöntem tanıtıldı. Ardından, Dirac delta fonksiyonları içeren potansiyeller bazı fiziksel sistemleri betimlemek için kullanıldı. Bir boyutta, rasgele yerleştirilmiş, sonlu sayıda Dirac delta fonksiyonu içeren harmonik ve çizgisel potansiyellerinin özdeğer denklemleri türetildi. Çizgisel potansiyelin, temel ve birinci uyarılmış seviyelerinin özdeğerlerinin davranışı Dirac delta fonksiyonlarının çeşitli güç ve pozisyonları için incelendi. İki Dirac delta fonksiyonundan oluşan $\mathcal{PT}$-symmetric sistemin, bağlı durumlarının sayısı ve özdeğerleri araşırtıldı. Değme etkileşimi bulunması durumunda, çizgisel potansiyelle oluşan farkı gözlemlemek için çarmonyumun s hallerinin kütle değerlerindeki değişim elde edildi. Üçgensel bir kuyunun Fermi enerjisinin kuyuda safsızlık bulunması halinde değişeceği de gösterildi. Çukur potansiyel bir Dirac delta fonksiyonu ile betimlenerek, derin bir çukur potansiyelin, Bose-Einstein yoğuşuk maddenin yoğuşukluk oranını ve kritik sıcaklığını arttırdığı gösterildi. Sonuç olarak, Dirac delta fonksiyonu ile betimlenebilen noktasal etkileşimlerin eklenmesinin, fiziksel sistemlerin özelliklerini önemli ölçüde değiştirdiği gözlemlenmiştir.

TABLE OF CONTENTS

LIST OF FIGURES

LIST OF TABLES

LIST OF SYMBOLS/ABBREVIATIONS

$\mathbb{M}$	Transfer Matrix
$\mathbb{X}$	Total Transfer Matrix
σ	Strength of the Dirac delta function
BEC	Bose-Einstein condansate
RHP	Right half part of the complex plane
WKB	Wentzel-Kramer Brillouin

1. INTRODUCTION

Point interactions are commonly used to model contact or very short range interactions. An operator with a point interaction may have the form [1],

$$L_{\alpha_1\alpha_2} = -\frac{d^2}{dx^2} + \alpha_1\delta(x) + \alpha_2\delta^{(1)}(x) \ , \tag{1.1}$$

where $\delta^{(1)}$ denotes the derivative of the Dirac delta function. Albeverio et al showed that the operator $L_{\alpha_1\alpha_2}$ is a self adjoint extension of the operator $-\frac{d^2}{dx^2}$. They also proved that any self adjoint extension of of the operator $-\frac{d^2}{dx^2}$ can be represented by one of the following boundary conditions [1]:

1.

$$\begin{pmatrix} \Psi(+0) \\ \Psi'(+0) \end{pmatrix} = \Lambda \begin{pmatrix} \Psi(-0) \\ \Psi'(-0) \end{pmatrix} \ . \tag{1.2}$$

Here, the matrix Λ is equal to

$$\Lambda = e^{i\theta} \begin{pmatrix} a & b \\ c & d \end{pmatrix} \ , \tag{1.3}$$

where $\theta \in [0, \pi)$ and $a, b, c, d, \in \mathbb{R}$ fulfill the condition $ad - bc = 1$. Here $\Psi(x)$' s are the eigenfunctions of the operator $-d^2/dx^2$.

2.

$$\Psi'(+0) = h^+\Psi(+0) \qquad \Psi'(-0) = h^-\Psi(-0) \tag{1.4}$$

with the parameters $h^\pm \in \mathbb{R} \bigcup \infty$. If $h^+ = \infty$, then the first equation of (1.4) reads $\Psi(+0) = 0$. Similarly for $h^- = \infty$.

As seen from the Equation (1.1), Dirac delta potentials are special types of point interactions ($\alpha_2 = 0$). These type of potentials are called by various names such as "point interactions", "zero-range potentials", "delta interactions", "Fermi pseudopotentials", and "contact interactions" in the literature [2].

Dirac delta functions are defined in various ways. The easiest way to define a Dirac delta function $\delta(x)$ is to represent it as a limiting case ($\epsilon \to 0$ where $\epsilon > 0$) of rectangular function, i.e. as (See, e.g. Appendix II of [3].)

$$\begin{aligned} \delta^{(\epsilon)}(x) &= \frac{1}{\epsilon} \quad \text{for} \quad -\frac{\epsilon}{2} < x < \frac{\epsilon}{2} \\ &= 0 \quad \text{for} \quad |x| > \frac{\epsilon}{2} \, , \end{aligned} \tag{1.5}$$

Using this definition, one can write for an arbitrary smooth function

$$\lim_{\epsilon \to 0} \int_{-\infty}^{\infty} \delta^{(\epsilon)}(x) f(x) dx = \int_{-\infty}^{\infty} \delta(x) f(x) dx = f(0) \, . \tag{1.6}$$

The equation

$$\int_{-\infty}^{\infty} \delta(x) f(x) dx = f(0) \, , \tag{1.7}$$

can also be used as the definition of a Dirac delta function [3]. Moreover, the Dirac delta function can be represented by one of the functions

$$\begin{aligned} (i) \quad & \delta(x) = \lim_{\epsilon \to 0} \frac{1}{2\epsilon} e^{-|x|/\epsilon} \, , \\ (ii) \quad & \delta(x) = \lim_{\epsilon \to 0} \frac{1}{\pi} \frac{\epsilon}{x^2 + \epsilon^2} \, , \\ (iii) \quad & \delta(x) = \lim_{\epsilon \to 0} \frac{1}{\epsilon \sqrt{\pi}} e^{-|x|^2/\epsilon^2} \, , \\ (iv) \quad & \delta(x) = \lim_{\epsilon \to 0} \frac{1}{\pi} \frac{\sin(x/\epsilon)}{x} \, , \\ (v) \quad & \delta(x) = \lim_{\epsilon \to 0} \frac{\epsilon}{\pi} \frac{\sin^2(x/\epsilon)}{x^2} \, , \end{aligned} \tag{1.8}$$

because all these functions satisfy the Equation (1.7). More generally, $\delta(x - x_0)$ is defined by:

$$\int_{-\infty}^{\infty} \delta(x - x_0) f(x) dx = f(x_0) \tag{1.9}$$

Finally, we state some important properties of Dirac delta functions,

$$\begin{aligned} &(i) \quad \delta(-x) = \delta(x) \\ &(ii) \quad \delta(cx) = \frac{1}{|c|}\delta(x) \\ &(iii) \quad \delta[g(x)] = \sum_j \frac{1}{g^{'}(x_j)}\delta(x - x_j) \end{aligned} \tag{1.10}$$

where $g^{'}(x)$ is the derivative of $g(x)$ and x_j are the simple zeros of the function g(x) $g(x_j) = 0, \;\; g^{'}(x_j) \neq 0$.

Dirac delta potentials are useful to describe very short ranged interactions. They can be used when the de Broglie wavelength of the particles are large compared to the interaction range or the wave function, of the particles can be taken as constant in the interaction region.

1.1. The Point Interactions as Physical Models

Dirac delta potentials were used frequently for describing short ranged interactions. Kronig-Penney model with Dirac delta functions is a widely known application of Dirac delta potentials. It approximates the potential of an electron in a metal by strongly localized scattering centers which allows a simplified potential $V(x)$ represented by Dirac delta functions. The model is quite successful to explain energy band structure of electrons in a metal [4, 5]. Mendez et.al. showed that the dynamics of particles in general periodic potentials may be studied by means of an equivalent generalized Kronig-Penney model, in which there exist several Dirac delta potentials in each unit cell [6]. The transfer matrix method is then used in a simple form to compute

the energy band edges and the dispersion relation for an arbitrary potential. [7]. The generalized Kronig-Penney model is also utilized to find the transmission coefficient and density of states for disordered systems [8]. Assuming the atoms as strongly localized scattering centers, Maksymowicz et al modelled a disordered system by Dirac delta functions located at random positions. Solving the Schrödinger equation for the system and utilizing the corresponding wave function they calculated the density of states of various alloys [9].

Extremely narrow one-dimensional quantum wells, such as layered GaAs/GaAlAs structures, are possible to synthesize [10]. Bound states of a charged particle in the presence of an external constant electric field in a medium with multiple ultrathin quantum wells (or impurities) can be investigated by modelling ultra thin quantum wells (or impurities) using Dirac delta functions. Particle scattering, photoionization, photodetachment and resonances related to such systems can be studied by introducing Dirac delta potentials [11]-[15]. The quantum dots are described by Dirac delta potentials in the calculation of spin dependent transport through a quantum wire with a finite array of quantum dots [16].

The Dirac delta functions are also utilized as a limiting case of various potentials. For example, Cox et.al. showed that the potential describing the interaction between a C_{60} fullerene and a single walled carbon nanotube can be approximated by Dirac delta functions where they used continuum approximation for C_{60} fullerene and the corbon nanotube [17]. Similarly, the dimple type potentials which are used to increase the phase space density of a Bose-Einstein condensate (BEC) can be approximated by a Dirac delta function [18].

The studies mentioned above, stimulated theoretical investigations of potentials with Dirac delta functions. Atkinson et al gave an exact treatment for the potentials with a Dirac delta function at the origin [19]. Avakian et al studied the spectrum of a harmonic potential with a Dirac delta function at the center of the potential [20]. Monoukian gave an explicit derivation for the propagator of a Dirac delta potential [21]. Demiralp et al presented a systematic investigation for the solutions of the potentials

with a finite number of Dirac delta shells in $\mathbb{R}^n$ [22]. Demiralp applied this method to harmonic potential in $\mathbb{R}^n$ [23]. Erkol et al studied the s sates of three dimensional Woods-Saxon potential with a finite number of Dirac delta functions [24]. Meanwhile, Altunkaynak et.al. investigated point interactions on Riemanian manifolds $\mathcal{S}^2$, $\mathcal{H}^2$ and $\mathcal{H}^3$. In this study, a lower bound estimate for the ground state energy is found by renormalization utilizing the heat kernel method [25, 26].

There are possible extensions of quantum mechanics such as supersymetric and $\mathcal{PT}$-symmetric quantum mechanics [27, 28]. The simplicity of the solution of the Schrödinger equation attracted researchers to investigate Dirac delta potentials in these formalisms. Uchino et.al and Goldstein et.al studied supersymmetric quantum mechanics under point singularities using Dirac delta functions [29, 30]. The systems with point interactions having $\mathcal{PT}$-symmetry have also attracted a lot of interest [31]-[45]. By studying two Dirac Delta functions in a one-dimensional box potential, Znojil et al showed that $\mathcal{PT}$-symmetric point interactions simplify calculations and clarified our understanding on this field [31]. Albeverio et al studied symmetries and general characteristics of point interactions having $\mathcal{PT}$-symmetry with different boundary conditions [33]. Weigert discussed the physical meaning of $\mathcal{PT}$ invariant potentials by studying scattering from $\mathcal{PT}$-symmetric Dirac delta potentials [34]. Eigenvalues and bound states of a $\mathcal{PT}$-symmetric Hamiltonian for a harmonic oscillator potential together with Dirac delta functions were investigated by Demiralp [35]. Cervero et al and Ahmed studied band structures of periodic $\mathcal{PT}$-symmetric Dirac delta potentials [36, 37, 38].

1.2. Main Results of This Thesis

First, the bound state solution of the one-dimensional Schrödinger equation for a general solvable potential decorated with a finite number (P) of Dirac delta functions is presented. This solution is generalized to higher dimensions for central, solvable potentials decorated with P Dirac delta shells. Moreover, a theorem on the bound state energy eigenvalues for potentials with Dirac delta shells is stated and proven.

Various potentials with a finite number (P) of Dirac delta potentials is studied for one-dimensional systems. First of all constant potential with a finite number of Dirac delta functions is investigated in Sections 3.1 The eigenvalue equation and the transfer matrix for this potential is found. Then for two Dirac delta functions, the condition for two bound states is presented.

A linear potential ($V(x) = f\,x$ where f is a real constant and $x > 0$) with a finite number of P Dirac delta functions is studied in Section 3.2. After presenting the eigenvalue equation and the transfer matrix for this potential, the cases for $P = 1, 2, 4, 8$ are studied in detail. For $P = 1$, the behavior of the ground and first excited states with respect to the strength and position of the Dirac delta functions is examined. For $P = 2, 4, 8$, the change in the ground and first excited state energies of linear potential is calculated with respect to various strengths of repulsive and attractive Dirac delta potentials. It is observed that the attractive Dirac delta potentials change the energy eigenvalues more than the repulsive Dirac delta potentials [46].

Hamiltonians which commute with the parity time operator ($\mathcal{PT}$) are called $\mathcal{PT}$-symmetric. The bound state solutions of the Schrödinger equation for $\mathcal{PT}$-symmetric Dirac delta potentials are derived in Section 3.4. The $\mathcal{PT}$-symmetric potential with two Dirac delta functions is studied in detail. The conditions for the symmetry breaking with respect to the positions and the strengths of Dirac delta functions are found. In addition, the number of bound states for various cases is calculated. The differences and similarities between the two $\mathcal{PT}$-symmetric and hermitian Dirac delta potentials are mentioned [47].

In Section 3.5, the Schrödinger equation for the potential $V(x) = \frac{1}{2\hbar}m^2\omega^3x^4 - \frac{\hbar^2}{2m}\sigma\delta(x)$ is solved using a numerical method. The ground state wave functions for $\sigma = 0, \sqrt{\frac{m\omega}{\hbar}}$ and $2\sqrt{\frac{m\omega}{\hbar}}$ are compared and the change of the ground state energy with respect to σ is presented.

The mathematical methods for potentials with Dirac delta functions are applied to charmonium, one dimensional triangular quantum wells with randomly located im-

purities and BEC in a harmonic trap with a dimple potential. The charmonium system is described by linear potential in quantum theory [48]. Assuming that there can also be contact interaction in addition to linear potential, the difference in the masses of the first ten s states is calculated in Section 5.1. In Section 5.2, triangular quantum wells with randomly located impurities are investigated. The change in the energies of the ground and first excited states are calculated modelling the impurities by Dirac delta potentials. Moreover, the effect of an impurity on the Fermi energy at the junction of GaAs and GaAlAs heterostructure is calculated both for attractive and repulsive type of impurities.

By considering an ideal gas consisting of bosons, Einstein showed that "from a certain temperature on, the molecules condense without attractive forces ... " and discovered the Bose-Einstein condensation in 1925 [49]. Seventy years after the prediction of Einstein, BEC of dilute gases have been observed at very low temperatures by using ingenious experimental designs [50, 51, 52]. Experimentally available condensates are systems with finite number of atoms N, confined in spatially inhomogeneous trapping potentials which are obtained by using magnetic fields. Modification of the shape of the trapping potential can be used to increase the phase space density [53]. 'Dimple' type potentials are most favorable potentials for this purpose [54, 55, 56]. Phase space density can be enhanced by an arbitrary factor by using a small dimple potential at the equilibrium point of the harmonic trapping potential [54]. Utilizing the harmonic potential with a Dirac delta function, the condensate fraction, the critical temperature and the density profile of a BEC in harmonic trap with a dimple potential is studied. It is shown that the tight and deep dimple potentials can increase the condensate fraction and critical temperature of a BEC by considerable amounts [57].

2. BOUND STATE SOLUTIONS OF THE SCHRÖDINGER EQUATION FOR SOLVABLE POTENTIALS WITH DIRAC DELTA FUNCTIONS

In this chapter, we briefly summarize how the bound state solutions of the Schrödinger equation changes for a solvable potential by adding finite number of Dirac delta functions in one and n ($n \geq 2$) dimensions [22, 23]. This process is called the decoration of the potential with Dirac delta functions [22, 23, 24, 46, 47]. Here, we consider the bound state solutions of the Schrödinger equation for solvable potentials. A potential $V(\mathbf{r})$ for which the time independent Schrödinger equation

$$-\frac{\hbar^2}{2m}\nabla^2\Psi(\mathbf{r}) + V(\mathbf{r})\Psi(\mathbf{r}) = E\Psi(\mathbf{r}) \; ; \tag{2.1}$$

can be solved analytically is called a solvable potential.

2.1. Decoration of a Solvable Potential with Dirac Delta Functions for One-Dimensional Systems

The Equation (2.1) reduces to

$$-\frac{\hbar^2}{2m}\frac{d^2\Psi(x)}{dx^2} + V(x)\Psi(x) = E\Psi(x) \; , \tag{2.2}$$

for one dimensional systems. Introducing a new parameter k as

$$E = -\frac{\hbar^2 k^2}{2m} \; , \tag{2.3}$$

the Equation (2.2) for energies of the bound states can be put in homogenous form

$$\frac{d^2\Psi(x)}{dx^2} - \left(\frac{2m}{\hbar^2}V(x) + k^2\right)\Psi(x) = 0 \; . \tag{2.4}$$

It is convenient to write the Equation (2.2) in terms of a dimensionless variable $u = k\,x$ as[1] :

$$\frac{d^2\Psi(u)}{du^2} - \left(\frac{2m}{\hbar^2 k^2}V(u) + 1\right)\Psi(u) = 0\ . \tag{2.5}$$

Since the Equation (2.5) is a second order linear differential equation, it has two linearly independent solutions $\psi_1(u)$ and $\psi_2(u)$ which form a basis set:

$$\{\psi_1(u)\,, \psi_2(u)\}\ . \tag{2.6}$$

All solutions of the equation (2.5) can be expressed as a linear combination of $\psi_1(u)$ and $\psi_2(u)$.

The potential decorated with a finite number (P) of Dirac delta functions can be written as

$$U(x) = V(x) - \frac{\hbar^2}{2m}\sum_{i=1}^{P}\sigma_i\delta(x - x_i)\ . \tag{2.7}$$

Here, x_i's are the positions of Dirac delta functions and σ_i 's are arbitrary real numbers (Positive σ_i represents an attractive potential while negative σ_i represents a repulsive one). The strengths of the Dirac delta functions is taken as $\left(-\frac{\hbar^2}{2m}\sigma_i\right)$ for computational convenience. The time independent Schrödinger equation for this potential is written as

$$-\frac{\hbar^2}{2m}\frac{d^2\Psi(x)}{dx^2} + \left(V(x) - \frac{\hbar^2}{2m}\sum_{i=1}^{P}\sigma_i\delta(x - x_i)\right)\Psi(x) = E\Psi(x)\ . \tag{2.8}$$

This equation reduces to the Schrödinger equation of the solvable potential $V(x)$ for

[1]For some potentials the dimensionless variable is chosen other than $u = k\,x$ according to the natural length scale determined by the potential.

$x \neq x_i$. The Equation (2.8) is written in terms of k and u as:

$$\frac{d^2\Psi(u)}{du^2} + \left(-\frac{2m}{\hbar^2 k^2} V(u) + \sum_{i=1}^{P} \frac{\sigma_i}{k} \delta(u - u_i) - 1 \right) \Psi(u) = 0 \,, \tag{2.9}$$

where $u_i = k\, x_i$. By deriving the Equation (2.9) from the Equation (2.8), we used the fact that $\delta(ax) = \delta(x)/a$. For $u \neq u_i$, the Equation (2.9) reduces to the Equation (2.5) and both equations have the same set of solutions whose basis is given in the Equation (2.6). However, P Dirac delta functions divide the position space into $P + 1$ intervals (see Figure 2.1). Using the basis set given in the Equation (2.6), one can form another

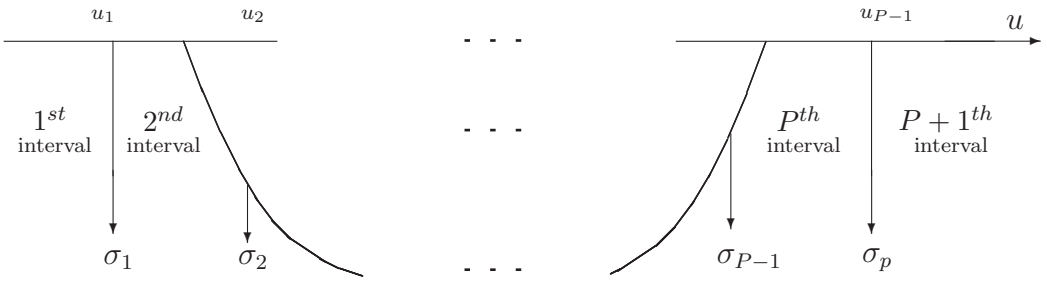

Figure 2.1. Intervals

two linearly independent solutions of the Equation (2.5) such that

$$\begin{aligned} \Psi_A(u_L) = \infty \quad &, \quad \Psi_A(u_R) = 0 \\ \Psi_B(u_L) = 0 \quad &, \quad \Psi_B(u_R) = \infty \,, \end{aligned} \tag{2.10}$$

where u_L and u_R represent the value of u at the left and right boundary, respectively. For bound states, the wave functions of the 1^{st} (leftmost) and $(P+1)^{th}$ (rightmost) intervals are defined in terms of Ψ_B and Ψ_A as

$$\Psi_1(u) = b_1 \Psi_B(u) \tag{2.11}$$

and

$$\Psi_{P+1}(u) = a_{P+1} \Psi_A(u) \,, \tag{2.12}$$

respectively. The wave functions of intermediate regions are chosen as linear combinations of Ψ_A and Ψ_B:

$$\Psi_i(u) = b_i \Psi_B(u) + a_i \Psi_A(u), \tag{2.13}$$

where b_i and a_i are determined by applying the boundary conditions at the interfaces of the intervals and normalizing the wave function. By integrating the Equation (2.9) from $u_i - \epsilon$ to $u_i + \epsilon$ and taking the limit $\epsilon \to 0^+$, we find that the derivative of $\Psi(u)$ will have a finite jump at $u = u_i$ i.e. there is a finite difference between the derivatives at $u = u_i + \epsilon$ and $u = u_i - \epsilon$. The conditions for the continuity of the wave function and the jump of its derivative is obtained by the following equations at the interfaces of the intervals (at u_i's)

$$b_i \Psi_B(u_i) + a_i \Psi_A(u_i) = b_{i+1} \Psi_B(u_i) + a_{i+1} \Psi_A(u_i) \tag{2.14}$$

and

$$\begin{aligned} & b_{i+1} \frac{d\Psi_B(u_i)}{du} + a_{i+1} \frac{d\Psi_A(u_i)}{du} - \left(b_i \frac{d\Psi_B(u_i)}{du} + a_i \frac{d\Psi_A(u_i)}{du} \right) \\ & = -\frac{\sigma_i}{k} \left(b_i \Psi_B(u_i) + a_i \Psi_A(u_i) \right) , \end{aligned} \tag{2.15}$$

where $\frac{d\Psi_B(u_i)}{du}$ and $\frac{d\Psi_A(u_i)}{du}$ denote the values of the derivatives of $\Psi_B(u)$ and $\Psi_A(u)$ with respect to u at point u_i. The Equations (2.14) and (2.15) can be unified in a matrix equation as:

$$\begin{bmatrix} \Psi_A(u_i) & \Psi_B(u_i) \\ \Psi_A'(u_i) & \Psi_B'(u_i) \end{bmatrix} \begin{bmatrix} a_{i+1} \\ b_{i+1} \end{bmatrix} = \begin{bmatrix} \Psi_A(u_i) & \Psi_B(u_i) \\ \Psi_A'(u_i) - \frac{\sigma_i}{k} \Psi_A(u_i) & \Psi_B'(u_i) - \frac{\sigma_i}{k} \Psi_B(u_i) \end{bmatrix} \begin{bmatrix} a_i \\ b_i \end{bmatrix}, \tag{2.16}$$

where primes denote the derivative with respect to u. A recursion relation between the coefficients of the wave functions of successive intervals is obtained by multiplying both

sides of the Equation (2.16) by the matrix $\begin{bmatrix} \Psi_A & \Psi_B \\ \Psi_A^{'} & \Psi_B^{'} \end{bmatrix}^{-1} = \frac{1}{\mathbb{W}_{AB}} \begin{bmatrix} \Psi_B^{'} & -\Psi_B \\ -\Psi_A^{'} & \Psi_A \end{bmatrix}$:

$$\begin{bmatrix} a_{i+1} \\ b_{i+1} \end{bmatrix} = \left(\mathbb{I} + \frac{\sigma_i}{k\ \mathbb{W}_{AB}} \begin{bmatrix} \Psi_A(u_i)\Psi_B(u_i) & \Psi_B(u_i)^2 \\ -\Psi_A(u_i)^2 & -\Psi_A(u_i)\Psi_B(u_i) \end{bmatrix} \right) \begin{bmatrix} a_i \\ b_i \end{bmatrix} . \quad (2.17)$$

where $\mathbb{I}$ is two by two identity matrix and $\mathbb{W}_{AB} = \Psi_A(u)\Psi_B^{'}(u) - \Psi_A^{'}(u)\,\Psi_B(u)$ is the Wronskian of the functions $\Psi_A(u)$ and $\Psi_B(u)$ which is a constant for the two linearly independent solutions of the Equation (2.5) [58]. The transfer matrix which gives the relation between the coefficients of the wave functions for two successive intervals is denoted as $\mathbb{M}_i(k)$, that is,

$$\mathbb{M}_i(k) = \mathbb{I} + \frac{\sigma_i}{k\ \mathbb{W}_{AB}} \begin{bmatrix} \Psi_A(u_i)\Psi_B(u_i) & \Psi_B(u_i)^2 \\ -\Psi_A(u_i)^2 & -\Psi_A(u_i)\Psi_B(u_i) \end{bmatrix} . \quad (2.18)$$

A relation for the coefficients of the wave functions of the leftmost and rightmost intervals is obtained by multiplying all the transfer matrices,

$$\begin{bmatrix} a_{P+1} \\ b_{P+1} \end{bmatrix} = \mathbb{M}_P(k) \ldots \mathbb{M}_2(k)\mathbb{M}_1(k) \begin{bmatrix} a_1 \\ b_1 \end{bmatrix} . \quad (2.19)$$

The total transfer matrix which relates the coefficients of the rightmost interval to the coefficients of the leftmost interval is defined as:

$$\mathbb{X}(k) = \mathbb{M}_P(k) \ldots \mathbb{M}_2(k)\mathbb{M}_1(k) . \quad (2.20)$$

The boundary conditions require $a_1 = 0,\ \ b_{P+1} = 0$, so the Equation (2.20) reads

$$\begin{bmatrix} a_{P+1} \\ 0 \end{bmatrix} = \mathbb{X}(k) \begin{bmatrix} 0 \\ b_1 \end{bmatrix} = \begin{bmatrix} x_{11} & x_{12} \\ x_{21} & x_{22} \end{bmatrix} \begin{bmatrix} 0 \\ b_1 \end{bmatrix} \quad (2.21)$$

for bound state solutions. This equation can be satisfied if and only if

$$x_{22}(k) = 0 \tag{2.22}$$

which in turn yields the bound state energy spectrum of the potential $U(x)$.

2.2. Decoration of Central, Solvable Potentials with Dirac Delta Functions for n-Dimensional Systems

In this section, the decoration of solvable, central potentials $V(r)$ with a finite number of concentric Dirac delta hyper-shells in $\mathbb{R}^n$ is presented. The decoration of $V(r)$ with Dirac delta functions ($\delta(r - r_i)$) leads to the potential,

$$U(r) = V(r) - \frac{\hbar^2}{2m} \sum_{i=1}^{P} \sigma_i \delta(r - r_i) \ . \tag{2.23}$$

The time independent Schrödinger equation equation for $U(r)$ in $\mathbb{R}^n$ is:

$$\left(-\frac{\hbar^2}{2m} \nabla^2 \Psi_{n,l}(\mathbf{r}) + V(r) - \frac{\hbar^2}{2m} \sum_{i=1}^{P} \sigma_i \delta(r - r_i) \right) \Psi_{n,l}(\mathbf{r}) = E\Psi(\mathbf{r}) \ , \tag{2.24}$$

where $\nabla^2 = \sum_{i=1}^{N} \frac{\partial^2}{\partial x_i^2}$, $r = \sqrt{\sum_{i=1}^{N} x_i^2}$, σ_i' s are real numbers and $r_1 < r_2, ... < r_i < ... < r_P$. Here, the Dirac delta functions $\delta(r - r_i)$' s define concentric hyperspherical shells.

The Equation (2.24) is a partial differential equation. However, utilizing the fact that the potential depends only on the radial distance r, for $n \geq 2$ one can apply the method of separation of variables. Thus, the wave function can be written in terms of n-dimensional spherical coordinates as:

$$\Psi_{n,l}(\mathbf{r}) = R_{n,l}(r) Y_{l,n}(\omega) \tag{2.25}$$

where $Y_{l,n}(\omega)$ is an n-dimensional spherical harmonic of degree l and $\omega = (\theta_1, ..., \theta_{n-1})$.

The angles $\theta_i \;\; i = 1, 2, ..., n-1$ are defined as

$$\begin{aligned} x_1 &= r\cos\theta_1 \\ x_2 &= r\sin\theta_1\cos\theta_2 \\ &... \\ x_{n-1} &= r\sin\theta_1\sin\theta_2...\sin\theta_{n-2}\cos\theta_{n-1} \\ x_n &= r\sin\theta_1\sin\theta_2...\sin\theta_{n-2}\sin\theta_{n-1} \end{aligned} \tag{2.26}$$

where $0 \leq r < \infty$, $0 \leq \theta_j \leq \pi$ for $j \leq n-2$ and $0 \leq \theta_{n-1} \leq 2\pi$ [59]. The Laplacian in $\mathbb{R}^n$ is written in terms of spherical coordinates as [59]:

$$\nabla^2 = \frac{1}{r^{n-1}}\frac{d}{dr}\left(r^{n-1}\frac{d(.)}{dr}\right) + \frac{\Omega_{LB}}{r^2} \tag{2.27}$$

where the Laplace-Beltrami operator Ω_{LB}, on the sphere $\mathbf{S^{n-1}}$, satisfies

$$\Omega_{LB}Y_{l,n}(\omega) = -l(l+n-2)Y_{l,n}(\omega)\ . \tag{2.28}$$

The degeneracy of $Y_{l,n}$ is $m_{l,n} = \frac{(2l+n-2)(l+n-3)!}{l!(n-2)!}$ for $n \geq 2$ and $l \geq 0$ [59]. By using another index (μ or ν) for these degenerate states, one gets an orthonormal set $\{Y_{l,n;\mu}\}$ for $\mu = 1, 2, ..., m_{l,n}$, that is [23, 59],

$$\int_{S^{n-1}} Y^*_{l,n;\mu}\, Y_{l,n;\nu} d\Theta = \delta_{\mu,\nu}\ . \tag{2.29}$$

It is possible to define $m_{0,2} = 1$ by substituting $l = 0$ into the general formula of $m_{l,n}$, doing the cancellations and then inserting n=2 [23].

By substituting the Equation (2.25) into the Equation (2.24) and using (2.27), after little algebra a differential equation for the radial part of the wave function is

obtained,

$$\frac{1}{r^{n-1}}\frac{d}{dr}\left(r^{n-1}\frac{dR_{n,l}(r)}{dr}\right)-\left[\frac{2m}{\hbar^2}V(r)-\sum_{i=1}^{P}\sigma_i\delta(r-r_i)+k^2+\frac{\alpha_l}{r^2}\right]R_{n,l}(r)=0 \quad (2.30)$$

for $l=0,1,2,...$, where $k=-\frac{2mE}{\hbar^2}$ and $\alpha_l=l(l+n-2)$. The transformation

$$f_{n,l}(r)=r^{\frac{n-1}{2}}R_{n,l}(r) \quad (2.31)$$

is necessary to put the Equation (2.30) into invariant form [58]

$$\left(\frac{d^2}{dr^2}-\frac{\left(l+\frac{n}{2}-\frac{1}{2}\right)\left(l+\frac{n}{2}-\frac{3}{2}\right)}{r^2}-\frac{2mV(\mathbf{r})}{\hbar^2}+\sum_{i=1}^{P}\sigma_i\delta(r-r_i)-k^2\right)f_{n,l}(r)=0\ . \quad (2.32)$$

Defining a dimensionless variable as $v=k\,r$ for a solvable potential the Equation (2.32) becomes[2]

$$\left(\frac{d^2}{dv^2}-\frac{\left(l+\frac{n}{2}-\frac{1}{2}\right)\left(l+\frac{n}{2}-\frac{3}{2}\right)}{v^2}-\frac{2mV(v)}{\hbar^2k^2}+\sum_{i=1}^{P}\frac{\sigma_i}{k}\delta(v-v_i)-1\right)f_{n,l}(v)=0\ . \quad (2.33)$$

For $v\neq v_i$, the Equation (2.33) reduces to

$$\left(\frac{d^2}{dv^2}-\frac{\left(l+\frac{n}{2}-\frac{1}{2}\right)\left(l+\frac{n}{2}-\frac{3}{2}\right)}{v^2}-\frac{2mV(v)}{\hbar^2k^2}-1\right)f_{n,l}(v)=0\ . \quad (2.34)$$

This differential equation is a second order, linear, ordinary differential equation. Hence it has two linearly independent solutions

$$\{f_{I,n,l}(v),\ \ f_{II,n,l}(v)\}\ . \quad (2.35)$$

Using these two functions, one can form another linearly independent (bound state)

[2]For some potentials the dimensionless variable is chosen other than $v=k\,r$ according to the natural length scale determined by the potential.

solutions of the Equation (2.32) for solvable potentials such that

$$\begin{aligned} f_A(0) = \infty \quad &, \quad f_A(\infty) = 0 \\ f_B(0) = 0 \quad &, \quad f_B(\infty) = \infty \ . \end{aligned} \tag{2.36}$$

In $\mathbb{R}^n$, spherical Dirac delta shells divide the space into $P+1$ regions. The radial factor of the wave function of the $(P+1)^{th}$ (outer most) region should satisfy $f_{n,l}(\infty) = 0$ for square integrability. Consequently, the wave functions of the 1^{st} and $P+1^{th}$ regions become

$$f_{1,n,l}(v) = b_1 f_B(v) \tag{2.37}$$

and

$$f_{P+1,n,l}(v) = a_{P+1} f_A(v) \ , \tag{2.38}$$

respectively. The wave functions of intermediate regions are chosen as linear combinations of $f_{A,n,l}(v)$ and $f_{B,n,l}(v)$:

$$f_{i,n,l}(v) = b_i f_B(v) + a_i f_A(v) \ . \tag{2.39}$$

After this point the procedure is the same with the one dimensional case. By integrating equation (2.33) from $v_i - \epsilon$ to $v_i + \epsilon$ and taking the limit $\epsilon \to 0^+$, one finds that the derivative of $f_{n,l}(v)$ will have a finite jump at $v = v_i$. Therefore, using the continuity of the wave function and the jump condition the transfer matrix which relates the coefficients of two successive regions is obtained as:

$$\mathbb{M}_i(k) = \mathbb{I} + \frac{\sigma_i}{k\mathbb{W}_{AB}} \begin{bmatrix} f_A(v_i) f_B(v_i) & f_B(v_i)^2 \\ -f_{A,n,l}(v_i)^2 & -f_A(v_i) f_B(v_i) \end{bmatrix} \tag{2.40}$$

where $\mathbb{W}_{AB} = f_A(v) f_B^{'}(v) - f_A^{'}(v) f_B(v)$ is the Wronskian of the functions $f_A(v)$ and $f_B(v)$ which is a constant for the two linearly independent solutions of the Equation

(2.34) [58]. For this case, the primes denote the derivative with respect to v. The total transfer matrix which relates the coefficients of the outermost region to the coefficients of the innermost region is defined in the same way as one dimensional case,

$$\mathbb{X}(k) = \mathbb{M}_P(k) \dots \mathbb{M}_2(k)\mathbb{M}_1(k) \ . \tag{2.41}$$

Since $a_1 = 0$ and $b_{P+1} = 0$ because of the boundary conditions, the energy eigenvalues are again obtained by the condition

$$x_{22}(k) = 0 \ . \tag{2.42}$$

2.3. A Theorem on Bound States of a Hamiltonian Decorated with a Finite Number of Dirac Delta Functions

The estimation of the energy eigenvalues of a Hamiltonian is a challenging problem when the Schrödinger equation can not be solved for this Hamiltonian. There are some approximation techniques such as variational method, WKB approximation, etc. developed to this aim. Therefore, it is useful to prove a theorem on the energy eigenvalues of bound states for a Hamiltonian decorated with a finite number of Dirac delta functions.

The Hamiltonian corresponding to the potential with a finite number of Dirac delta function is defined as $\mathcal{H}_0$ [23],

$$\mathcal{H}_0 = -\frac{\hbar^2}{2m}\nabla^2 - \frac{\hbar^2}{2m}\sum_{i=1}^{P}\sigma_i\delta(r - r_i) \ . \tag{2.43}$$

For a potential $V(r)$ we define $V_\lambda(r)$ as $V_\lambda(r) = \lambda^d V(r)$ where λ is a parameter independent of r and d is a positive integer. So, $V_{\lambda=1}(r) = V(r)$. Thus, $U_\lambda(r, \{\sigma_i\}) = V_\lambda(r) - \frac{\hbar^2}{2m}\sum_{i=1}^{P}\sigma_i\delta(r - r_i)$ depends on r, λ and $\{\sigma_i\}$. The Hamiltonian corresponding

to $U_\lambda(r, \{\sigma_i\})$ will be denoted by $\mathcal{H}_{\lambda\sigma}$,

$$\mathcal{H}_{\lambda\sigma} = -\frac{\hbar^2}{2m}\nabla^2 + V_\lambda(r) - \frac{\hbar^2}{2m}\sum_{i=1}^{P}\sigma_i\delta(r - r_i)\ . \tag{2.44}$$

THEOREM 1: *If a potential* $V_\lambda(r) = \lambda^d V(r)$ *in* $\mathbb{R}^n$ *where* $d \in \mathbb{Z}^+$ *satisfies the following conditions*:

(i) *It is a smooth function of* r *and has an absolute minimum* V_0.

(ii) *The expectation value of the potential* $V_{\lambda=1}(r)$ *in its eigenstates*

$$\langle \Psi_{l,n;\,\mu}\,(kr, \Theta)|V_{\lambda=1}(r)|\Psi_{l,n;\,\mu}\,(kr, \Theta)\rangle$$

is finite where $\Psi_{l,n;\,\mu}$*'s are bound state eigenfunctions of* $\mathcal{H}_{\lambda=1\sigma}$.

(iii) $V(r)$ *does not diverge exponentially as* $r \to \infty$ *and does not diverge faster than* $1/r^{n-1}$ *as* $r \to 0$.

Then, for given n *and* l *and for* $\mathcal{H}_{\lambda\sigma}$ *with arbitrary positive real* σ_i *and* r_i*, the following statements are valid:*

(a) *"Bound state energies are continuous functions of* $\lambda, \sigma_1, ..., \sigma_P$*".*

(b) *"There can be at most* P *energy eigenvalues less than* V_0*".*

Proof:

(a) For given n and l, $R_{n,l;\,q}$ is defined as the radial part of the bound state eigenfunction of $\mathcal{H}_{\lambda=1,\sigma}$ with q nodes. By dropping the subscripts n and l, one can take $R_q \equiv R_{n,l;\,q}$. The energy surface is defined as $f_q = E_q(\lambda, \sigma_1, ..., \sigma_P)$ for the energy of bound state $\Psi_{l,n;\,\mu}\,(kr, \Theta) = R_q(kr)Y_{l,n;\,\mu}(\Theta)$ [23]. By Hellmann-Feynmann

theorem, one gets for the normalized wave function $\Psi \equiv \Psi_{l,n;\mu}(kr,\Theta)$ of $\mathcal{H}_{\lambda\sigma}$ [3],

$$\begin{aligned}\frac{\partial E_q}{\partial \lambda} &= \langle\Psi|\frac{\partial \mathcal{H}_{\lambda\sigma}}{\partial \lambda}|\Psi\rangle = d\lambda^{d-1}\int_\tau V(r)\,|\Psi|^2\,r^{n-1}\,d\tau \\ &= d\lambda^{d-1}\int_0^\infty V(r)\,|R_q(kr)|^2\,r^{n-1}\,dr \end{aligned} \tag{2.45}$$

where orthonormality of $Y_{l,n;\,\mu}$ is used and $d\tau$ represents n-dimensional "volume element". This integral converges by assumption (ii) of the theorem. Thus the derivative $\frac{\partial E_q}{\partial \lambda}$ exists for all r, and hence $f_q = E_q(\lambda,\sigma_1,...,\sigma_P)$ is a continuous function of λ. Similarly,

$$\begin{aligned}\frac{\partial E_q}{\partial \sigma_i} &= \langle\Psi|\frac{\partial \mathcal{H}_{\lambda\sigma}}{\partial \sigma_i}|\Psi\rangle = \int_0^\infty \left(-\frac{\hbar^2}{2m}\delta(r-r_i)\right)\,|R_q(kr)|^2\,r^{n-1}dr \\ &= \frac{\hbar^2}{2m}|R_q(kr_i)|^2 r_i^{n-1}\,. \end{aligned} \tag{2.46}$$

Assumption (i) states that $V(r)$ is a smooth function of r. Hence, $|R_q(kr)|^2$ is finite and $\frac{\partial E_q}{\partial \sigma_i}$ exists for all r and $f_q = E_q(\lambda,\sigma_1,...,\sigma_P)$ is a continuous function of σ_i for $i = 1,...,P$.

(b) Since all σ_i' s are positive, all the Dirac delta potentials are attractive. With this choice, $\mathcal{H}_0$ will have at most P bound state solutions with negative energies for given n and l (See Theorem 7 in Reference [22]). Assume that there are N bound states of $\mathcal{H}_0$ with negative energies α_j, where $0 \le N \le P$ and j represents the number of nodes of the corresponding radial part of the bound state eigenfunction. For given n and l, $\tilde{R}_j$ and T_j^0 are the exact radial (bound state) eigenfunctions with j nodes of $\mathcal{H}_{\lambda\sigma}$ and $\mathcal{H}_0$, respectively [23]. Among the admissible functions F_j which satisfy boundary conditions and have j nodes, for a Hamiltonian $\mathcal{H}$, $\langle F_j|\mathcal{H}|F_j\rangle$ is the minimum for the exact eigenfunction (See pp. 399 of [60]). Adding the negative of absolute minimum $-V_0$ to the potential $V_\lambda(r)$, a new potential can be defined as $V_\lambda^{'}(r) = V_\lambda(r) - V_0$ which is non-negative for all r, where $r > 0$. The corresponding Hamiltonian for $V_\lambda^{'}(r)$ with P Dirac delta potentials added can be denoted by $\mathcal{H}_{\lambda\sigma}^{'} = \mathcal{H}_{\lambda\sigma} - V_0$. Then, the eigenfunctions $\tilde{R}_j$ of $\mathcal{H}_{\lambda\sigma}$ with $E_j(\lambda,\sigma_1,...,\sigma_P)$ are eigenfunctions of $\mathcal{H}_{\lambda\sigma}^{'}$ with $E_j^{'}(\lambda,\sigma_1,...,\sigma_P) =$

$E_j(\lambda, \sigma_1, ..., \sigma_P) - V_0$. Thus, one gets

$$\begin{aligned} \langle T_j^0|\mathcal{H}_0|T_j^0\rangle &\leq \langle \tilde{R}_j|\mathcal{H}_0|\tilde{R}_j\rangle \leq \langle \tilde{R}_j|\mathcal{H}'_{\lambda\sigma} = \mathcal{H}_0 + V'_\lambda(r)|\tilde{R}_j\rangle \\ &\leq \langle T_j^0|\mathcal{H}'_{\lambda\sigma}|T_j^0\rangle = \langle T_j^0|\mathcal{H}_{\lambda\sigma}|T_j^0\rangle - V_0 \ . \end{aligned} \tag{2.47}$$

This leads to

$$\begin{aligned} E_j(0, \sigma_1, ..., \sigma_P) &= \alpha_j \leq E'_j(\lambda, \sigma_1, ..., \sigma_P) \\ &\leq \alpha_j + \int_0^\infty V'_\lambda(r)|T_j^0|^2 r^{n-1} dr \ . \end{aligned} \tag{2.48}$$

Since $T_j^0 \to ce^{-kr}$ with k positive as $r \to \infty$, $I'_\lambda = \int_0^\infty V'_\lambda(r)|T_j^0|^2 r^{n-1} dr$ converges by the assumption $V(r)$ is not exponentially divergent as $r \to \infty$ and does not diverge faster than $1/r^{n-1}$ as $r \to 0$ [3] . Thus,

$$\alpha_j \leq E'_j(\lambda, \sigma_1, ..., \sigma_P) \leq \alpha_j + I'_\lambda \tag{2.49}$$

Therefore, for some particular values $\sigma_i > 0$ such that $\alpha_j < -I'_\lambda$, one gets

$$E'_j(\lambda, \sigma_1, ..., \sigma_P) < 0 \Rightarrow E_j(\lambda, \sigma_1, ..., \sigma_P) < V_0 \tag{2.50}$$

If the index j of R_j with the corresponding negative energy is bigger than $P-1$, then the Equation (2.49) implies that there can be more than P bound states of $\mathcal{H}_0$ with negative energies. However, this is impossible since there exists at most P bound states of $\mathcal{H}_0$ with negative energies [22]. Thus, there are at most P bound states of $\mathcal{H}_{\lambda\sigma}$ with the eigenvalues less than V_0.

[3] These conditions are met by almost all physical potentials.

3. SPECIFIC POTENTIALS WITH DIRAC DELTA FUNCTIONS FOR ONE-DIMENSIONAL SYSTEMS

3.1. Constant Potential with a Finite Number of Dirac Delta Functions

The constant potential can be chosen as $V(x) = 0\,(\Rightarrow V(u) = 0)$ without loss of generality, where $u = kx$ and k is defined in the Equation (2.3). Therefore, the Equation (2.9) becomes

$$\frac{d^2\Psi\,(u)}{du^2} + \left(\sum_i^P \frac{\sigma_i}{k}\delta(u-u_i) - 1\right)\Psi\,(u) = 0 \tag{3.1}$$

where σ_i' s are positive real constants and $u_1 < u_2 < ... < u_P$. The linearly independent solutions of the Equation (3.1) for $u \neq u_i$ are e^u and e^{-u} which satisfy the necessary boundary conditions at $u \to -\infty$ and $u \to \infty$, respectively. Therefore, the wave functions of the different intervals can be written as

$$\begin{aligned} \Psi_1(u) &= b_1\,e^u &&= b_1 e^{kx} \\ \Psi_{P+1}(u) &= a_{P+1}\,e^{-u} &&= a_{P+1}\,e^{-kx} \\ \Psi_i(u) &= a_i\,e^{-u} + b_i\,e^u &&= a_i\,e^{-kx} + b_i\,e^{kx}\ , \end{aligned} \tag{3.2}$$

where $2 \leq i \leq P-1$ and $k > 0$ for bound states. Using the method developed in Section 2.1, the transfer matrix $\mathbb{M}_i(k)$ calculated at point $u_i = k\,x_i$ is:

$$\mathbb{M}_i(k) = \begin{bmatrix} 1 + \frac{\sigma_i}{2\,k} & \frac{\sigma_i\,e^{2u_i}}{2k} \\ -\frac{\sigma_i\,e^{-2ku_i}}{2k} & 1 - \frac{\sigma_i}{2k} \end{bmatrix}\ . \tag{3.3}$$

The total transfer matrix defined in the Equation (2.20) reads for this case,

$$\mathbb{X}(k) = \mathbb{M}_P(k)\ldots\mathbb{M}_2(k)\,\mathbb{M}_1(k)\ . \tag{3.4}$$

where $\{\sigma_i\}$ is the set of all σ_is as defined in Section 2.1. $x_{22}(k) = 0$ gives the energy eigenvalues of the potential. If the potential consists of only one Dirac delta function, $U(x) = -\frac{\hbar^2}{2m}\sigma_1\delta(x - x_1)$, the eigenvalue equation is immediately obtained by using the Equation (3.3), since $\mathbb{X}(k) = \mathbb{M}_1(k)$ and one gets

$$k = \sigma_1/2 \ , \tag{3.5}$$

for bound state eigenvalue.

The Dirac delta quantum well is used for modelling different physical systems mentioned in the Introduction [14, 15]. Therefore, it is useful to derive the eigenvalue equation for this case. The potential for double Dirac delta well is defined as:

$$V(x) = -\frac{\hbar^2}{2m}\left[\sigma_1\,\delta(x - x_1) + \sigma_2\,\delta(x - x_2)\right] \tag{3.6}$$

where $x_2 > x_1$. The total transfer matrix for this potential is

$$\begin{aligned}
&\mathbb{X}(k) = \mathbb{M}_2(k)\mathbb{M}_1(k) \\
&= \begin{bmatrix} 1 + \frac{\sigma_2}{2\,k} & \frac{\sigma_2\,e^{2kx_2}}{2k} \\ -\frac{\sigma_2\,e^{-2kx_2}}{2k} & 1 - \frac{\sigma_2}{2k} \end{bmatrix} \begin{bmatrix} 1 + \frac{\sigma_1}{2\,k} & \frac{\sigma_1\,e^{2kx_1}}{2k} \\ -\frac{\sigma_1\,e^{-2kx_1}}{2k} & 1 - \frac{\sigma_1}{2k} \end{bmatrix} \\
&= \begin{bmatrix} 1 + \frac{\sigma_1+\sigma_2}{2\,k} + \frac{\sigma_1\sigma_2\left(1-e^{2k(x_2-x_1)}\right)}{4\,k^2} & \frac{\sigma_1\,e^{2kx_1}+\sigma_2\,e^{2kx_2}}{2k} + \frac{\sigma_1\sigma_2\left(e^{2kx_1}-e^{2kx_2}\right)}{4\,k^2} \\ \frac{\sigma_1\sigma_2\left(e^{-2kx_1}-e^{-2kx_2}\right)}{4\,k^2} - \frac{\sigma_1\,e^{-2kx_1}+\sigma_2\,e^{-2kx_2}}{2k} & 1 - \frac{\sigma_1+\sigma_2}{2\,k} + \frac{\sigma_1\sigma_2\left(1-e^{-2k(x_2-x_1)}\right)}{4\,k^2} \end{bmatrix} .
\end{aligned} \tag{3.7}$$

The spectrum equation found by the condition $x_{22}(k) = 0$ becomes,

$$1 - \frac{\sigma_1 + \sigma_2}{2\,k} + \frac{\sigma_1\sigma_2\left(1 - e^{-2k(x_2-x_1)}\right)}{4\,k^2} = 0 \ , \tag{3.8}$$

Assuming real $k \neq 0$, the Equation (3.8) can be written as [4] :

$$(2k - \sigma_1)(2k - \sigma_2) = \sigma_1\sigma_2 e^{-2k(x_2-x_1)} \ . \tag{3.9}$$

[4]There is no loss of generality, since $k = 0 \Rightarrow E = 0$ which is not a bound state energy value for $V(x) = 0$

Both the polynomial at the left hand side and exponential at the right hand side of the Equation (3.9) are equal to $\sigma_1 \times \sigma_2$ at $k = 0$ and the polynomial is equal to zero for positive $k = \sigma_1/2$ and $k = \sigma_2/2$. The right hand side of the Equation (3.5) decreases monotonically from $\sigma_1 \times \sigma_2$ to zero as k goes from zero to ∞. Hence, they intersect at least one and therefore the double Dirac delta well has at least one bound state. Both the polynomial at the left hand side and the exponential at the right hand side of the Equation (3.9) have negative derivatives at $k = 0$ and if $x_2 - x_1 > \frac{\sigma_1+\sigma_2}{\sigma_1\sigma_2}$, the decrease of the exponential is larger than the decrease of the polynomial. So, for $x_2 - x_1 > \frac{\sigma_1+\sigma_2}{\sigma_1\sigma_2}$ Dirac delta well has two bound states. As the Dirac delta functions get closer to each other or get weaker (smaller σ_i values), there can be only one bound state. These results are the specific examples of the general result:
There exist at least one and at most P bound states of the Schrödinger equation for the potential $V(x) = \sum_i^P -\frac{\hbar^2}{2m}\sigma_i\delta(x - x_i)$ [22].

3.2. Linear Potential with a Finite Number of Dirac Delta Functions

In this Section, we obtain the wave functions of the Schrödinger equation

$$-\frac{\hbar^2}{2m}\frac{d^2\Psi(x)}{dx^2} + U(x)\,\Psi(x) = E\,\Psi(x) \tag{3.10}$$

where the potential is given as

$$U(x) = f\,x - \frac{\hbar^2}{2m}\sum_{i=1}^{P}\sigma_i\,\delta(x - x_i) \tag{3.11}$$

for $x \geq 0$ and the potential is infinite for $x < 0$. Here, the positions of Dirac delta functions x_i's and the coefficient of the linear potential f are positive real constants and σ_i 's are arbitrary real numbers (Positive σ_i represents an attractive potential while negative σ_i represents a repulsive one). Introducing $E = \frac{\hbar^2k^2}{2m}$ for bound states, we obtain from the Equation (3.10)

$$\frac{d^2\Psi(x)}{dx^2} - \left(\frac{2mfx}{\hbar^2} - \sum_{i=1}^{P}\sigma_i\delta(x - x_i) - k^2\right)\Psi(x) = 0\ . \tag{3.12}$$

We denote $(0, x_1)$ as the 1^{st}, (x_i, x_{i+1}) for $i = 1, ..., P-1$ as the $(i+1)^{th}$ and (x_P, ∞) as the $(P+1)^{th}$ interval. Defining [5]

$$l = \left(\frac{\hbar^2}{2mf}\right)^{\frac{1}{3}} \text{ and } u = \frac{x}{l} - k^2\, l^2 \tag{3.13}$$

the Equation(3.12) becomes

$$\frac{d^2\Psi\,(u)}{du^2} - \left(u - l\sum_{i=1}^{P}\sigma_i\delta(u-u_i)\right)\Psi = 0 \tag{3.14}$$

where $u_i = \frac{x_i}{l} - k^2\, l^2$. This equation reduces to Airy differential equation for $u \neq u_i$. The solutions of this differential equation are the Airy functions $Ai\,(u)$ and $Bi\,(u)$ [61]. The boundary conditions at $x = 0\,(u = -k^2l^2)$ and $x = \infty\,(u = \infty)$ force us to choose

$$\Psi\left(-k^2l^2\right) = 0 \ , \ \ \Psi\,(\infty) = 0 \ . \tag{3.15}$$

The function $Ai\,(x)$ satisfies $Ai(\infty) = 0$ whereas $Bi(\infty) = \infty$. Therefore, we define $\Psi_A = Ai\,(u)$ and $\Psi_B = Ai\,(u) - \lambda\, Bi\,(u)$ where $\lambda = \frac{Ai\left(-k^2\, l^2\right)}{Bi(-k^2\, l^2)}$ as the functions which satisfy the boundary conditions at $x = \infty$ and $x = 0$, respectively. Hence, the wave function for the first (leftmost) interval is

$$\Psi_1 = b_1\Psi_B\,(u) = b_1\,(Ai\,(u) - \lambda\, Bi\,(u)) \tag{3.16}$$

where b_1 is a constant. By varying σ_i's, $Bi\,(-k^2\, l^2)$ may become zero, thus λ goes to infinity. However, we first consider $Bi\,(-k^2\, l^2) \neq 0$ and then study the cases $Bi\,(-k^2\, l^2) = 0$. Similarly, by using the boundary condition at $x = \infty$

$$\Psi_{P+1} = a_{P+1}\Psi_A\,(u) = a_{P+1}Ai\,(u) \tag{3.17}$$

[5] Here we choose another dimensionless variable than defined for the general case in Section 2.1 to obtain a natural length scale for the potential.

is taken as the wave function of the $(P+1)^{th}$ (rightmost) interval. For the intermediate regions, we choose the wave functions as linear combinations of Ψ_A and Ψ_B,

$$\Psi_i(u) = a_i\ \Psi_A(u) + b_i\ \Psi_B(u) \tag{3.18}$$

where a_i and b_i are determined by applying the boundary conditions at the interfaces of the intervals and normalizing the wave function. By using the methodology of Section 2.1 we find the transfer matrix, $\mathbb{M}_i(k)$ as

$$\mathbb{M}_i(k) = \begin{bmatrix} 1 - \frac{\sigma_i \pi l Ai(u_i)[Ai(u_i) - \lambda Bi(u_i)]}{\lambda} & -\frac{\sigma_i \pi l}{\lambda}\left[Ai(u_i) - \lambda Bi(u_i)\right]^2 \\ \frac{\sigma_i \pi l}{\lambda} Ai^2(u_i) & 1 + \frac{\sigma_i \pi l Ai(u_i)[Ai(u_i) - \lambda Bi(u_i)]}{\lambda} \end{bmatrix} \tag{3.19}$$

in terms of $Ai(u)$ and $Bi(u)$. The total transfer matrix is written as

$$\mathbb{X}(k) = \mathbb{M}_P(k) \ldots \mathbb{M}_2(k)\mathbb{M}_1(k)\ , \tag{3.20}$$

and

$$x_{22}(k) = 0 \tag{3.21}$$

yields the bound state energy spectrum of the linear potential.

It is instructive to obtain the energy spectrum equation for P=1 case in order to observe how the energy eigenvalues change as the dimensionless parameter $(\sigma_1 l)$ varies. Since we have derived the energy equation for the general case, it is now easy to obtain it for P=1 where the total transfer matrix reduces to $\mathbb{M}_1(k)$ and the Equation (3.21) gives

$$\sigma_1 l = \frac{Ai(-k^2 l^2)}{\pi Ai(u_1)\left[Ai(-k^2 l^2)\, Bi(u_1) - Bi(-k^2 l^2)\, Ai(u_1)\right]}\ . \tag{3.22}$$

Here, we have used $\lambda = \frac{Ai\left(-k^2 l^2\right)}{Bi\left(-k^2 l^2\right)}$ and $u_1 = \frac{x_1}{l} - k^2 l^2$. Note that equation(3.22) reduces

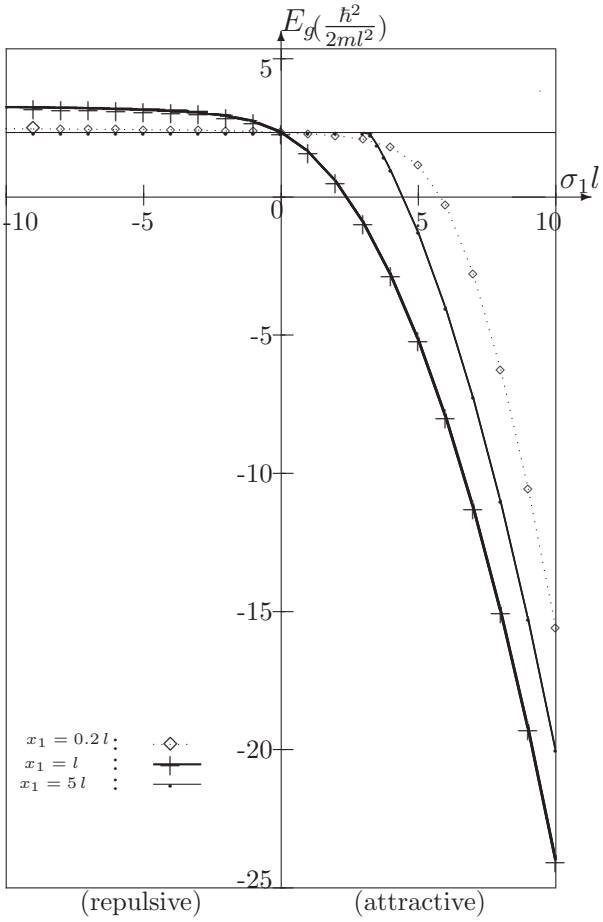

Figure 3.1. The ground state energies (E_g) vs. ($\sigma_1 l$).

to the well-known energy eigenvalue equation of the linear potential

$$Ai\left(-k^2 l^2\right) = 0 \tag{3.23}$$

as $\sigma_1 \to 0$. For different x_1 values ($x_1 = 0.2l,\ l,\ 5l$), we solve the Equation (3.22) numerically for $\frac{2ml^2}{\hbar^2}E_g$ where E_g is the ground state energy. We observe that E_g is a monotonically decreasing function of $\sigma_1 l$ as shown in Figure 3.1. We also show how the ground state energy changes with the position x_1/l of Dirac delta function for $\sigma_1 l = 2$ in Figure 3.2. ΔE_g is negative since we have used attractive Dirac delta interaction. For very small and very large x_1 values, ΔE_g will go to zero due to the boundary conditions. By using the first order perturbation theory, it can be shown that $\Delta E_n \propto \left|Ai\left(\frac{x_1}{l} - r_n\right)\right|^2$ where r_n is the n^{th} root of Ai. However, there will be two minima of ΔE_2 for the first excited state which has a node and also becomes zero at

Table 3.1. Configuration Numbers (N_{conf}) for ordered P=1, 2, 4, 8 Dirac delta functions.

N_{conf}	P=1	P=2	P=4	P=8
1	A	A^2	A^4	A^8
2	R	AR	A^3R	A^4R^4
3	-	RA	A^2RA	R^4A^4
4	-	R^2	A^2R^2	R^8
5	-	–	ARA^2	–
6	-	–	$ARAR$	–
7	-	–	AR^2A	–
8	-	–	AR^3	–
9	-	–	RA^3	–
10	-	–	RA^2R	–
11	-	–	$RARA$	–
12	-	–	RAR^2	–
13	-	–	R^2A^2	–
14	-	–	R^2AR	–
15	-	–	R^3A	–
16	-	–	R^4	–

the boundaries. Figure 3.3 shows the graph of ΔE_2 as a function of the position, x_1/l, of Dirac delta function. ΔE_2 is zero at the node of the first excited state wave function. In general, the change in the energy levels as a function of the positions of Dirac delta functions will be a complicated function since there will be several extremum points of $|\Psi_n|^2$ for excited states, $n \geq 2$.

For $P > 1$, the energy spectrum can be found by using the Equation (3.21). However, one obtains complicated eigenvalue equations for these cases. For investigating the effects of attractive (A) and repulsive (R) Dirac delta potentials at $x_1 = l, \ldots, x_P = Pl$ on energy levels, we solve the Equation (3.21) for P=1, 2, 4, 8 cases with several different configurations. For demonstrating all these results together in a figure, we define

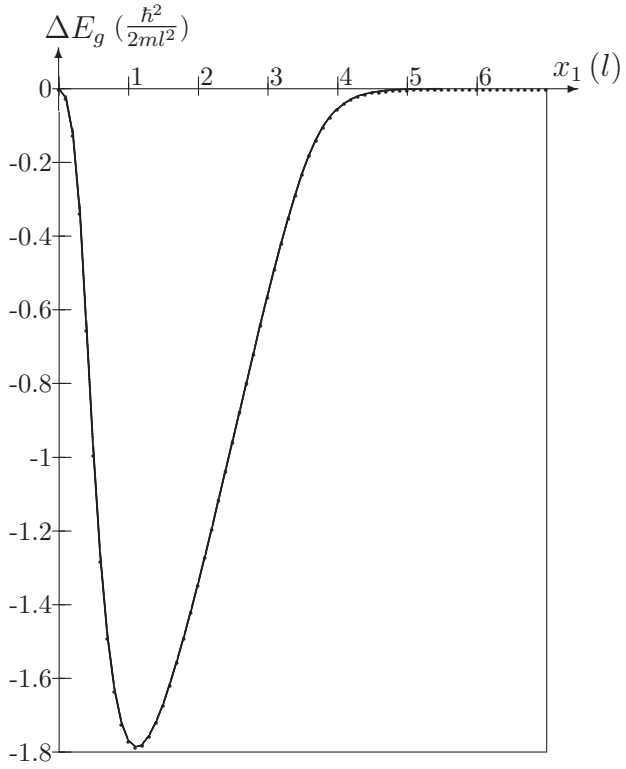

Figure 3.2. The change of ground state energy (ΔE_g) vs. x_1 for $\sigma_1 l = 2$.

configuration numbers for different ordered configurations which are presented in Table 3.1. For example, for P=4, four ordered Dirac delta functions is shown as $AAAA$ or A^4 has the configuration number 1 and $ARRA$ or AR^2A has the configuration number 7 which has successive A, R, R, A Dirac delta functions at points x_1, x_2, x_3, x_4 where $x_1 < x_2 < x_3 < x_4$. We choose configuration numbers such that configurations with attractive Dirac delta functions at larger x_i values have higher configuration numbers.

The ground state and first excited state energies as a function of these configuration numbers are presented in Figures (3.4)-(3.7) with the strengths $\sigma_1 = |\frac{1}{l}|$ and $\sigma_2 = |\frac{5}{l}|$ ($\sigma_1 = \frac{1}{l}, \frac{5}{l}$ and $\sigma_2 = -\frac{1}{l}, -\frac{5}{l}$ for attractive (A) and repulsive (R) delta functions respectively). In these figures, the lines are drawn as a guide to the eye.

We notice that for the same strength the attractive Dirac delta functions decrease E_g more than the repulsive Dirac delta functions increase it. For example, compare A^4 and R^4 cases with zero delta function values in Figures 3.5 and 3.6. This can also be seen in Figure 3.1 for P=1 case. One can qualitatively explain this effect by

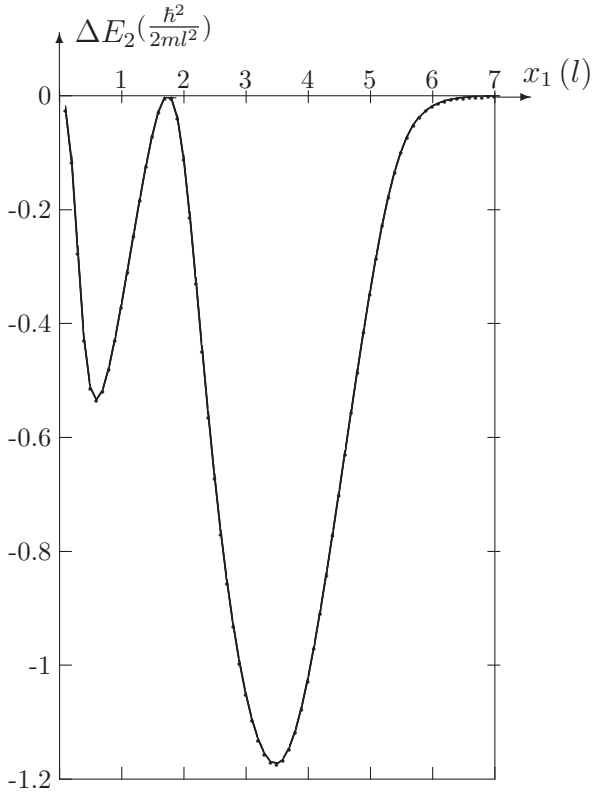

Figure 3.3. The change of the energy in first excited state (ΔE_2) vs. x_1 for $\sigma_1 l = 2$.

considering the change of the wave function. The wave function should have a kink at $x = x_i$ with a finite jump for derivatives at $x = x_i - \epsilon$ and $x = x_i + \epsilon$ in order to satisfy $\frac{d\Psi}{dx}|_{x=x_i+\epsilon} - \frac{d\Psi}{dx}|_{x=x_i-\epsilon} = -\sigma\Psi$. Thus, the wave function forms an outward kink and increase the value of $|\Psi|^2$ for attractive Dirac delta potential and forms an inward kink and decrease the value of $|\Psi|^2$ for repulsive Dirac delta potential. Thus, the attractive Dirac delta functions will cause much bigger changes in energy E_n since the energy change due to Dirac delta functions is $\Delta E_n \propto |\Psi_n|^2$.

Until this point, we have assumed $Bi\,(-k^2\,l^2) \neq 0$. However, as σ_1 varies, the solution of the Equation (3.22) may yield k values that satisfy

$$Bi\left(-k^2\,l^2\right) = 0\ . \tag{3.24}$$

In this case, $Bi\,(u)$ part of the wave function in the Equation (3.16) satisfies the boundary condition at $x = 0$. Then, for this specific value of k, only the wave function

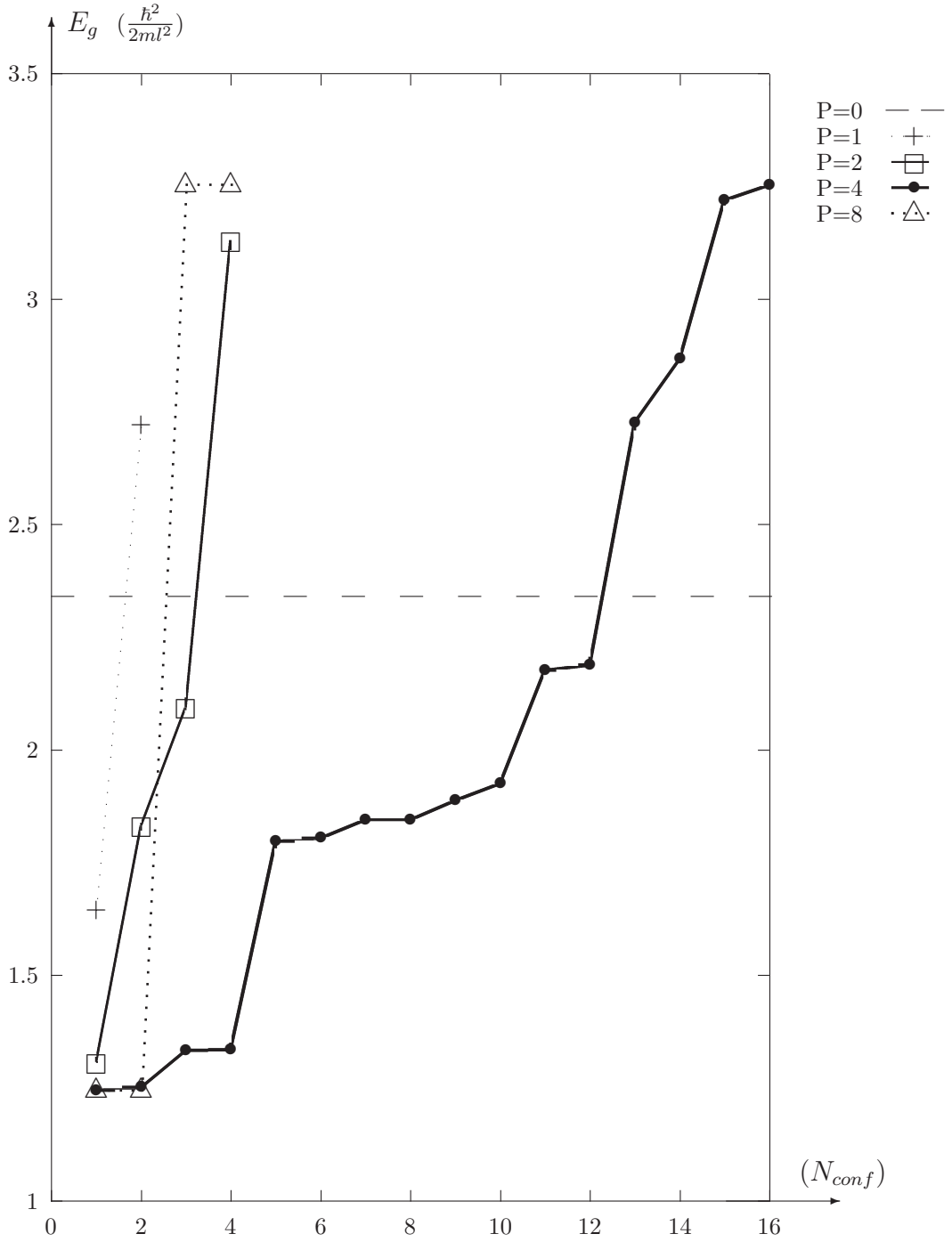

Figure 3.4. The ground state energy E_g vs. configuration number (N_{conf}) for $x_1 = l, \ldots, x_P = Pl$ and $|\sigma|l = 1$.

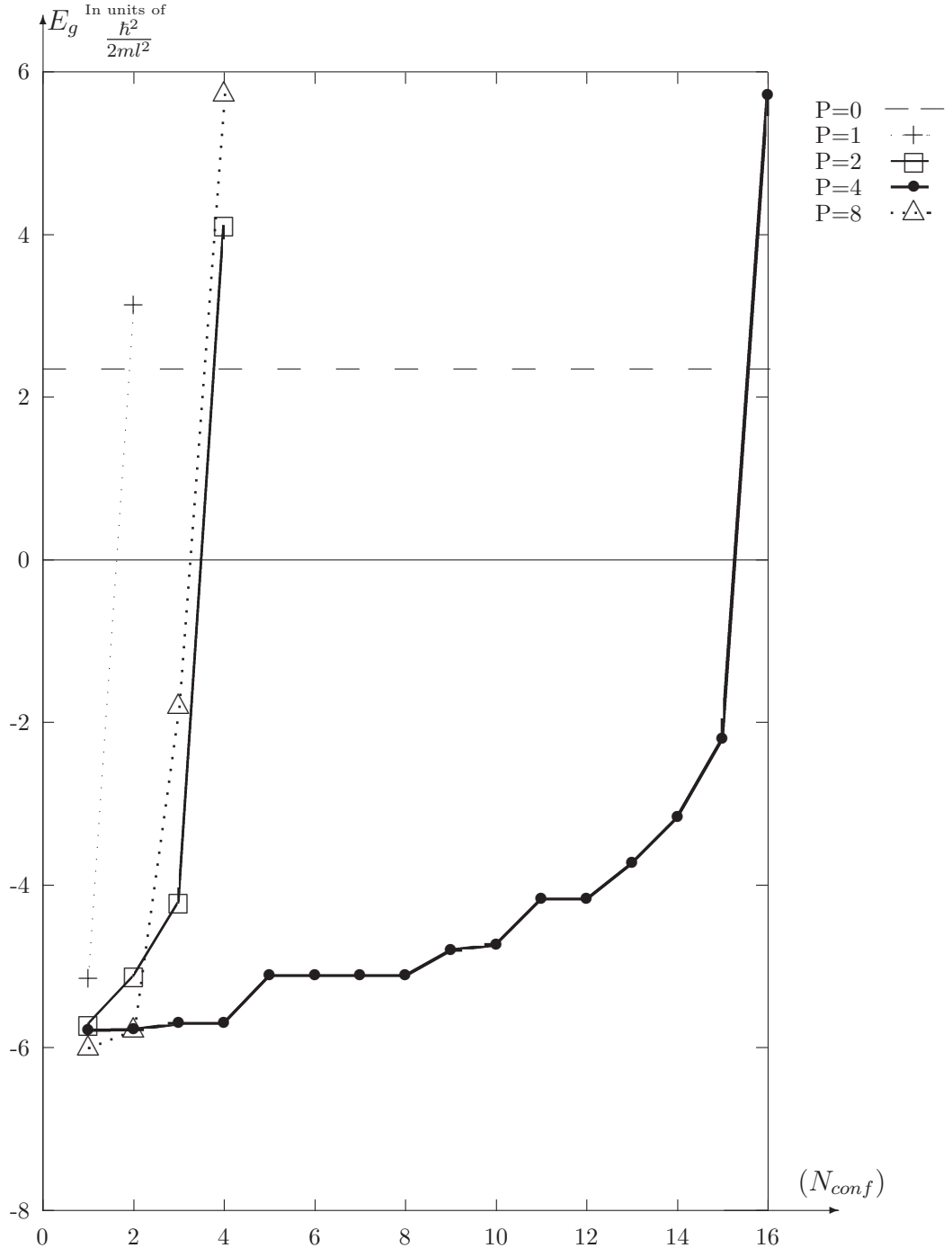

Figure 3.5. The ground state energy E_g (in units of $\frac{\hbar^2}{2ml^2}$) vs. configuration number (N_{conf}) for $x_1 = l\,, \ldots\,, x_P = Pl$ and $|\sigma|l = 5$.

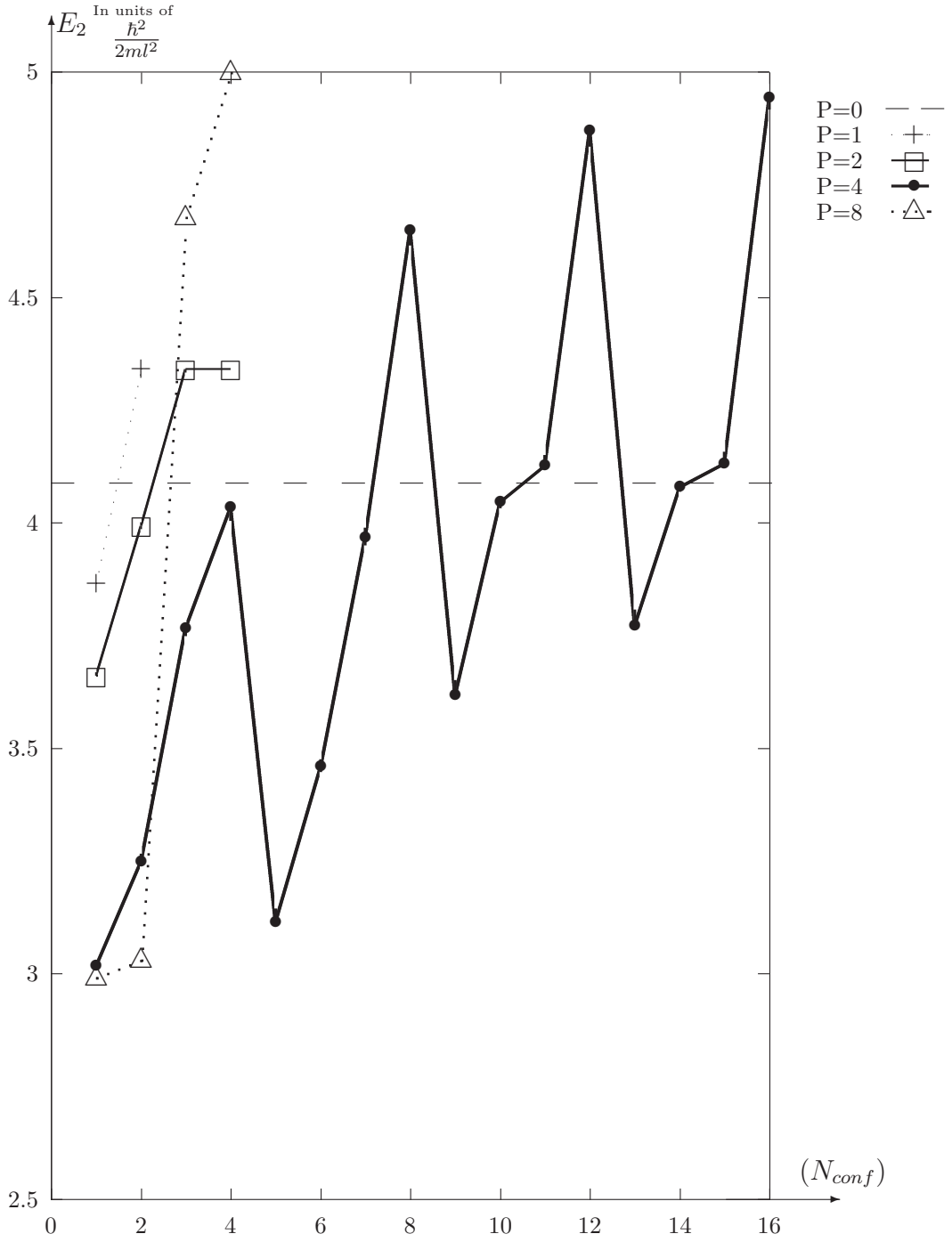

Figure 3.6. The first excited state E_2 (in units of $\frac{\hbar^2}{2ml^2}$) vs. configuration number (N_{conf}) for $x_1 = l\,, \ldots\,, x_P = Pl$ for $|\sigma|l = 1$.

of the 1^{st} interval should be modified as

$$\Psi_1 = b_1 \Psi_B\,(u) = b_1 Bi\,(u)\ . \tag{3.25}$$

The wave functions for all intervals except $i = 1$ preserve their forms as given in the

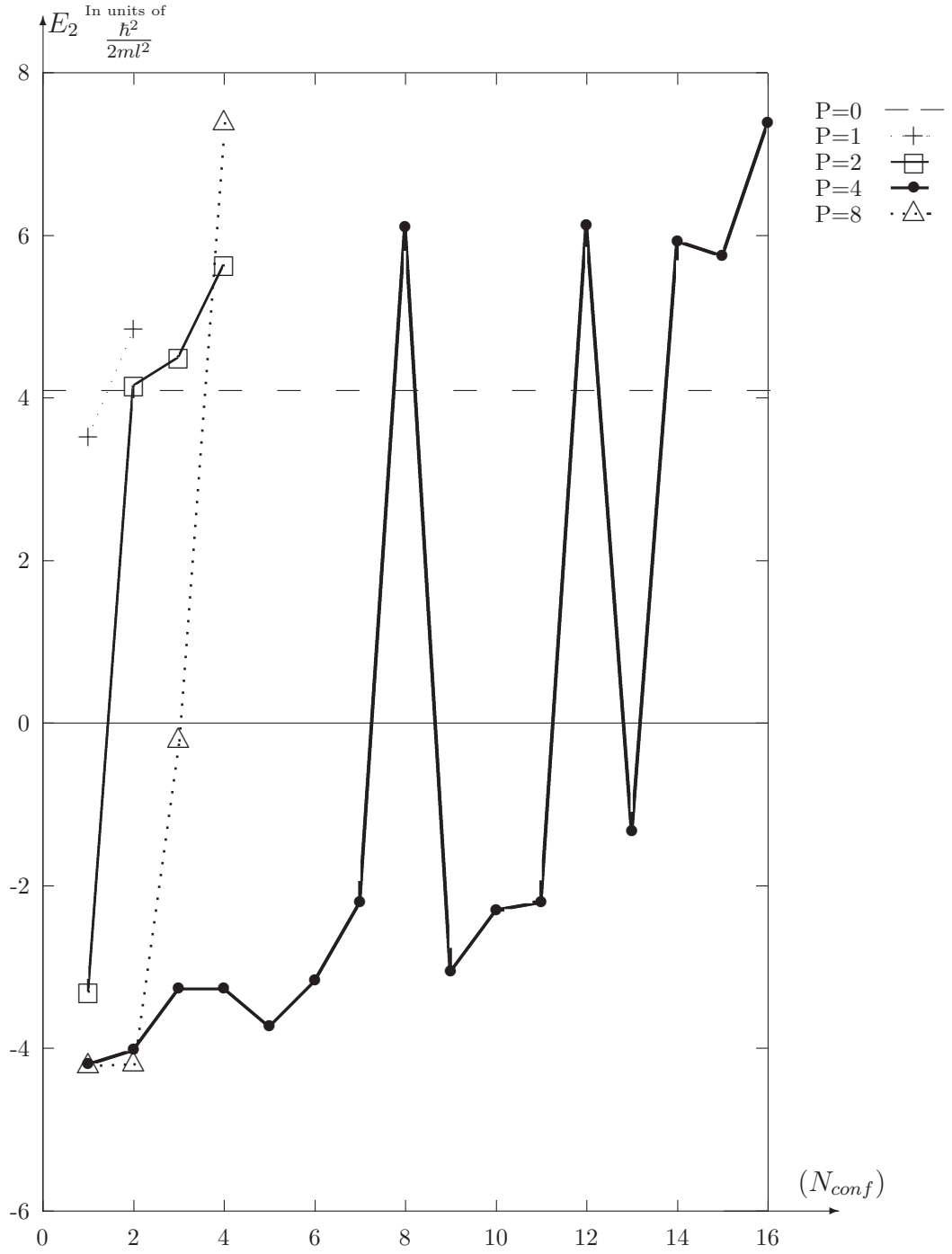

Figure 3.7. The first excited state E_2 (in units of $\frac{\hbar^2}{2ml^2}$) vs. configuration number (N_{conf}) for $x_1 = l\,, \ldots\,, x_P = Pl$ and $|\sigma|l = 5$.

Equations (3.17) and (3.18). Note that for $Bi\,(-k^2l^2) = 0$ case, the Equation (3.22) for P=1 reduces to

$$\sigma_1 l = \frac{1}{\pi Ai\left(\frac{x_1}{l} - k^2l^2\right)\, Bi\left(\frac{x_1}{l} - k^2l^2\right)}\,. \tag{3.26}$$

By using $\Psi(r) = \frac{F(r)}{r}$ for the radial function, above calculations may also be used to find the exact s state solutions ($L = 0$) of the three-dimensional Schrödinger equation with linear potential.

3.3. Harmonic Potential with a Finite Number of Dirac Delta Potential

The harmonic potential with a finite number of Dirac delta functions is given as [62]:

$$V(x) = \frac{1}{2}m\omega^2 x^2 - \frac{\hbar^2}{2m}\sum_i^P \sigma_i \delta(x - x_i) \; . \tag{3.27}$$

The time-independent Schrödinger equation for this potential is

$$-\frac{\hbar^2}{2m}\frac{d^2\Psi(x)}{dx^2} + V(x)\Psi(x) = E\Psi(x) \; . \tag{3.28}$$

By inserting $E = (\xi + \frac{1}{2})\hbar\omega$, with ξ a real number, and introducing dimensionless quantities $z = x/x_0$, and $z_i = x_i/x_0$ with $x_0 = \sqrt{\hbar/2m\omega}$, the natural length scale of the harmonic potential, we can reexpress the Equation (3.28) as

$$\frac{d^2\Psi(z)}{dz^2} + \left[\xi + \frac{1}{2} - \frac{z^2}{4} + \sum_i^P \Lambda_i \delta(z - z_i)\right]\Psi(z) = 0, \tag{3.29}$$

where $\Lambda_i = x_0\sigma_i$. For $z \neq z_i$, the Equation (3.29) has two linearly independent solutions. For $\xi \neq 0, 1, 2, ...$ these linearly independent solutions are parabolic cylinder functions $D_\xi(z)$ and $D_\xi(-z)$, defined as:

$$\begin{aligned} &D_\xi(z) = 2^{\frac{\xi}{2}} e^{-\frac{z^2}{4}} \times \\ &\left\{ \frac{\sqrt{\pi}\;{}_1F_1\left(-\frac{\xi}{2}, \frac{1}{2}; \frac{z^2}{2}\right)}{\Gamma\left(\frac{1-\xi}{2}\right)} - \frac{\sqrt{2\pi}z\;{}_1F_1\left(\frac{1-\xi}{2}, \frac{3}{2}; \frac{z^2}{2}\right)}{\Gamma\left(-\frac{\xi}{2}\right)} \right\} \end{aligned} \tag{3.30}$$

$$D_\xi(-z) = 2^{\frac{\xi}{2}} e^{-\frac{z^2}{4}} \times$$
$$\left\{ \frac{\sqrt{\pi}\ {}_1F_1\left(-\frac{\xi}{2}, \frac{1}{2}; \frac{z^2}{2}\right)}{\Gamma\left(\frac{1-\xi}{2}\right)} + \frac{\sqrt{2\pi} z\ {}_1F_1\left(\frac{1-\xi}{2}, \frac{3}{2}; \frac{z^2}{2}\right)}{\Gamma\left(-\frac{\xi}{2}\right)} \right\}, \tag{3.31}$$

where ${}_1F_1\left(-\xi/2, 1/2; z^2/2\right)$ and ${}_1F_1\left((1-\xi)/2, 3/2; z^2/2\right)$ are the confluent hypergeometric functions ${}_1F_1\left(a, b; z^2/2\right)$ defined in the Reference [61] for $a = -\xi/2$, $b = 1/2$ and $a = (1-\xi)/2$, $b = 3/2$, respectively. $D_\xi(-z)$ is regular as $z \to -\infty$, but $|D_\xi(-z)| \to +\infty$ as $z \to \infty$ and $D_\xi(z)$ is regular as $z \to \infty$, but $|D_\xi(z)| \to +\infty$ as $z \to -\infty$ [61]. Thus, the general solution of the Equation (3.29) is

$$\begin{aligned} \Psi_1(z) &= b_1 D_\xi(-z) \\ \Psi_i(z) &= a_i\, D_\xi(z) + b_i D_\xi(-z) \\ \Psi_{P+1}(z) &= a_{P+1} D_\xi(z)\ , \end{aligned} \tag{3.32}$$

for the intervals $1, i$ and $P+1$ respectively where $i = 2, ..., P$. These wave functions are normalizable, because

$$I = \int_0^\infty (D_\xi(t))^2 dt = \int_{-\infty}^0 (D_\xi(-t))^2 dt = \sqrt{\pi} 2^{-3/2} \left[\frac{\psi(1/2 - \xi/2) - \psi(-\xi/2)}{\Gamma(-\xi)} \right] \tag{3.33}$$

is finite. Here

$$\psi(x) = \frac{\left(d\Gamma(x)\right)/dx}{\Gamma(x)}\ , \tag{3.34}$$

is the logarithmic derivative of $\Gamma(x)$ and should not be confused with wave functions. Both $\psi(x)$ and $\Gamma(x)$ have simple poles at negative integers. Therefore, the integral in the Equation (3.33) is defined for all real values of ξ [61].

By using the transfer matrix method explained in Section 2.1, one finds the

transfer matrix $\mathbb{M}_i(k)$ as:

$$\mathbb{M}_i(k) = \begin{bmatrix} 1 + \frac{\Lambda_i D_\xi(z) D_\xi(-z)}{\mathcal{W}_z} & \frac{\Lambda_i \left(D_\xi(-z)\right)^2}{\mathcal{W}_z} \\ -\frac{\Lambda_i \left(D_\xi(z)\right)^2}{\mathcal{W}_z} & 1 - \frac{\Lambda_i D_\xi(z) D_\xi(-z)}{\mathcal{W}_z} \end{bmatrix} , \tag{3.35}$$

where $\mathcal{W}_z = \mathcal{W}_z \left[D_\xi(z), D_\xi(-z)\right]$ is the Wronskian of the functions $D_\xi(z), D_\xi(-z)$ and it is constant for a given ξ,

$$\mathcal{W}_z = \frac{2^{\xi+3/2}\pi}{\Gamma(-\xi/2)\Gamma((1-\xi)/2)} . \tag{3.36}$$

The total transfer matrix $\mathbb{X}$ is defined as in the previous sections and $x_{22} = 0$ gives the spectrum for the harmonic potential with a finite number of Dirac delta functions.

For a special case of the potential given in the Equation (3.27), harmonic potential with one Dirac delta function at its center $P = 1,\ x_1 = 0$ is [20]

$$V(x) = \frac{1}{2} m\omega^2 x^2 - \frac{\hbar^2}{2m} \sigma \delta(x) . \tag{3.37}$$

The total transfer matrix for this potential is

$$\mathbb{X}(k) = M_1(k) = \begin{bmatrix} 1 + \frac{\Lambda_i (D_\xi(0))^2}{\mathcal{W}_z} & \frac{\Lambda_i \left(D_\xi(0)\right)^2}{\mathcal{W}_z} \\ -\frac{\Lambda_i \left(D_\xi(0)\right)^2}{\mathcal{W}_z} & 1 - \frac{\Lambda_i (D_\xi(0))^2}{\mathcal{W}_z} \end{bmatrix} , \tag{3.38}$$

which gives the equation

$$\frac{\Lambda_1 (D_\xi(0))^2}{\mathcal{W}_z} = 1 . \tag{3.39}$$

for the eigenvalues. In this case, the odd solutions of the harmonic potential are unaffected because the Dirac delta function is located at the center of the harmonic potential and does not break the symmetry of the wave functions. On the other hand, energy eigenvalues of even states change as a function of σ_1. The eigenvalue equation

of the even states is written in terms of Γ functions as:

$$\frac{\Gamma((1-\xi)/2)}{\Gamma(-\xi/2)} = \frac{\Gamma(3/4 - E/2\hbar\omega)}{\Gamma(1/4 - E/2\hbar\omega)} = \frac{\sigma\sqrt{\hbar/m\omega}}{4}, \tag{3.40}$$

by calculating $D_\xi(0)$ and $\mathcal{W}_z$ from the Equations (3.30) and (3.36), respectively. The ground state energy eigenvalue decreases unlimitedly as σ increases (attractive case). However, the energies of the excited even states are limited by the energies E_{2n+1} of odd states and as $\sigma \to \infty$, $E_{2n+2} \to E_{2n+1} = (2n+1+1/2)\hbar\omega$ where $n = 0, 1, ...$ Thus, as $\sigma_1 \to \infty$ the energy eigenvalues of these states go to the energy eigenvalue of the one lower eigenstate, and the odd energy eigenstates asymptotically become doubly degenerate [62].

We will use the Equation (3.40) in Section 5.3.

3.4. $\mathcal{PT}$ - Symmetric Potential with Dirac Delta Functions

The pioneering work of Bender et al [28] revealed that there may be a possible extension to standard quantum theory. In this study, it is shown that the class of non-hermitian Hamiltonians

$$\mathcal{H} = p^2 + x^2(ix)^\nu \ \text{ with } \ \nu \in \mathbb{R}^+ \tag{3.41}$$

have real, positive and discrete spectrum. The set of Hamiltonians given in the Equation (3.41) are invariant under the parity time reversal operator $\mathcal{PT}$. The parity operator $\mathcal{P}$ is linear and has the effect.

$$p \to -p \ \text{ and } \ x \to -x\ . \tag{3.42}$$

The time reversal operator $\mathcal{T}$ is anti linear and has the effect

$$p \to -p, \quad x \to -x \ \text{ and } \ i \to -i\ . \tag{3.43}$$

Therefore, the effect of the parity time operator $\mathcal{PT}$ (first $\mathcal{T}$ then $\mathcal{P}$ or vice versa since parity and time reversal operators commute) is

$$p \to p, \quad x \to -x \text{ and } i \to -i \,. \tag{3.44}$$

Now, it is easy to see that the set of Hamiltonians given in the Equation (3.41) are invariant under $\mathcal{PT}$ operation. Hamiltonians that are invariant under $\mathcal{PT}$ operator is called $\mathcal{PT}$-symmetric [63].

Although the $\mathcal{PT}$-symmetric Hamiltonians $\mathbf{H}$ are invariant under $\mathcal{PT}$ operation their eigenfunctions may not be. However, if all the eigenfunctions of $\mathcal{H}$ are simultaneously eigenfunctions of $\mathcal{PT}$ operator, then it is said that $\mathcal{PT}$-symmetry is unbroken. For this case, it is possible to show that the spectrum is real [63]. If the eigenfunctions of $\mathbf{H}$ are not simultaneously eigenfunctions of $\mathcal{PT}$ operator, then $\mathcal{PT}$-symmetry is broken. In this case, the eigenvalues of $\mathbf{H}$ are generally complex. For $\mathcal{PT}$-symmetric Hamiltonians, $\mathbf{H}$ and $\mathbf{H}^\dagger$ have the same spectrum [64].

$\mathcal{PT}$-symmetric Hamiltonians with complex potentials have very rich spectral structures for bound states which decay at infinities and eigenvalues are in general much harder to obtain. Even when we have two Dirac delta functions with complex strengths, investigations on the characteristics of eigenvalues (numbers of eigenvalues, realness, etc.) is not a simple problem. Rouche's theorem and the argument principle on the roots of complex functions (See e.g. pp. 230, 231 of Reference [65]) are helpful to investigate the domains where only real or complex conjugate roots (breakdown of $\mathcal{PT}$-symmetry) are possible.

The $\mathcal{PT}$ symmetric potential with a finite number of Dirac delta functions is

$$V(x) = -\frac{\hbar^2}{2m} \sum_{i=1}^{N} \sigma_i \, \delta(x - x_i) + \sigma_i^* \, \delta(x + x_i) \tag{3.45}$$

where $0 < x_1 < x_2 < ... < x_{N-1} < x_N$ and $x_i \in (0, \infty)$. σ_i s are arbitrary complex

numbers.

We label the interval containing the origin with zero, the intervals $[-x_{i+1}, -x_i]$ with negative integers $(-i)$ and intervals $[x_i, x_{i+1}]$ with positive integers (i) (See Figure (3.8)) where $i = 1, 2, ..., N$.

The time independent Schrödinger equation for the potential given in the Equation (3.45) reads,

$$-\frac{\hbar^2}{2m}\frac{d^2\Psi(x)}{dx^2} + V(x)\Psi(x) = E\Psi(x) \ . \tag{3.46}$$

Introducing $E = -\frac{\hbar^2\kappa^2}{2m}$, we obtain from the Equation (3.46)

$$\frac{d^2\Psi(x)}{dx^2} + \left\{ \sum_{i=1}^{N} \sigma_i \delta(x - x_i) + \sigma_i^* \delta(x + x_i) - \kappa^2 \right\} \Psi(x) = 0 \tag{3.47}$$

for bound states. We note that E and κ can be complex, since Hamiltonian is not hermitian. For $x \neq x_i$, the solutions are given by two linearly independent exponential functions $\Psi_A = e^{-\kappa x}$ and $\Psi_B = e^{\kappa x}$ where $\kappa = k_1 + ik_2$ with k_1, $k_2 \ \epsilon \ \mathbb{R}$ [6] . We take $\mathbf{Re}(\kappa) = k_1 > 0$ so that the functions Ψ_A and Ψ_B are (decaying) wave functions for bound states as x goes to $+\infty$ and $-\infty$, respectively. Thus, the wave functions of leftmost, rightmost and intermediate intervals between two Dirac delta functions are

$$\begin{aligned} \Psi_{(-N)}(x) &= b_{-N}\Psi_B(x) \\ \Psi_N(x) &= a_N\Psi_A(x) \\ \Psi_i(x) &= a_i\Psi_A(x) + b_i\Psi_B(x) \end{aligned} \tag{3.48}$$

By using the method developed in Section 2.1, we calculate the transfer matrix as:

$$\mathbb{M}_i(k) = \begin{bmatrix} 1 + \frac{\sigma_i}{2\kappa} & \frac{\sigma_i}{2\kappa}e^{2\kappa x_i} \\ -\frac{\sigma_i}{2\kappa}e^{-2\kappa x_i} & 1 - \frac{\sigma_i}{2\kappa} \end{bmatrix} . \tag{3.49}$$

[6] We do not use the dimensionless variable convention because κ is not real.

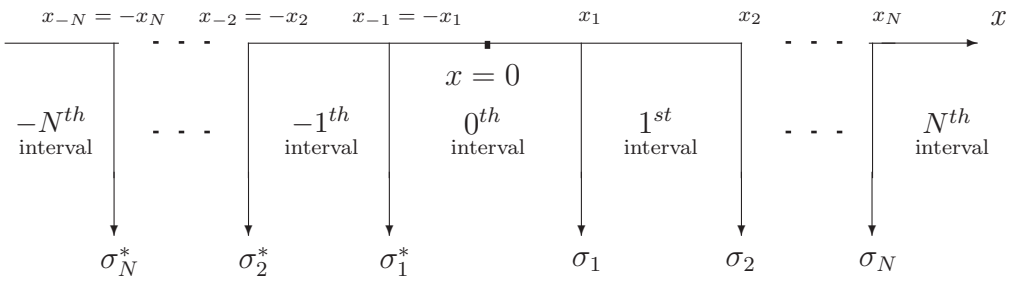

Figure 3.8. Intervals for a $\mathcal{PT}$-symmetric potential

The relations between the coefficients of the successive regions is found as

$$\begin{bmatrix} a_{i+1} \\ b_{i+1} \end{bmatrix} = \mathbb{M}_i(k) \begin{bmatrix} a_i \\ b_i \end{bmatrix} \tag{3.50}$$

for $i = -N, -N+1, ..., -1$ and

$$\begin{bmatrix} a_{i+1} \\ b_{i+1} \end{bmatrix} = \mathbb{M}_{i+1}(k) \begin{bmatrix} a_i \\ b_i \end{bmatrix} \tag{3.51}$$

for $i = 0, 1, ..., N-1$. By operating the transfer matrices successively, we can find total transfer matrix $\mathbb{X} \equiv \mathbb{X}(\kappa)$ which relates coefficients of the rightmost (N^{th}) region to the coefficients of the leftmost ($-N^{th}$) region:

$$\begin{bmatrix} a_N \\ b_N \end{bmatrix} = \mathbb{X} \begin{bmatrix} a_{(-N)} \\ b_{(-N)} \end{bmatrix} \quad \text{where } \mathbb{X}(\kappa) = \mathbb{M}_N(\kappa) \dots \mathbb{M}_1(\kappa) \mathbb{M}_{-1}(\kappa) \dots \mathbb{M}_{-N}(\kappa) \ . \tag{3.52}$$

Since boundary conditions require $b_N = 0$ and $a_{(-N)} = 0$, we get

$$\begin{bmatrix} a_N \\ 0 \end{bmatrix} = \mathbb{X}(\kappa) \begin{bmatrix} 0 \\ b_{(-N)} \end{bmatrix} \Rightarrow \begin{bmatrix} a_N \\ 0 \end{bmatrix} = \begin{bmatrix} X_{11} & X_{12} \\ X_{21} & X_{22} \end{bmatrix} \begin{bmatrix} 0 \\ b_{(-N)} \end{bmatrix} , \tag{3.53}$$

and

$$X_{22}(\kappa) = 0 \ . \tag{3.54}$$

condition gives the energy spectrum for the bound states.

3.4.1. Two $\mathcal{PT}$-Symmetric Dirac Delta Functions

In this section, we will investigate the simplest case (N=1) and obtain an analytical expression of the eigenvalue equation. The potential constitutes of two Dirac delta functions at $x = x_1$ and $x = -x_1$ with strengths σ_1 and σ_1^*, respectively.

We utilize the Equation (3.52) to obtain total transfer matrix for two $\mathcal{PT}$-symmetric Dirac delta functions

$$\mathbb{X}(\kappa) = \mathbb{M}_1(\kappa)\mathbb{M}_{-1}(\kappa) = \begin{bmatrix} 1+\frac{\sigma_1}{2\kappa} & \frac{\sigma_1}{2\kappa}e^{2\kappa x_1} \\ -\frac{\sigma_1}{2\kappa}e^{-2\kappa x_1} & 1-\frac{\sigma_1}{2\kappa} \end{bmatrix} \begin{bmatrix} 1+\frac{\sigma_1^*}{2\kappa} & \frac{\sigma_1^*}{2\kappa}e^{-2\kappa x_1} \\ -\frac{\sigma_1^*}{2\kappa}e^{2\kappa x_1} & 1-\frac{\sigma_1^*}{2\kappa} \end{bmatrix} = \begin{bmatrix} 1+\frac{\mathbf{Re}(\sigma_1)}{\kappa}+\frac{|\sigma_1|^2\left(1-e^{4\kappa x_1}\right)}{4\kappa^2} & \frac{\sigma_1 e^{2\kappa x_1}+\sigma_1^* e^{-2\kappa x_1}}{2\kappa}-\frac{|\sigma_1|^2\sinh 2\kappa x_1}{2\kappa^2} \\ -\frac{\sigma_1 e^{-2\kappa x_1}+\sigma_1^* e^{2\kappa x_1}}{2\kappa}+\frac{|\sigma_1|^2\sinh 2\kappa x_1}{2\kappa^2} & 1-\frac{\mathbf{Re}(\sigma_1)}{\kappa}+\frac{|\sigma_1|^2\left(1-e^{-4\kappa x_1}\right)}{4\kappa^2} \end{bmatrix}. \quad (3.55)$$

Then, $X_{22} = 0$ leads to the equation

$$1 - \frac{\mathbf{Re}\,(\sigma_1)}{\kappa} - \frac{|\sigma_1|^2\,(e^{-4\kappa x_1}-1)}{4\kappa^2} = 0 \quad (3.56)$$

which gives the spectrum of bound states.

As we mentioned above, for $\mathcal{PT}$-symmetric potentials, $\mathbf{H}$ and $\mathbf{H}^\dagger$ have the same spectrum [64]. By taking complex conjugate of the Equation(3.56), it can be shown that both κ and κ^* satisfy the Equation (3.56) for given σ_1 and x_1. Thus, both κ and κ^* are in the spectrum for complex κ values. Therefore, if there is only one root of the Equation(3.56), it is real.

3.4.2. Number of Bound States and Regions of $\mathcal{PT}$- Symmetry

We will use the Equation (3.56) to find the number of bound states and regions of $\mathcal{PT}$-symmetry. Then, we solve it numerically. Defining $\sigma_1 = \sigma_{1r} + i\,\sigma_{1i}$, the Equation

(3.56) leads to:

$$(2\kappa - \sigma_{1r})^2 + \sigma_{1i}^2 = \left(\sigma_{1r}^2 + \sigma_{1i}^2\right) e^{-4\kappa x_1} \tag{3.57}$$

for $\kappa \neq 0$. In the $\mathcal{PT}$-symmetric region, κ should be real since we want the bound state eigenvalues $E = -\frac{\hbar^2\kappa^2}{2m}$ to be a negative number. Moreover, κ should be positive since the wave functions of the bound states should vanish at infinities. Since $e^{-4\kappa x_1} < 1$ for real and positive κ, we obtain

$$\frac{(2\kappa - \sigma_{1r})^2 + \sigma_{1i}^2}{\sigma_{1r}^2 + \sigma_{1i}^2} < 1 \tag{3.58}$$

from the Equation (3.57). This leads to

$$0 < \kappa < \sigma_{1r}; . \tag{3.59}$$

It is interesting that the same inequality is obtained if σ_1 is a pure real number [22]. Thus, real κ values can not be equal or greater than σ_{1r} for any value of σ_{1i}. Hence, if σ_1 is a purely imaginary number or has a negative real part, we cannot have $\mathcal{PT}$-symmetric bound states.

The solution of the Equation(3.57) for σ_{1r} is

$$\sigma_{1r} = \frac{4\kappa \mp \sqrt{16\kappa^2 - 4[\sigma_{1i}^2(1 - e^{-4\kappa x_1}) + 4\kappa^2](1 - e^{-4\kappa x_1})}}{2(1 - e^{-4\kappa x_1})} . \tag{3.60}$$

Since σ_{1r} is a real number, the discriminant inside the square root of the Equation(3.60) should be non-negative. Thus, after some algebra, we get

$$\frac{1}{4x_1^2}\frac{(2\kappa x_1)^2}{(sinh(2\kappa x_1))^2} \geq \sigma_{1i}^2 \tag{3.61}$$

for $\mathcal{PT}$-symmetric regions. The left hand side of the inequality above is monotonically decreasing function of positive κ and the maximum value is attained at $\kappa = 0$ which is

equal to $\frac{1}{4x_1^2}$. Therefore, $\mathcal{PT}$-symmetry breaks down for sufficiently large x_1 and $|\sigma_{1i}|$ values such that

$$x_1|\sigma_{1i}| > \frac{1}{2} \, . \tag{3.62}$$

As a result of this, we have only complex conjugate eigenvalues for $x_1|\sigma_{1i}| > \frac{1}{2}$.

The values of σ_1 and x_1 determine the reality and number of roots of the system. By writing the Equation(3.56) in the following form

$$f(\kappa) = \kappa^2 - \sigma_{1r}\kappa + \frac{|\sigma_1|^2}{4} - \frac{|\sigma_1|^2 e^{-4\kappa x_1}}{4} = 0 \, , \tag{3.63}$$

We utilize the argument principle and Rouche's theorem to find the number of bound states. Here, we state the argument principle and Rouche's theorem [65]:

Argument Principle: *Let a function f be meromorphic in the domain interior to positively oriented simple closed contour C, and suppose that f is analytic and nonzero*

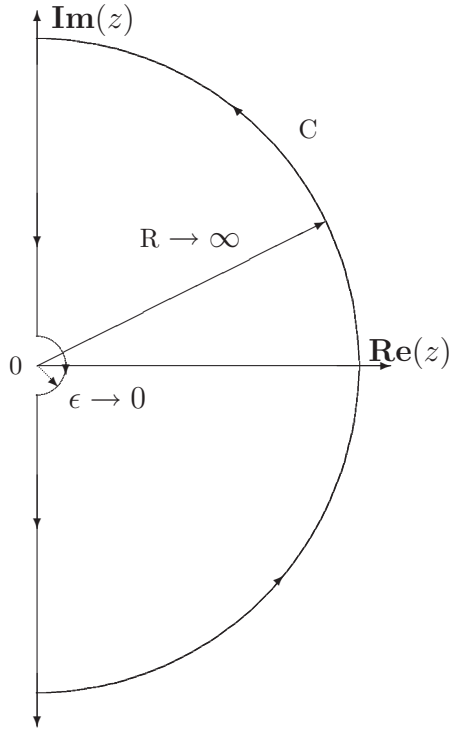

Figure 3.9. The contour C

on C. If, counting multiplicities, Z is the number of zeros and P is the number of poles inside C, then

$$\frac{1}{2\pi}\Delta_C \arg f(z) = Z - P$$

where $\Delta_C \arg f(z)$ *denotes the argument change of* $f(z)$ *around the contour.*
Rouche's theorem: *Let two functions f(z) and g(z) be analytic inside and on a simple closed contour C, and suppose*

$$|f(z)| > |g(z)|$$

at every point of C. Then, $f(z)$ *and* $f(z)+g(z)$ *have the same number of zeros, counting multiplicities, inside C.*

For $\frac{\sigma_{1r}}{|\sigma_1|^2 x_1} > 1$, the change of the argument of $f(\kappa)$

$$f(\kappa) = \kappa^2 - \mathbf{Re}(\sigma_1)\kappa + \frac{|\sigma_1|^2}{4} - \frac{|\sigma_1|^2 e^{-4\kappa x_1}}{4} = 0 \,, \tag{3.64}$$

around contour C in the right half part of the complex plane (RHP) shown in Figure 3.9, can be calculated using argument principle. Since $f(\kappa)$ is an analytic function and has no poles inside the contour C the total change of argument of $f(\kappa)$ around C gives us the number of roots, that is

$$\frac{\Delta(\alpha)}{2\pi} = m \tag{3.65}$$

where $\Delta(\alpha)$ and m denote the change of argument and the total number of roots, respectively. On the semicircle with infinite radius the parameter κ can be written as $\kappa = Re^{i\theta}$, where R$\rightarrow \infty$. As R goes to infinity, the κ^2 term of $f(\kappa)$ dominates. Thus, traversing the semicircle counter clockwise the argument of $f(\kappa)$ goes from $-\pi$ to π since θ changes from $-\frac{\pi}{2}$ to $\frac{\pi}{2}$ and the total change of argument is 2π.

On the imaginary axis $\kappa = i\,y$ and $f(\kappa)$ becomes,

$$\begin{aligned} f(y) &= -y^2 - i\,\sigma_{1r}\,y - \frac{|\sigma_1|^2\,(e^{-i4x_1y}-1)}{4} \\ &= \left[-y^2 - \tfrac{|\sigma_1|^2}{4}\,(\cos(4x_1y)-1)\right] + i\left[-\sigma_{1r}\,y + \tfrac{|\sigma_1|^2}{4}\sin(4x_1y)\right]\,. \end{aligned} \tag{3.66}$$

Therefore the argument of $f(\kappa)$ on the imaginary axis can be found from

$$\tan(\alpha) = \frac{-\sigma_{1r}\,y + \frac{|\sigma_1|^2}{4}\sin(4x_1y)}{-y^2 - \frac{|\sigma_1|^2}{4}\,[\cos(4x_1y)-1]}\,. \tag{3.67}$$

By multiplying both denominator and numerator of the equation with $-\frac{4}{|\sigma|^2}$ and performing some arrangements, we get

$$\tan(\alpha) = \frac{\frac{\sigma_{1r}}{|\sigma_1|^2x_1}\,(4x_1y) - \sin(4x_1y)}{\frac{4}{|\sigma_1|^2}y^2 + \cos(4x_1y) - 1}\,. \tag{3.68}$$

If $\frac{\sigma_{1r}}{|\sigma_1|^2x_1} > 1$, the numerator has no root. Since the denominator $D(y) = \frac{4}{|\sigma_1|^2}y^2 + \cos(4x_1y) - 1$ is an even function, excluding zero it has even number of roots. We exclude zero bypassing it with a semicircle of infinitesimal radius to satisfy the condition $|f(\kappa)| \neq 0$ on the contour. As y decreases from $+\infty$ to the largest root on the imaginary axis, $\tan(\alpha) \to +\infty$ and $\alpha \to \frac{3\pi}{2}^-$. We note that there are no roots of numerator and denominator on the semicircle with infinitesimal radius. Thus, after y crosses even number of roots of the denominator, α will be in the range $(\pi, \frac{3\pi}{2})$. Therefore, as $y \to -\infty$, after crossing all roots of the denominator, α decreases from $\frac{3\pi}{2}^-$ to π. Hence, the total change of the argument of $f(\kappa)$ around C is $\Delta(\alpha) = \pi - (-\pi) = 2\pi$. Thus, the number of roots of $f(\kappa)$ for $\frac{\sigma_r}{|\sigma_1|^2x_1} > 1$ is $\frac{\Delta(\alpha)}{2\pi} = 1$. Consequently, two $\mathcal{PT}$-symmetric Dirac delta functions has only one bound state for this case.

The total change of argument of $f(\kappa)$ is also 2π and the Equation (3.56) has again one real root if

$$\frac{\sigma_{1r}}{|\sigma_1|^2x_1} = 1 \qquad \text{and} \qquad |\sigma_1|x_1 > \frac{1}{2}\,. \tag{3.69}$$

On the other hand, the change of the argument of $f(\kappa)$ vanishes around the same contour if

$$\frac{\sigma_{1r}}{|\sigma_1|^2 x_1} = 1 \qquad \text{and} \qquad |\sigma_1| x_1 \leq \frac{1}{2} \, . \tag{3.70}$$

Hence, the Equation (3.56) has no root in this case.

We will find the number of roots of $f(\kappa)$ in the Equation (3.63) by using Rouche's theorem for the case $\frac{\sigma_{1r}}{|\sigma_1|^2 x_1} < 1$ and $|\sigma_{1i}| < \sigma_{1r}$. We write $f(\kappa) = g(\kappa) + h(\kappa)$ where

$$g(\kappa) = \kappa^2 - \sigma_{1r}\kappa + \frac{|\sigma_1|^2}{4} \tag{3.71}$$

and

$$h(\kappa) = -\frac{|\sigma_1|^2 e^{-4\kappa x_1}}{4} \, . \tag{3.72}$$

In order to apply Rouche's theorem, we should have

$$|h(\kappa)| < |g(\kappa)| \, . \tag{3.73}$$

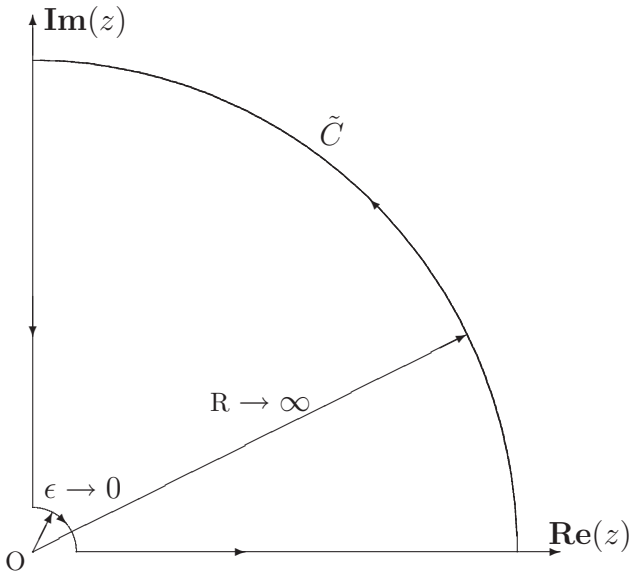

Figure 3.10. The contour $\tilde{C}$

Since $\cos\theta > 0$ on the semicircle at infinity, $|h(\kappa)| \to 0$, whereas $|g(\kappa)| \to \infty$ on that semicircle. So, on the semicircle at infinity, we have $|h(\kappa)| < |g(\kappa)|$. The condition(3.73) is satisfied on the imaginary axis excluding the origin if

$$|\sigma_{1i}| < \sigma_{1r} \ . \tag{3.74}$$

Since $|g(0)| = |h(0)|$, we have to bypass the origin with a semicircle of infinitesimal radius. By inserting $\kappa = \epsilon e^{i\theta}$ where $\epsilon \to 0$, and expanding $g(\kappa)$ and $h(\kappa)$ up to order ϵ, we find

$$\begin{aligned} |g(\epsilon,\theta)|^2 &\approx \frac{|\sigma_1|^4}{16} - \left(\frac{|\sigma_1|^2}{2}\sigma_{1r}\cos\theta\right)\epsilon \\ |h(\epsilon,\theta)|^2 &\approx \frac{|\sigma_1|^4}{16} - \left(\frac{|\sigma_1|^4}{2}x_1\cos\theta\right)\epsilon \ . \end{aligned} \tag{3.75}$$

The condition $|h(\kappa)| < |g(\kappa)|$ leads to

$$\frac{\sigma_{1r}}{|\sigma_1|^2 x_1} < 1 \ . \tag{3.76}$$

on that semicircle. We notice that if inequalities (3.74 and 3.76) are satisfied, the condition (3.73) is satisfied on the whole of contour C shown in Figure 3.9. Therefore under these conditions, $f(\kappa) = g(\kappa) + h(\kappa)$ and $g(\kappa)$ have same number of roots in RHP by Rouche's theorem [65]. $g(\kappa)$ is a polynomial of order 2 and both of its roots (σ_1 and σ_1^*) are in RHP since $\sigma_{1r} > 0$. Thus, $f(\kappa)$ has also two roots if $\frac{\sigma_{1r}}{|\sigma_1|^2 x_1} < 1$ and $|\sigma_{1i}| < \sigma_{1r}$ in RHP. Consequently, two $\mathcal{PT}$-symmetric Dirac delta functions has two bound states for this case.

Since g has only one root (σ_1 or σ_1^*, the one with positive imaginary part) inside $\tilde{C}$ shown in Figure 3.10, the Equation (3.56) has also only one complex root inside $\tilde{C}$. Moreover, the system has two bound states with complex eigenvalues, i.e. $\mathcal{PT}$-symmetry breaks down, if conditions $\frac{\sigma_{1r}}{|\sigma_1|^2 x_1} < 1$ and $|\sigma_{1i}| < \sigma_{1r}$ in RHP are satisfied

because the complex conjugate of this root is also in the spectrum. However, if

$$\frac{\sigma_{1i}^2}{|\sigma_1|^2} \leq e^{-2\sigma_{1r}x_1} \ , \tag{3.77}$$

then $|g|$ and $|h|$ intersect at two real κ values for $\frac{\sigma_{1r}}{|\sigma_1|^2 x_1} < 1$. To show this, consider the values of $|g|$ and $|h|$ at some certain points. Since $|g(0)| = |h(0)|$, $|g(\epsilon)| > |h(\epsilon)|$ $(0 < \epsilon \ll 1)$, $|g(\frac{\sigma_{1r}}{2})| < |h(\frac{\sigma_{1r}}{2})|$ and $|g(\infty)| > |h(\infty)|$, the parabola $|g(\kappa)|$ intersects $|h(\kappa)|$ at two points. Thus, we get $|g| - |h| = 0$ at two points on the positive real axis. Since $|g| - |h| = 0$ is exactly the Equation (3.56), we get two real roots of the Equation (3.56) under the conditions $\frac{\sigma_{1r}}{|\sigma_1|^2 x_1} < 1$ and $|\sigma_{1i}| < \sigma_{1r}$.

Finally, we will investigate the case

$$\frac{\sigma_{1r}}{|\sigma_1|^2 x_1} < 1 \qquad \text{and} \qquad |\sigma_{1r}| < |\sigma_{1i}| \ . \tag{3.78}$$

First, we consider the special case, purely imaginary strengths. As shown in the beginning of this section, there are no real roots and $\mathcal{PT}$-symmetry breaks down for this case. The eigenvalue equation is found easily by taking $\sigma_{1r} = 0$ in the Equation (3.57) and reads

$$\left(\frac{2\kappa}{\sigma_{1i}}\right)^2 - e^{-4\kappa x_1} + 1 = 0 \ . \tag{3.79}$$

The change of the argument of the left hand side of the Equation (3.79) around C is not a fixed value but depends on the values of σ_{1i} and x_1. As the product $|\sigma_{1i}|x_1$ gets larger, the number of roots increases. The Hamiltonian with two $\mathcal{PT}$-symmetric Dirac delta functions and purely imaginary strengths has

$$\begin{aligned} &\text{no root if} && |\sigma_{1i}| \cdot x_1 \leq \tfrac{\sqrt{2}\pi}{4} \\ &\text{2n roots if} && (2n-1)\tfrac{\sqrt{2}\pi}{4} < |\sigma_{1i}| \cdot x_1 \leq (2n+1)\tfrac{\sqrt{2}\pi}{4} \end{aligned} \tag{3.80}$$

where n =1,2,... . This is an interesting deviation from the case of Dirac delta potentials

with real strengths. For the latter case, we can have at most two bound states; but for imaginary strengths, we can have many bound states by increasing the value of $|\sigma_{1i}|x_1$.

For the general case with $\sigma_{1r} \neq 0$, we perform numerical calculations to obtain number of roots of the Equation (3.56). We investigate the number of roots of the Equation (3.56) in terms of $\beta = \frac{\sigma_{1r}}{|\sigma_1|^2 x_1}$ and $\gamma = |\sigma_1|x_1$. Pure imaginary σ_1 cases suggest that there can be regions of (β, γ) values on ($\beta - \gamma$) plane, which lead to different number of roots of the Equation (3.56). By using β and γ, we plot the results of numerical calculations for regions of 0,1,2,4,6 roots in the Figure 3.11. The regions above $\beta = 1/\gamma$ and below $\beta = -1/\gamma$ curves are not considered since $|\beta \cdot \gamma| = \frac{\sigma_{1r}}{|\sigma_1|} \leq 1$. Moreover, on the curve $\beta \cdot \gamma = 1$, there are two roots and on the $\beta \cdot \gamma = -1$ curve, there is no root. We also analyze the number of roots on the common boundary curves between the regions (See Figure 3.11). For the regions with 0,2,4,... roots, the number of roots on the common boundary of two such regions will be equal to the value with the larger number of roots of these regions. An interesting situation arises for the boundary between the regions of 0,1,2 roots ($\beta = 1$): For $\gamma \leq \frac{\sqrt{2}}{2}$, there is no root and for $\gamma > \frac{\sqrt{2}}{2}$, there is one root. Note that there will be always even number (2n) of roots for $\beta < 1$. For non-positive β values ($\sigma_{1r} \leq 0$), we have already shown analytically that $\mathcal{PT}$-symmetry breaks down and the roots of the Equation (3.56) are always complex conjugate pairs. Moreover, we also proved that for $0 < \beta < 1$ and $\gamma \leq \frac{\sqrt{2}}{2}$, there is no root. The real roots of the Equation (3.56) can be at most 2. For $0 < \beta < 1$ and $\gamma \geq \frac{\sqrt{2}}{2}$, by considering the intersections of the polynomial $|g(\kappa)|$ and the exponential $|h(\kappa)|$ (the Equations (3.71) and (3.72)) for real and positive κ, we find that the Equation (3.56) can not have *only one* real root. Thus, for $\beta < 1$ there are always even number of roots (0,2,...,2n,...).

Finally, we summarize our results on two $\mathcal{PT}$-symmetric Dirac delta functions in Table 3.2.

We also present some numerical solutions of the Equation (3.56), first for purely imaginary and then for complex σ_1 with nonzero real part, in Tables 3.3 and 3.4. For $\sigma_1 = i\sigma_{1i}$ and $x_1 = 1.0$, some of the eigenvalues of the bound states are presented in

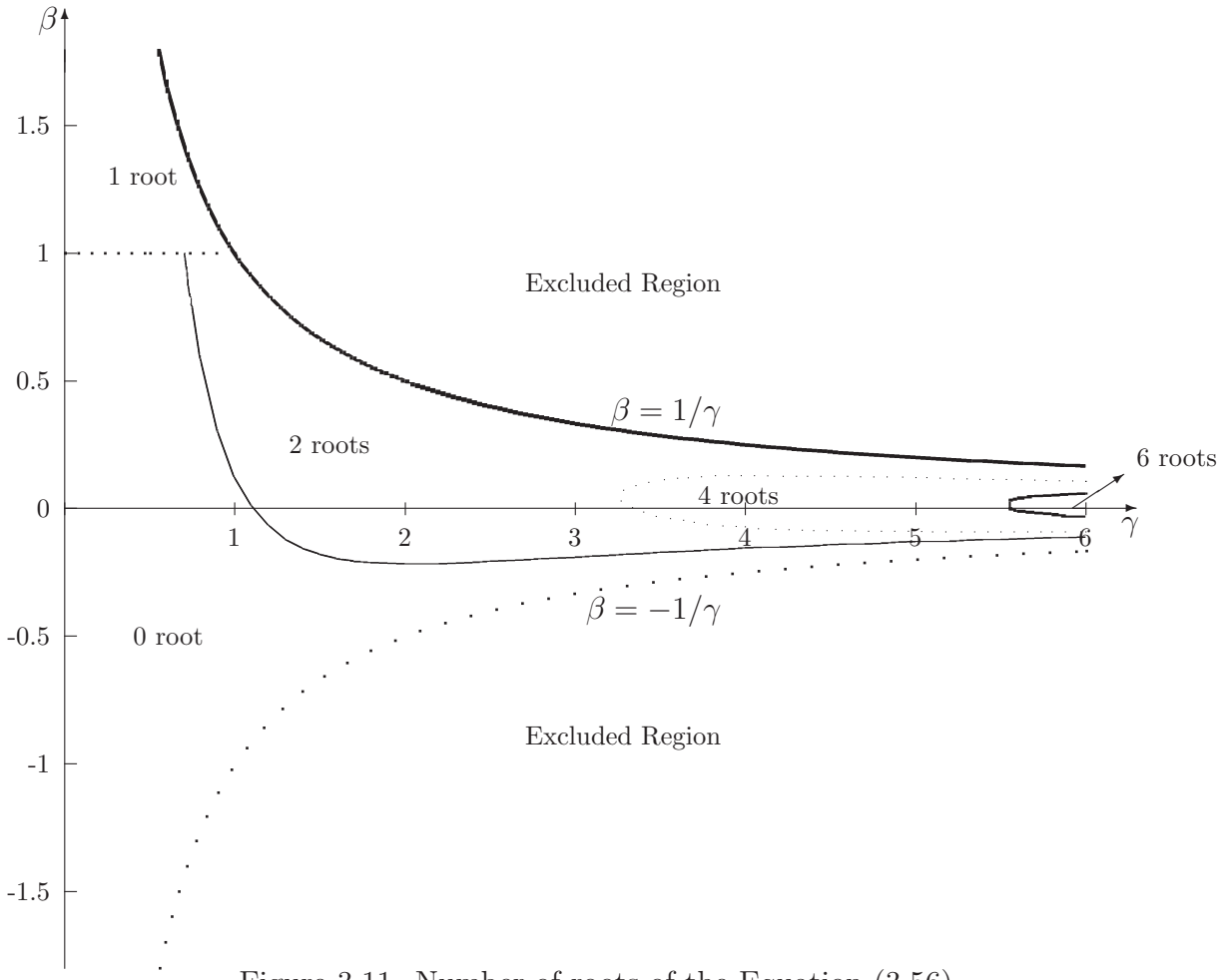

Figure 3.11. Number of roots of the Equation (3.56).

Table 3.2. Number of bound states of two $\mathcal{PT}$-symmetric delta functions.

β	γ	Number of Roots
$\beta > 1$	for all values	One root
$\beta = 1$	$\gamma \leq \frac{\sqrt{2}}{2}$	No root
	$\gamma > \frac{\sqrt{2}}{2}$	One root
$0 < \beta < 1$	$\gamma \leq \frac{\sqrt{2}}{2}$	No root
	$\gamma > \frac{\sqrt{2}}{2}$	2 roots if $\lvert\sigma_{1i}\rvert \leq \sigma_{1r}$
$\beta = 0$	$(2n-1)\frac{\sqrt{2}\pi}{4} < \gamma \leq (2n+1)\frac{\sqrt{2}\pi}{4}$	$2n$ roots $(n = 1, 2, ...)$
	$\gamma \leq \frac{\sqrt{2}\pi}{4}$	No root

Table 3.3. The values of κ for two Dirac delta functions with $\sigma_1 = i\,\sigma_{1i}$ and $x_1 = 1.0$.

σ_1	κ_1	κ_2	κ_3
1.12i	0.0032+ 0.7894	-	-
1.5 i	0.1094+0.9351 i	-	-
2.0 i	0.1964+1.0920 i	-	-
3.0 i	0.2472+1.3420 i	-	-
3.34 i	0.2352+1.4073 i	-	-
4.0 i	0.1880+1.4951 i	0.1584+2.4497 i	-
5.0 i	0.1187+1.5472 i	0.3124+2.6513 i	-
5.6 i	0.3480+2.7793 i	0.0918+1.5576 i	0.0079+3.9290 i

Table 3.3. As we expect from analytical results there are no roots for $\sigma_{1i} \leq 1.11 \approx \frac{\sqrt{2}\pi}{4}$, there are two roots for $\frac{\sqrt{2}\pi}{4} \approx 1.11 < \sigma_{1i} \leq \frac{3\sqrt{2}\pi}{4} \approx 3.33$ and the number of roots increase according to general formula given in the Equation (3.80).

Table 3.4. The values of κ for two Dirac delta functions with $\sigma_1 = 2.0 + \sigma_{1i}$ and $x_1 = 1.0$.

σ_1	κ_1	κ_2
2+0.0 i	1.1089	0.7968
2+0.1 i	1.0992	0.8071
2+0.2 i	1.0652	0.8429
2+0.3 i	0.9556+0.0506 i	0.9556-0.0506 i
2+0.5 i	0.9602+0.2231 i	0.9602-0.2231 i
2+0.7 i	0.9666+0.3452 i	0.9666-0.3452 i
2+1.0 i	0.9783+0.5118 i	0.9783-0.5118 i

Moreover, we obtain numerical values of eigenvalues for $\sigma_1 = 2.0 + i\,0.1\,p$ where $p = 0, 1, ..., 10$ and $x_1 = 1.0$ and present these results in Table 3.4. For $|\sigma_{1i}| \leq \sigma_{1r} = 2.0$ and $x_1 = 1.0$, we expect always two roots since the inequalities $\frac{\sigma_{1r}}{|\sigma_1|^2 x_1} < 1$ and $|\sigma_1| x_1 > \frac{\sqrt{2}}{2}$ are satisfied. The roots are real for $\sigma_{1i} < 0.2$ because $e^{-2\sigma_{1r}x_1} = e^{-2\cdot 2\cdot 1} \approx 0.0183$; $\frac{\sigma_{1i}^2}{|\sigma_1|^2} = 0.01$ for $\sigma_{1i} = 0.2$ and $\frac{\sigma_{1i}^2}{|\sigma_1|^2} = 0.02$ for $\sigma_{1i} = 0.3$.

Therefore, as σ_{1i} increases, beginning at a value between 0.2 and 0.3, $\mathcal{PT}$-symmetry breaks down and the eigenvalues of the bound states are complex numbers. By Rouche's Theorem, the eigenvalues of bound states presented in this Table are the only bound states for the corresponding σ_1 and x_1.

3.4.3. Four $\mathcal{PT}$-Symmetric Dirac Delta Functions

The eigenvalue equation for bound states of a $\mathcal{PT}$-symmetric potential containing four Dirac delta functions are obtained from the Equation (3.54) as

$$\begin{aligned}
&(1-\tfrac{\mathbf{Re}(\sigma_1)}{\kappa}+\tfrac{|\sigma_1|^2}{4\kappa^2}(1-e^{-4\kappa x_1}))(1-\tfrac{\mathbf{Re}(\sigma_2)}{\kappa}+\tfrac{|\sigma_2|^2}{4\kappa^2}(1-e^{-4\kappa x_2}))\\
&+\tfrac{|\sigma_1|^2\,|\sigma_2|^2}{8\kappa^4}e^{-2\kappa x_2}(e^{-2\kappa x_2}\sinh 4\kappa x_1-2\sinh 2\kappa x_1)\\
&+\tfrac{|\sigma_1|^2\,\mathbf{Re}(\sigma_2)}{2\kappa^3}e^{-2\kappa x_2}\sinh 2\kappa x_1+\tfrac{|\sigma_2|^2\mathbf{Re}(\sigma_1)}{2\kappa^3}e^{-2\kappa x_2}(-e^{-2\kappa x_2}+\cosh 2\kappa x_1)\\
&-\tfrac{\mathbf{Re}(\sigma_1)\mathbf{Re}(\sigma_2)}{\kappa^2}e^{2\kappa(x_1-x_2)}+\tfrac{\mathbf{Re}(\sigma_1\sigma_2^*)}{\kappa^2}e^{-2\kappa x_2}\sinh 2\kappa x_1=0\ \ .
\end{aligned}\tag{3.81}$$

The Equation (3.81) is a very complicated equation to obtain the number of bound states and some conditions for real eigenvalues as we did in the case of two Dirac delta functions. Thus, for obtaining some information about the breakdown of $\mathcal{PT}$-symmetry, we solve it numerically for different $\sigma_1=\sigma_{1r}+i\sigma_{1i}$ and $\sigma_2=\sigma_{2r}+i\sigma_{2i}$ values, where σ_1 and σ_2 are the strengths of Dirac delta functions at positions $x_1=1$ and $x_2=2$, respectively.

We present the bound state eigenvalues for purely imaginary σ_1 and $\sigma_2\in\Re$ in Table (3.5). In Section 3, we found that for two $\mathcal{PT}$-symmetric Dirac delta functions with purely imaginary strengths, there are no bound states for $|\sigma_{1i}|<1.11$ and all the eigenvalues are complex. However, we notice that adding two real Dirac delta functions at $x_2=2$ and $x_{-2}=-2$, the system becomes $\mathcal{PT}$-symmetric for small and large σ_2 values when $\sigma_1=0.1\,i$. However, $\mathcal{PT}$-symmetry breaks down for $3.6<\sigma_2<8.0$.

Moreover, we study the case where σ_1 and σ_2 are complex numbers with nonzero real and imaginary parts and present the results in Table (3.6). The system remains $\mathcal{PT}$-symmetric only for small σ_{1i} and σ_{2i} compared to σ_{1r} and σ_{2r}, in these cases.

Table 3.5. The values of κ for four Dirac delta functions with purely imaginary σ_1 and $\sigma_2 \in \Re$.

σ_1	σ_2	κ
0.1 i	0.1	0.0781
0.1 i	1.0	0.5518
0.1 i	2.0	0.9812
0.1 i	4.0	2.0000+0.0006 i
0.1 i	6.0	3.0000+0.0001 i
0.1 i	8.0	4.0000
0.1 i	20.0	10.0000

Table 3.6. The values of κ for four Dirac delta functions with complex σ_1 and σ_2.

σ_1	σ_2	κ_1
1.0+0.1 i	1.0+0.1 i	0.6219
1.0+0.1 i	1.0+0.2 i	0.6557
1.0+0.1 i	1.0+0.3 i	0.7126+0.0593 i
1.0+0.1 i	1.0+0.4 i	0.7105+0.1107 i
1.0+0.1 i	1.0+0.6 i	0.7025+0.1884 i
1.0+0.1 i	1.0+0.8 i	0.6891+0.2579 i
1.0+0.1 i	1.0+1.0 i	0.6700+0.3250 i

3.5. Solution of Schrödinger Equation for $U(x) = ((1/2)m^2\omega^3/\hbar)x^4 - (\hbar^2/2m)\sigma\,\delta(x)$

It is possible to obtain the energy eigenvalues of the ground and some of the low-lying states of non-solvable symmetric potentials by means of numerical methods using the symmetry of the potential. The symmetry condition is needed to guess the derivative of the wave function at some point (see for example Appendix G of Reference [71]). Since it is difficult to guess the value of the derivative of the wave function for a delta decorated potential at some point, the numerical method used in this section

is useful only if a Dirac delta functions is added to the symmetry center. We use an iterative algorithm to find the ground state energy eigenvalue. Therefore, it is useful to obtain a first guess for the energy eigenvalue of a decorated potential by running the program first for $\sigma = 0$. The first guess for the non-decorated case can be found by approximation methods such as WKB method. In other words, one should find the energy eigenvalue for the potential without any Dirac delta potential choosing $\sigma = 0$ at first and then use this energy value as the first guess for the decorated harmonic potential.

We apply the process summarized above for the potential

$$U(x) = \frac{m^2\omega^3}{\hbar}x^4 - \frac{\hbar^2}{2m}\sigma\delta(x) \tag{3.82}$$

The Schrödinger equation for this potential is

$$-\frac{\hbar^2}{2m}\frac{d^2\Psi(x)}{dx^2} + (\frac{1}{2}\frac{m^2\omega^3}{\hbar}x^4 - \frac{\hbar^2}{2m}\sigma\delta(x))\psi\left(x\right) = E\Psi\left(x\right) \ . \tag{3.83}$$

It is useful to write the computer program in terms of dimensionless variables. Therefore, we define the variables $u = \sqrt{\frac{m\omega}{\hbar}}x$, $\epsilon = \frac{E}{\hbar\omega}$ and $\Lambda = \sqrt{\frac{\hbar}{m\omega}}\sigma$. We write the Equation (3.83) in terms of these variables as

$$\frac{d^2\Psi(u)}{du^2} - (u^4 - \Lambda\delta(u) - 2\epsilon)\psi\left(u\right) = 0 \ . \tag{3.84}$$

For $u \neq 0$ the second derivative of $\Psi(u)$ with respect to u is easily calculated from the Equation (3.84),

$$\frac{d^2\Psi(u)}{du^2} - (u^4 - 2\epsilon)\psi\left(u\right) = 0 \ . \tag{3.85}$$

The Dirac delta function cause to a jump in the second derivative of the wave function at $u = 0$, which changes all the values of the wave function and its derivative at other positions.

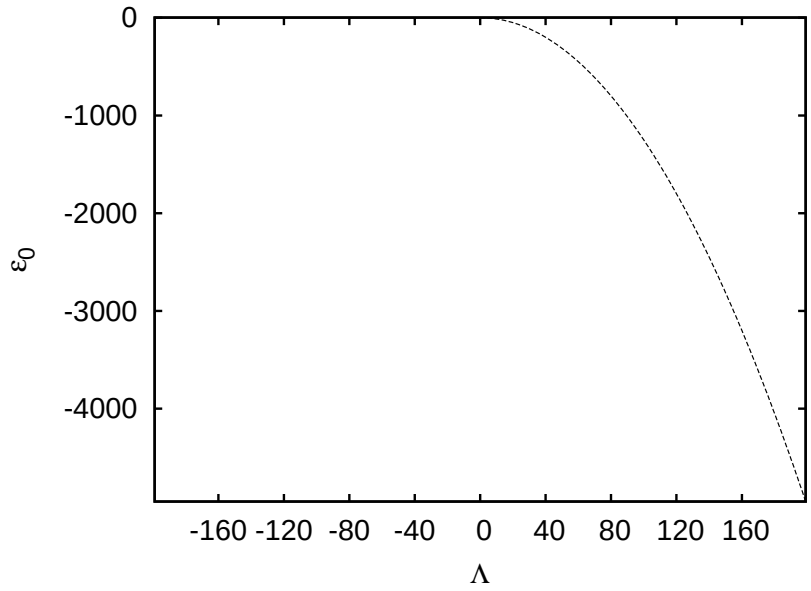

Figure 3.12. The change of the ground state energy with respect to Λ.

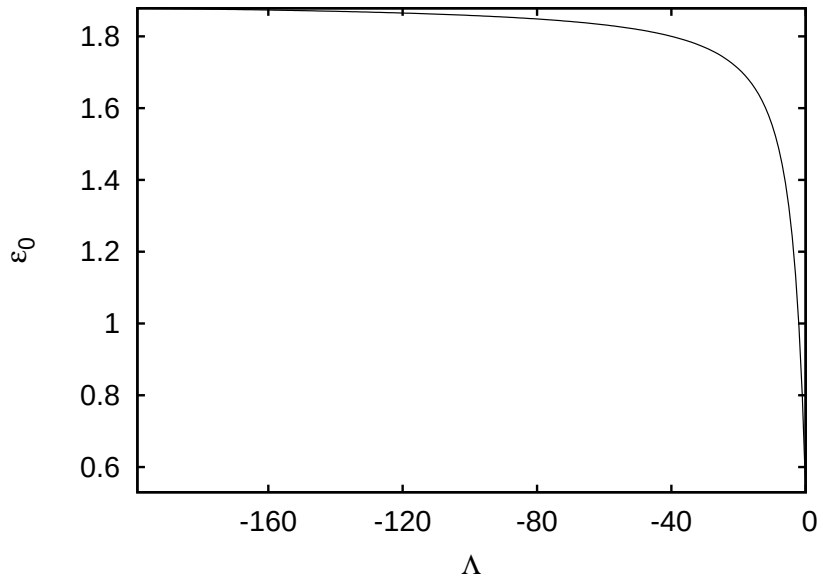

Figure 3.13. The change of the ground state energy with respect to negative Λ.

We show the change of the ground state energy with respect to α in Figure 3.12. The ground state decreases for positive α without a limit. However, the first excited state of the potential $V(x) = ((1/2)m^2\omega^3/\hbar)x^4$ limits the increase of the energy value for negative Λ. Since it is difficult to observe the increase of energy for negative Λ we enlarge this part of the Figure 3.12 in Figure 3.13.

We compare the normalized wave functions of the ground states for $\Lambda = 0, 1$ and 2 in Figure 3.14. In this figure, the solid dashed and dotted curves show the wave functions for $\Lambda = 0, 1$ and 2, respectively.

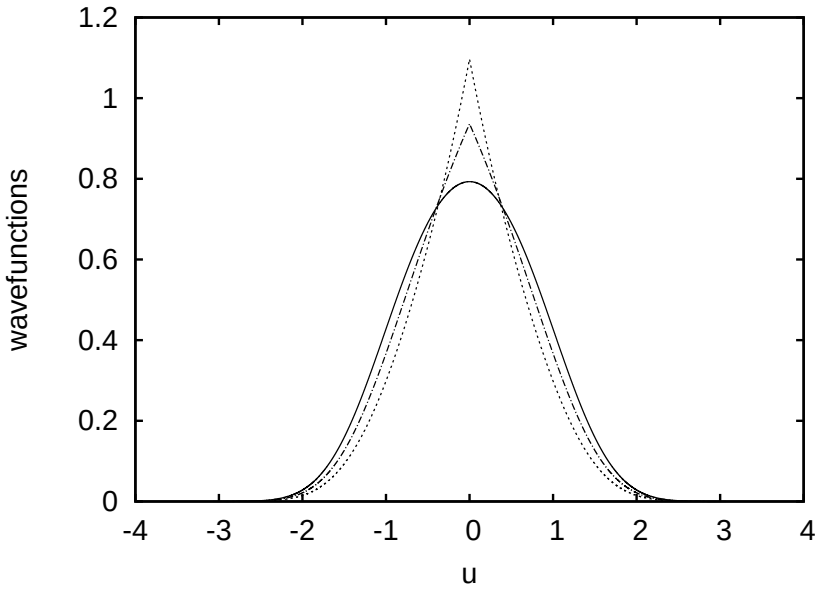

Figure 3.14. The wave functions of the ground states with respect to u, for $\Lambda = 0, 1$ and 2.

In Appendix A, we present the fortran program we used to draw the graphics of the wave functions. In this program we use the Runge-Kutta method to calculate the second derivatives. The algorithm can be used to solve any symmetric potential with a Dirac delta potential at the symmetry center or for potentials with Dirac delta potentials are distributed symmetrically around the symmetry center of the potential.

4. SPECIFIC POTENTIALS WITH DIRAC DELTA FUNCTIONS FOR n-DIMENSIONAL SYSTEMS

This chapter is a brief review of References [22] and [23] and written to give some examples about the Dirac delta decorated potentials for n dimensional case.

4.1. Constant Potential with a Finite Number of Dirac Delta Shells

The constant potential ($V(r) = 0$) with a finite number of the Dirac delta functions

$$U(r) = -\frac{\hbar^2}{2m}\sum_{i=1}^{P}\sigma_i\delta(r - r_i)\ . \tag{4.1}$$

In terms of the dimensionless variable $v = k\,r$, this potential can be written as:

$$U(v) = -\frac{\hbar^2}{2m}\sum_{i=1}^{P}\frac{\sigma_i}{k}\delta(v - v_i) \tag{4.2}$$

Substituting $U(v)$ to the Equation (2.33), one gets

$$\left(\frac{d^2}{dv^2} + -\frac{\left(l+\frac{n}{2}-\frac{1}{2}\right)\left(l+\frac{n}{2}-\frac{3}{2}\right)}{v^2} + \sum_{i=1}^{P}\frac{\sigma_i}{k}\delta(v - v_i) - 1\right) f_{n,l}(v) = 0\ . \tag{4.3}$$

The Equation (4.3) reduces to

$$\left(\frac{d^2}{dv^2} - \frac{\left(l+\frac{n}{2}-\frac{1}{2}\right)\left(l+\frac{n}{2}-\frac{3}{2}\right)}{v^2} - 1\right) f_{n,l}(v) = 0\ . \tag{4.4}$$

for $v \neq v_i$. Defining

$$f_{n,l}(v) = v^{1/2}\Phi_{n,l}(v)\ , \tag{4.5}$$

the Equation (4.4) becomes

$$\left(\frac{d^2}{dv^2}+\frac{1}{v}\frac{d}{dv}-\frac{\left(l+\frac{n}{2}-1\right)^2}{v^2}-1\right)\Phi_{n,l}(v)=0\ . \tag{4.6}$$

This equation is the Bessel's equation and has two linearly independent solutions. The solutions of the Bessel's equation that satisfy the boundary conditions at $v\to 0$ and at $v\to\infty$ are $I_{l+\frac{n-2}{2}}$ and $K_{l+\frac{n-2}{2}}$, respectively. $I_{l+\frac{n-2}{2}}\to\infty$ as $v\to\infty$ and $K_{l+\frac{n-2}{2}}$ as $v\to 0$. So the functions for the regions separated by Dirac delta shells can be written as:

$$\begin{aligned}
\Phi_{1_{n,l}}(v) &= b_1 I_{l+\frac{n-2}{2}}(v) \\
\Phi_{1_{n,l}}(v) &= b_i I_{l+\frac{n-2}{2}}(v)+a_i K_{l+\frac{n-2}{2}}(v) &(4.7)\\
\Phi_{P+1_{n,l}}(v) &= a_{P+1} K_{l+\frac{n-2}{2}}(v)\ . &(4.8)
\end{aligned}$$

where $i=2,3,...P$. Applying the method developed in Section 2.2 to find the transfer matrix $\mathbb{M}_i(k)$ one gets

$$\mathbb{M}_i(k)=\begin{bmatrix} 1+\frac{\sigma_i v_i I_{l+\frac{n-2}{2}}(v_i)K_{l+\frac{n-2}{2}}(v_i)}{k} & \frac{\sigma_i v_i (I_{l+\frac{n-2}{2}}(v_i))^2}{k} \\ -\frac{\sigma_i v_i (K_{l+\frac{n-2}{2}}(v_i))^2}{k} & 1-\frac{\sigma_i v_i I_{l+\frac{n-2}{2}}(v_i)K_{l+\frac{n-2}{2}}(v_i)}{k} \end{bmatrix} \tag{4.9}$$

The total transfer matrix is defined as usual

$$\mathbb{X}(k)=\mathbb{M}_P(k)\ldots\mathbb{M}_1(k) \tag{4.10}$$

and the equation $x_{22}(k)=0$ gives the energy spectrum of the potential. For one Dirac delta shell the energy eigenvalue equation is

$$k=\sigma_i v_i I_{l+\frac{n-2}{2}}(v_i)K_{l+\frac{n-2}{2}}(v_i)\ . \tag{4.11}$$

Finally, we state the theorem we have used to prove Theorem 1 in Section 2.3 [22].

THEOREM 2: *There exists at most P bound state energy levels of the Schrödinger equation for the potential* $V(r) = \sum_i^P \sigma_i \delta(r - r_i)$.

4.2. Decoration of Harmonic Potential

The harmonic potential decorated with P Dirac delta functions in $\mathbb{R}^n$ is given as:

$$U(r) = \frac{1}{2} m\omega^2 r^2 - \frac{\hbar^2}{2m} \sum_{i=1}^{P} \sigma_i \delta(r - r_i) \tag{4.12}$$

where r is defined in the Equation (2.26) for $\mathbb{R}^n$, $\omega > 0$, $0 < r_1 < \ldots < r_P$ and σ_is are arbitrary real numbers [23]. Since this potential is a central potential, one can use the Equation (2.32) to obtain a differential equation whose solution gives the radial part of the wave function for the potential given in the Equation(4.12),

$$\left(\frac{d^2}{dr^2} - \frac{\left(l + \frac{n}{2} - \frac{1}{2}\right)\left(l + \frac{n}{2} - \frac{3}{2}\right)}{r^2} - \frac{m^2\omega^2}{\hbar^2} r^2 + \sum_{i=1}^{P} \sigma_i \delta(r - r_i) - k^2 \right) f_{n,l}(r) = 0 \ . \tag{4.13}$$

where $f_{n,l}(r)$ is defined in the Equation (2.31). For this potential it is appropriate to use the dimensionless parameter $v = \sqrt{\frac{2m\omega}{\hbar}} r$, and which gives a natural unit length for this potential. Moreover, another dimensionless parameter Ω can be defined as

$$k^2 = -\frac{2m}{\hbar^2} (\Omega + \frac{n}{2})\, \hbar\omega \ . \tag{4.14}$$

for calculational convenience. In terms of the dimensionless variables Ω and v the Equation (4.13) reads,

$$\left(\frac{d^2}{dv^2} - \frac{\left(l + \frac{n}{2} - \frac{1}{2}\right)\left(l + \frac{n}{2} - \frac{3}{2}\right)}{v^2} - v^2 + \sqrt{\frac{\hbar}{2m\omega}} \sum_{i=1}^{P} \sigma_i \delta(v - v_i) + \Omega + \frac{n}{2} \right) f_{n,l}(v) = 0 \ , \tag{4.15}$$

where $v_i = \sqrt{\frac{2m\omega}{\hbar}} r_i$. For $v \neq v_i$ the Equation (4.15) reduces to

$$\left(\frac{d^2}{dv^2} - \frac{\left(l + \frac{n}{2} - \frac{1}{2}\right)\left(l + \frac{n}{2} - \frac{3}{2}\right)}{v^2} - v^2 + \Omega + \frac{n}{2} \right) f_{n,l}(v) = 0 \ . \tag{4.16}$$

Two linearly independent solutions of this differential equation in terms of the radial part of the wave function $R_{n,l}(v) = (\sqrt{\frac{\hbar}{2m\omega}}v)^{\frac{1-n}{2}} f_{n,l}(v)$ are

$$\begin{aligned} R_{I;n,l}(v) &= e^{-\frac{v^2}{4}}\, v^{2-l-n}\, {}_1F_1\left(1 - \frac{l+\Omega+n}{2}, 2-l-\frac{n}{2}; \frac{v^2}{2}\right) \\ R_{II;n,l}(v) &= e^{-\frac{v^2}{4}}\, v^{l}\, {}_1F_1\left(\frac{l-\Omega}{2}, l+\frac{n}{2}, \frac{v^2}{2}\right) . \end{aligned} \tag{4.17}$$

where ${}_1F_1(\alpha, \beta; y)$ denotes the confluent hypergeometric functions (See e.g. [58] pp.155). The solutions $R_{I;n,l}$ and $R_{II;n,l}$ are radial solutions of the Schrödinger equation and obtained as follows. The differential equation (4.16) has two regular singular points at $v = 0$ and $v = \infty$. The differential equation

$$\left(\frac{d^2}{dx^2} - (\frac{\beta}{x} - 1)\frac{d}{dx} - \frac{\alpha}{x}\right) {}_1F_1(\alpha, \beta; x) = 0 \tag{4.18}$$

whose solutions are the confluent hypergeometric functions ${}_1F_1(\alpha, \beta; y)$ has also two regular singular points at $v = 0$ and $v = \infty$. This suggests to search a solution of the Equation (4.16) in terms of confluent hypergeometric functions. We first transform the differential equation (4.18) into its invariant form. Any differential equation of the form

$$\left(\frac{d^2}{dx^2} - f_1(x)\frac{d}{dx} - f_0(x)\right) u(x) = 0 \tag{4.19}$$

can be put into the standard form by applying the transformation $e^{\frac{1}{2}\int f_1(x)dx} y(x)$ to the dependent variable $y(x)$ (See pp. 147 of [58]). In the Equation (4.18) $f_1(x) = -(\frac{\beta}{x} - 1)$ and applying the transformation $e^{\frac{1}{2}\int f_1(x)dx}\, {}_1F_1(\alpha, \beta; x)$ we get

$$\left(\frac{d^2}{dx^2} - (\frac{2\beta - \beta^2}{4x^2})\frac{d}{dx} - \frac{\beta - 2\alpha}{2x} - \frac{1}{4}\right) e^{-\frac{x}{2}} x^{\frac{\gamma}{2}}\, {}_1F_1(\alpha, \beta; x) = 0 . \tag{4.20}$$

Now, we change our independent variable to v where we assume $x \equiv x(v)$. Then, we write the Equation (4.20) in terms of v,

$$\left(\frac{d^2}{dv^2} - \left(\frac{\frac{d^2x}{dv^2}}{\frac{dx}{dv}} \right) \frac{d}{dv} - (\frac{2\beta - \beta^2}{4x^2} + \frac{\beta - 2\alpha}{2x} - \frac{1}{4})(\frac{dx}{dv})^2 \right) e^{-\frac{x}{2}} x^{\frac{\gamma}{2}} \, {}_1F_1(\alpha, \beta; x) = 0 \, . \tag{4.21}$$

Finally, we transform this equation to the invariant form:

$$\left(\frac{d^2}{dv^2} + \frac{\frac{d^3x}{dv^3}}{2\frac{dx}{dv}} - \frac{3}{4} \left(\frac{\frac{d^2x}{dv^2}}{\frac{dx}{dv}} \right)^2 + \left(\frac{2\beta - \beta^2}{4x^2} + \frac{\beta - 2\alpha}{2x} - \frac{1}{4} \right) (\frac{dx}{dv})^2 \right) e^{-\frac{x}{2}} \left(\frac{x^{\frac{\gamma}{2}}}{\frac{dx}{dv}} \right) \, {}_1F_1(\alpha, \beta; x) = 0 \, . \tag{4.22}$$

Comparing Equations (4.16) and (4.22), we find that the Equation (4.22) reduce to the Equation (4.16) if

$$x = \frac{v^2}{2}, \quad (\beta - \frac{3}{2})(\beta - \frac{1}{2}) = (l + \frac{n}{2} - \frac{3}{2})(l + \frac{n}{2} - \frac{1}{2}), \quad \beta - 2\alpha = \Omega + \frac{n}{2} \, . \tag{4.23}$$

The equation for β is satisfied for two β values: $\beta_1 = l + \frac{n}{2}$ and $\beta_2 = 2 - l - \frac{n}{2}$. Thus, we obtain two possible α values $\alpha_1 = \frac{l-\Omega}{2}$ and $\alpha_2 = 1 - \frac{l+n+\Omega}{2}$. Substituting these two different β and corresponding α values to the expression $e^{-\frac{x}{2}} \left(\frac{x^{\frac{\gamma}{2}}}{\frac{dx}{dv}} \right) \, {}_1F_1(\alpha, \beta; x)$ we find the solutions given in the Equation (4.17).

The function $R_{II;n,l}(v)$ goes to zero as $v \to \infty$. Therefore, the wave function satisfying the boundary condition as $r \to \infty$ can be chosen as

$$R_A(v) = R_{II;n,l}(v) \, . \tag{4.24}$$

The wave function which satisfies the boundary condition $r = 0$ can be defined as the linear combination of $R_{I;n,l}(v)$ and $R_{I;n,l}(v)$.

$$R_B(v) = (R_{I;n,l}(v) - \lambda_a \, R_{II;n,l}(v)) \tag{4.25}$$

where $\lambda_a = \frac{R_{I;n,l}(0)}{R_{II;n,l}(0))}$. Therefore, the wave functions of the innermost, i^{th} and outermost regions are

$$\begin{aligned} R_{1;n,l}(v) &= b_1\, R_B(v) \\ R_{i;n,l}(v) &= b_i\, R_B(v) + a_i\, R_A(v) \\ R_{P+1;n,l}(v) &= a_{P+1}\, R_A(v)\ , \end{aligned} \tag{4.26}$$

respectively. Using $f_A(v) = (\sqrt{\frac{\hbar}{2m\omega}}v)^{\frac{n-1}{2}}\ R_A(v)$ and $f_B(v) = (\sqrt{\frac{\hbar}{2m\omega}}v)^{\frac{n-1}{2}}\ R_B(v)$ the transfer matrix can be found by Equation (2.40) as:

$$\mathbb{M}_i(\Omega) = \begin{bmatrix} 1 + \frac{\sigma_i f_A(v) f_B(v)}{W_{AB}} & \frac{\sigma_i f_B^2(v)}{W_{AB}} \\ -\frac{\sigma_i f_A^2(v)}{W_{AB}} & 1 - \frac{\sigma_i f_A(v) f_B(v)}{W_{AB}} \end{bmatrix}\ , \tag{4.27}$$

where W_{AB} is the Wronskian of the functions $f_A(v)$ and $f_B(v)$ which is equal to $\lambda_a(1 - l - n/2)$. The total transfer matrix is the multiplication of all transfer matrices:

$$\mathbb{X}(k) = \mathbb{M}_P(k) \ldots \mathbb{M}_1(k)\ . \tag{4.28}$$

The energy eigenvalues are found by $x_{22}(k) = 0$.

The harmonic oscillator potential satisfies the conditions for the potentials given in Theorem 1 in Section 2.3 with $\lambda = \omega$ and $d = 2$. Therefore, the harmonic potential with P Dirac delta functions can have at most P bound states with negative energy eigenvalues where P is finite.

5. APPLICATIONS

5.1. Charmonium

In high energy physics, a quarkonium is a flavorless meson constituted by the association of a quark and its own antiquark. Charmonium is an example of a quarkonium with charmed quark (c) and its antiquark ($\overline{c}$). It is possible to apply linear potential with one Dirac delta functions to the charmonium problem to demonstrate how this potential may be employed to describe physical systems with point interactions. Greiner et al [48] used the first two experimental masses to fit the unknown parameters of the linear potential (f and m_c, mass of the charmed quark) and predicted the effective masses of s states for n=3, 4 levels. By including a very short range interaction which may be modelled by means of a Dirac delta function in addition to the linear potential, we predict effective masses, $2m_c + E_i$ (i^{th} bound state energy) of the charmonium system (Here we use natural units $\hbar = 1,\ c = 1$). In this case, we fit four parameters (m_c, f, σ_1, x_1) to the experimental data (only known lowest four levels) considering also the relativistic mass corrections and get optimum values of m_c, f, σ_1, x_1 as

$$m_c = 1.172\,GeV,\ f = (0.453)^2\,GeV^2,\ \sigma_1 = -0.433\,GeV,\ x_1 = 5.128\left(\frac{1}{GeV}\right),$$

in natural units (Here the reduced mass of the charmonium is $\frac{m_c}{2} = m$) [66]. These values represent a linear potential with a repulsive Dirac delta function at x_1. We obtain M^n_{rel} which contains the relativistic corrections due to the term $\left(\frac{p^4}{8m^3c^2}\right)$ and present it in the sixth column of Table 5.1. The masses without relativistic correction is given in the fourth column, $M^n_{non-rel}\,(opt)$. Comparison of these two columns exhibits the effect of the relativistic mass correction. As expected, these relativistic mass corrections increase from $0.028\,GeV$ to $0.705\,GeV$ when n increases from n=1 to n=10. These predictions of M^n_{rel} for $n = 5 - 10$ are yet to be tested by experimentalists.

In Table 5.1, $M^n\,(LP)$ shows the mass spectrum for the linear potential with the

Table 5.1. Masses, M^n, of s states of charmonium in unit of GeV.

n	$M^n(LP)$	$M^n(DDLP)$	$M^n_{non-rel}\,(opt)$	$M^n_{rel}(LP)$	$M^n_{rel}\,(opt)$	M_{exp}
1	3.097	3.106	3.124	3.070	3.096	3.097
2	3.686	3.775	3.780	3.604	3.695	3.686
3	4.168	4.168	4.165	4.019	4.031	4.040
4	4.595	4.624	4.615	4.368	4.447	4.415
5	4.983	5.081	5.001	4.674	4.714	-
6	5.347	5.362	5.332	4.948	4.922	-
7	5.689	5.690	5.656	5.195	5.202	-
8	6.016	6.019	6.981	5.421	5.483	-
9	6.328	6.339	6.297	5.629	5.715	-
10	6.628	6.646	6.597	5.841	5.892	-

parameters of [48], $m_c = 1.155\,GeV$ $f = (0.458)^2\,GeV^2$. The masses $M^n\,(DDLP)$ are for the Dirac delta decorated potential with $m_c = 1.155\,GeV$, $f = (0.458)^2\,GeV^2$, $\sigma_1 = -0.433\,GeV$, $x_1 = 5.128\left(\frac{1}{GeV}\right)$ so that we can determine the effect of a Dirac delta function on the mass spectrum since same m_c and f (parameters of [48]) are used for these calculations. Finally, we added relativistic mass corrections to the results of $M^n(LP)$ and obtain the column 5 of Table (5.1) to make a comparison of $M^n_{rel}(LP)$, $M^n_{rel}(opt)$ and experimental results M_{exp}. This comparison shows that Dirac delta decorated linear potential can give a good description of experimental mass spectrum.

5.2. Triangular Quantum Well Structure with Impurities

The linear potential can be used to describe the motion of a charged particle in a constant electric field. If there are impurities in the medium of the motion, this impurities can be modelled by Dirac delta potentials. In order to show how the energy levels of a charged particle change in case of one impurity located at $x_1 = l$ [7] , in Table 5.2, we have investigated the change in the bound state energy levels where one Dirac delta function is added to the linear potential. We have exhibited E_n in units of $\frac{\hbar^2}{2ml^2}$

[7] Here we use the l value defined in Equation (3.13)

for attractive ($\sigma l = 2$) and repulsive ($\sigma l = -2$) cases. The change in the ground state energy is the largest. As we have discussed above, this is due to the value of $|\Psi_n|^2$ at the position of Dirac function, $x_1 = l$.

Table 5.2. The energies E_n for the low-lying bound states with linear potential and linear potential decorated with one Dirac delta function.

n	E(DDLP)		E(LP)
	$\sigma l = 2$	$\sigma l = -2$	
1	0.568	2.923	2.338
2	3.717	4.554	4.088
3	5.347	5.829	5.521
4	6.704	6.941	6.787
5	7.909	8.000	7.944
6	9.012	9.036	9.023
7	10.040	10.041	10.040
8	11.007	11.01	11.009
9	11.925	11945	11.936
10	12.803	12.847	12.829

We also investigated the change in ground state energy for 8 Dirac delta functions at random locations between 0 and 10 l. By using the given electric field $E_s = 7.5\,10^4 V/cm$ and the effective mass of an electron $m^* = 0.067\,m_0$ for GaAs/GaAlAs heterostructure [67, 68], we estimate the parameter l given in the Equation (3.13) as $42\,A^\circ$. This result shows that there exists, on the average, one impurity per $50\,A^\circ$ along the one-dimensional wire, which is a realistic choice. We have studied four cases:

a) **Attractive impurities**: All the Dirac delta functions are attractive with strengths $\sigma_i l = 2$,

b) **Repulsive impurities**: All the Dirac delta functions are repulsive with strengths $\sigma_i l = -2$,

c) **Mixed aR-Type impurities**: The strengths of the Dirac delta functions are

also determined randomly, and it can be either $\sigma_i l = 1$ or $\sigma_i l = -2$,

d) **Mixed Ar-Type impurities**: Same as in part c) but randomly chosen strengths are with $\sigma_i l = 2$ or $\sigma_i l = -1$.

Case a) and b) represent the model of one type (attractive or repulsive) of impurities in a system. Case c) and d) are for the models of different type impurities in a system. For case c), repulsive impurities have the strengths twice the strength of attractive ones. For case d), it is the opposite. By performing these calculations, we have investigated the effects of locations, types and strengths of impurities on the ground state energy. We have done 1000 calculations for each cases. The number of ground states vs. ground state energy E_g in units of $\frac{\hbar^2}{2ml^2}$ are plotted in figures (5.1- 5.4) for cases a) - d). The intervals are chosen 0.1 unit on the x-axis to obtain box diagrams. Since the locations are chosen randomly, E_g can have values in a wide range of energies. For these 1000 calculations, average (E_{av}) and the maximally occurred energy (E_{peak}) are obtained and shown in Table 5.3. Comparisons of ground state energy $E_g = 2.338$ of linear potential with E_{av} values for these four cases again demonstrate that the attractive interactions are more effective than repulsive interactions.

Table 5.3. Energies for attractive and repulsive Dirac delta functions at random locations.

	Attractive $\sigma l = 2$	Repulsive $\sigma l = -2$	Attractive($\sigma l = 1$) Repulsive($\sigma l = -2$)	Attractive($\sigma l = 2$) Repulsive($\sigma l = -1$)
E_{peak}	-0.4	3.4	2.3	0.9
E_{av}	-1.061	3.322	1.886	1.095

Triangular quantum well structures have been studied to explain the electronic properties of semiconductor heterostructures. For GaAs/GaAlAs semiconductor, charge transfers create an electric field at the junction of GaAs and GaAlAs. This electric field can be approximately taken as constant [67]. Thus, we obtain a linear potential due to this constant electric field. If there exist impurities in this system, then the effect of impurities should be added to this linear potential. It is possible to investigate these effects by using Dirac delta functions which can model very short-range impurity

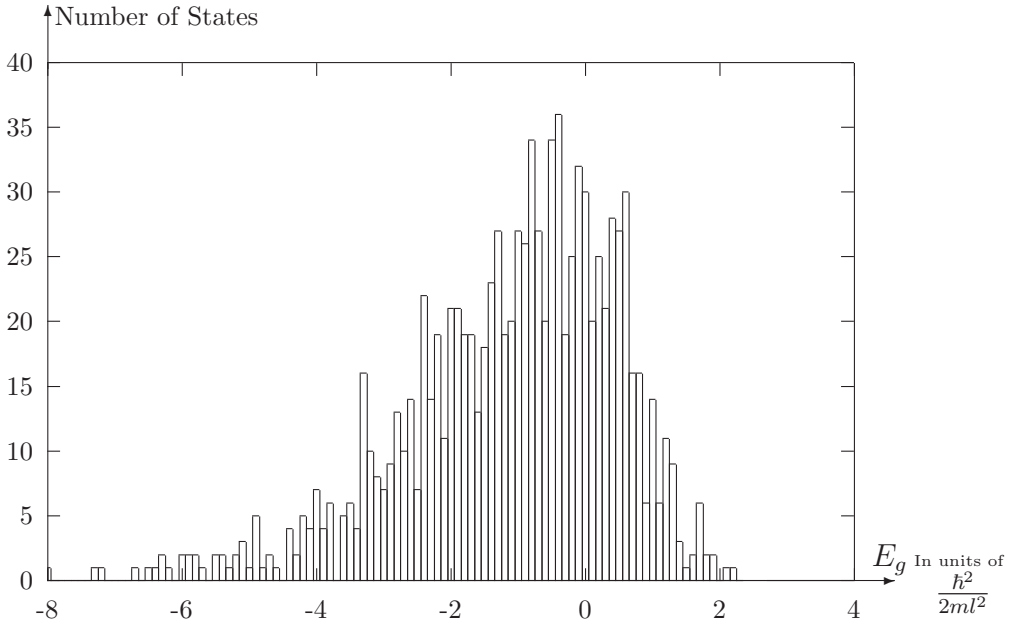

Figure 5.1. Number of states in an interval (0.1 unit) (box diagram) vs. E_g for $\sigma_{att}l = 2$.

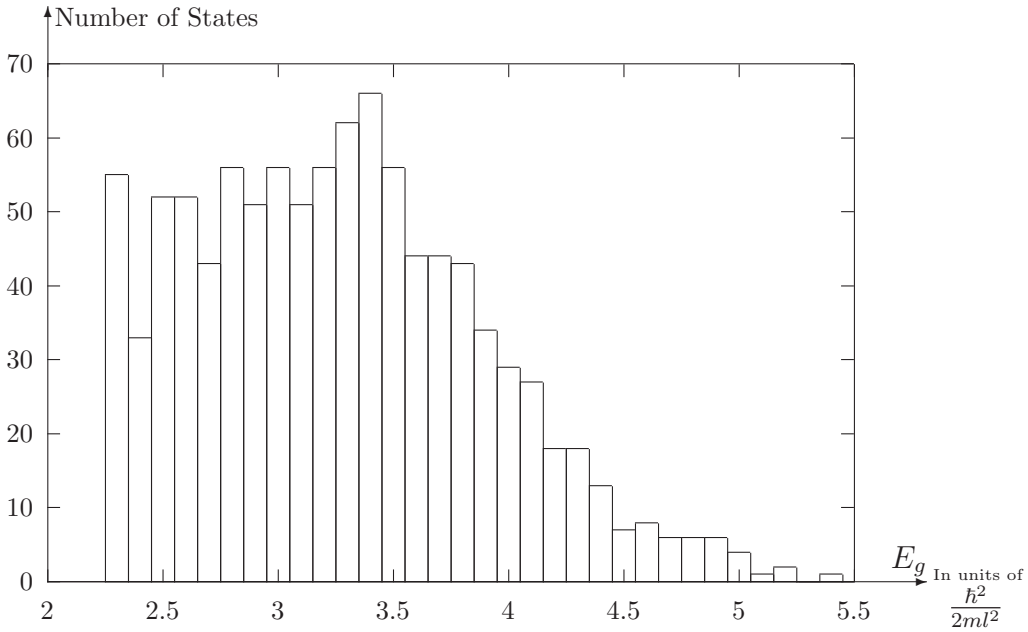

Figure 5.2. Number of states in an interval (0.1 unit) (box diagram) vs. E_g for $\sigma_{rep}l = -2$.

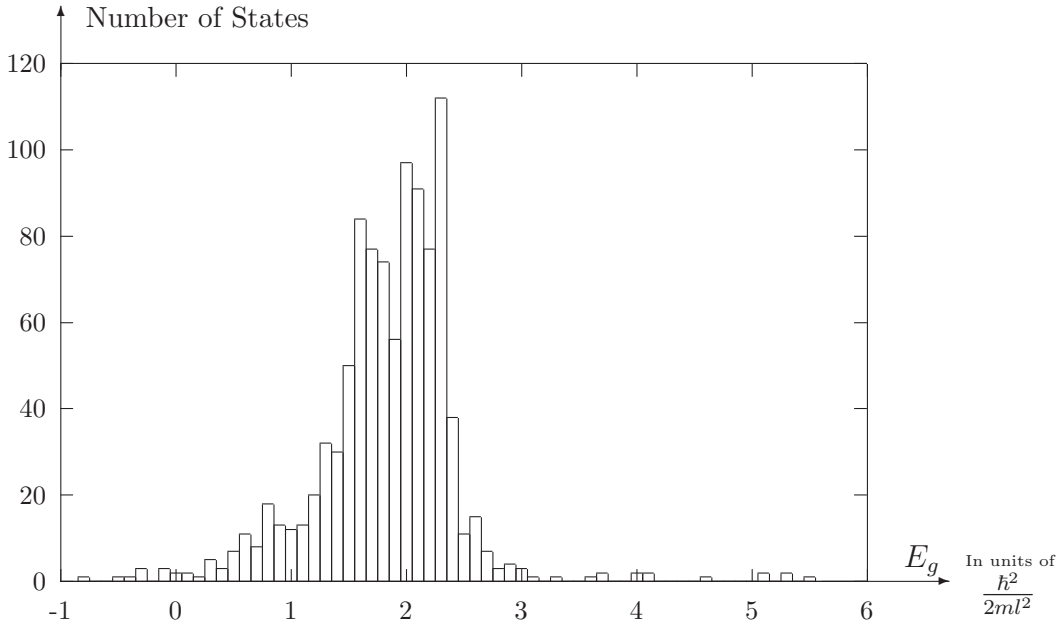

Figure 5.3. Number of states in an interval (0.1 unit) (box diagram) vs. E_g for $\sigma_{att}l = 1$, $\sigma_{rep}l = -2$.

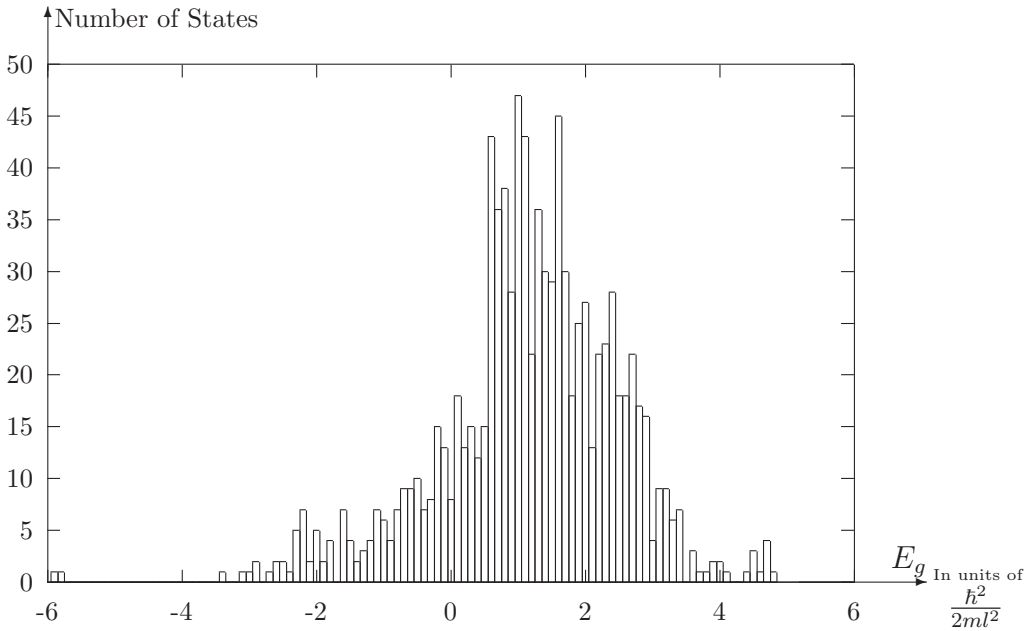

Figure 5.4. Number of states in an interval (0.1 unit) (box diagram) vs. E_g for $\sigma_{att}l = 2$, $\sigma_{rep}l = -1$.

potentials. As we mention above this one-dimensional model can be used to describe the bound state energy levels of a charged particle which moves in a constant electric field ($\overrightarrow{E} = -E_0\hat{x}$) on the positive half-line with impurities at $x = x_i$ and impenetrable boundary at x=0. The linear potential due to the constant electric field will shift the Fermi level of this heterostructure by the amount of the ground state energy of the linear potential [67]. Thus, the ground state energy for the linear potential and hence the Fermi energy of the system change by adding impurities. By using the calculated $l = 42\,A^\circ$ for GaAs/GaAlAs and Dirac delta interaction with the strength $\sigma_1 = \frac{2}{42}\frac{1}{A^\circ}$ ($\sigma_1 = -\frac{2}{42}\frac{1}{A^\circ}$), we find that Fermi energy lowers $57\,meV$ (rises $19\,meV$) for attractive (repulsive) Dirac delta function located at $x_1 = l$ (See Table 5.2). Fermi energy of a triangular well without an impurity depends on the number of charge carriers per area n_s and for a typical value $n_s = 5\ 10^{11}$ cm^{-2} [67], this energy is $93\,meV$. These values show even one impurity may have very substantial effect on the Fermi energy of the system.

5.3. Dimple Potentials for Bose-Einstein Condensation

Bose-Einstein condensation was perhaps one of the last major discoveries of Einstein [69, 70]. Einstein showed that "from a certain temperature on, the molecules condense without attractive forces ... " [49] and discovered the Bose-Einstein condensation in 1925. This theoretical prediction motivated the experimental studies for realizations of Bose-Einstein condensates of gases. Seventy years after the prediction of Einstein, Bose-Einstein condensates of dilute gases have been observed at very low temperatures by using ingenious experimental designs [50, 51, 52].

Bosons are particles with integer spin. The wave function for a system of identical bosons is symmetric under interchange of any two particles. As a result of this, bosons may occupy the same single-particle state. The general form of the Bose distribution which gives the mean occupation number of particles in a state ν is (See e.g. [71] pp.

399)

$$n(\varepsilon_\nu) = \frac{1}{e^{\beta(\varepsilon_\nu - \mu)} - 1} \ , \tag{5.1}$$

where ε_ν is the energy of the state ν, $\beta = 1/(k_B T)$, μ is the chemical potential and k_B is the Boltzmann constant. Since $n(\varepsilon_\nu)$ should be positive for all energy values, the chemical potential is less than ground state energy value ε_0. The total number of particles $\mathcal{N}$ is fixed in equilibrium for a given temperature. Therefore, the value of the chemical potential can be found by means of the formula:

$$N = \sum_\nu \frac{1}{e^{\beta(\varepsilon_\nu - \mu)} - 1} \ , \tag{5.2}$$

at a certain T. For high temperatures, temperatures such that $k_B T$ is large compared to the energy difference between successive states, the occupation number is very low $\frac{n(\varepsilon_\nu)}{\mathcal{N}} \ll 1$ for all states (and classical statistical mechanics can be applied to a Bose gas). However, as $T \to 0$ the chemical potential approximates to ground state and most of the particles occupy the ground state energy level. This phenomenon is called Bose-Einstein condensation.

The investigation of non-interacting Bose gas in a box reveals the ideas in the previous paragraph more clearly. The energy levels of a single particle state in a box of side a can easily be calculated as:

$$\varepsilon = \frac{\hbar^2}{8ma^2}(n_x^2 + n_y^2 + n_z^2) \ , \tag{5.3}$$

where $n_x, n_y, n_z = 1, 2, ...$ The sum in the Equation (5.2) can be approximated by an integral using the density of state approach. For non-interacting particles in a cube the number of states for ε and $\varepsilon + d\varepsilon$ is given as (See e.g. chapter 2 in [72]):

$$N(\varepsilon)d\varepsilon = \frac{4\pi V}{\hbar^3}(2m^3)^{1/2}\varepsilon^{1/2}d\varepsilon \ . \tag{5.4}$$

Using this expression for the number of states, the sum in the Equation (5.2) can be converted to an integral and the expression for the total number of particles becomes

$$N = \frac{4\pi V}{h^3}(2m^3)^{1/2}\int_0^\infty \frac{\varepsilon^{1/2}}{e^{\beta(\varepsilon_\nu-\mu)}-1}d\varepsilon \tag{5.5}$$

where V is the volume of the box. Calculating the integral, the Equation (5.5) becomes

$$\frac{N}{V} = \frac{(2\pi m k_b T)^{2/3}}{h^3}e^{\beta\mu}\left(1+\frac{1}{2^{3/2}}e^{\beta\mu}+\frac{1}{3^{3/2}}e^{2\beta\mu}+\ldots\right). \tag{5.6}$$

For large mass m and high temperature T, $e^{\beta\mu}$ must be very small since N is fixed.[8] However, as temperature decreases μ approaches to zero (or to the ground state for the general case) and the particles begin to condense in the ground state because as μ approaches to the ground state $\mu \to \varepsilon_0$ the number of particles in the ground state given by expression

$$n(\varepsilon_0) = \frac{1}{e^{\beta(\varepsilon_0-\mu)}-1} \tag{5.7}$$

grows very rapidly.

Experimentally available condensates are systems with finite number of atoms N, confined in spatially inhomogeneous trapping potentials. Their understanding requires theories that go beyond the usual treatments based upon London's continuous spectrum approximation [73] or the thermodynamic limit $N \to \infty$. Such studies [74, 75] reveal that BEC can occur in harmonically trapped lower-dimensional systems for finite N despite the enhanced importance of phase fluctuations [76]. Quasicondensates with large phase fluctuations may still occur [77]. This is in contrast to standard results [78], in agreement with the Mermin-Wagner-Hohenberg theorem [79, 80] in the thermodynamic limit. Bose-Einstein condensation in one-dimension with a harmonic trap is attractive due to enhanced critical temperature and condensate fraction [74, 75]. Recently, one and two dimensional BECs have been created in experiments [81]. One dimensional condensates were also generated on a microchip [82, 83] and in lithium

[8] We note that $\mu < 0$ because the lower limit of energy is taken as zero in the integral

mixtures [84].

Modification of the shape of the trapping potential can be used to increase the phase space density [53]. "Dimple" type potentials are most favorable potentials for this purpose [54, 55, 56]. Phase space density can be enhanced by an arbitrary factor by using a small dimple potential at the equilibrium point of the harmonic trapping potential [54]. Recent demonstration of caesium BEC exploits a tight dimple potential [55]. Quite recently, such potentials are proposed for efficient loading and fast evaporative cooling to produce large BECs [85]. Tight dimple potentials for one dimensional (or strictly speaking quasi-one-dimensional) BECs offer attractive applications, such as, controlling interaction between dark soliton and sound [86], introducing defects as atomic quantum dots in optical lattices [87], or quantum tweezers for atoms [88]. Such systems can also be used for spatially selective loading of optical lattices [89]. In combination with the condensates on atom chips, tight and deep dimple potentials can lead to rich novel dynamics for potential applications in atom lasers, atom interferometers and in quantum computations (see Ref. [90] and references therein). We investigate the effect of the tight dimple potential on the harmonically confined one dimensional BEC. We model the dimple potential with a Dirac delta function. This allows for analytical expressions for the eigenfunctions of the system and a simple eigenvalue equations greatly simplifying numerical treatment.

5.3.1. BEC in a One-Dimensional Harmonic Potential with a Dirac Delta Function

We begin our discussion about BEC in a one-dimensional harmonic potential decorated with a Dirac delta function by investigating the change of the critical temperature as a function of σ given in the Equation (3.40). One estimates a σ value using the parameters of Ref.[56]. In this paper, the minimum value of the dimple potential is given as $U_c = k_B\, 4\,\mu\mathrm{K}$ and the average potential width is given as $r = 1 - 100\,\mu\mathrm{m}$. We equate the strength $(-\hbar^2\sigma/2m)$ to the product $U_c\, r$ to get an estimate of σ. We find that σ varies approximately between $10^8\,1/\mathrm{m}$ and $10^{10}\,1/\mathrm{m}$ as r changes from

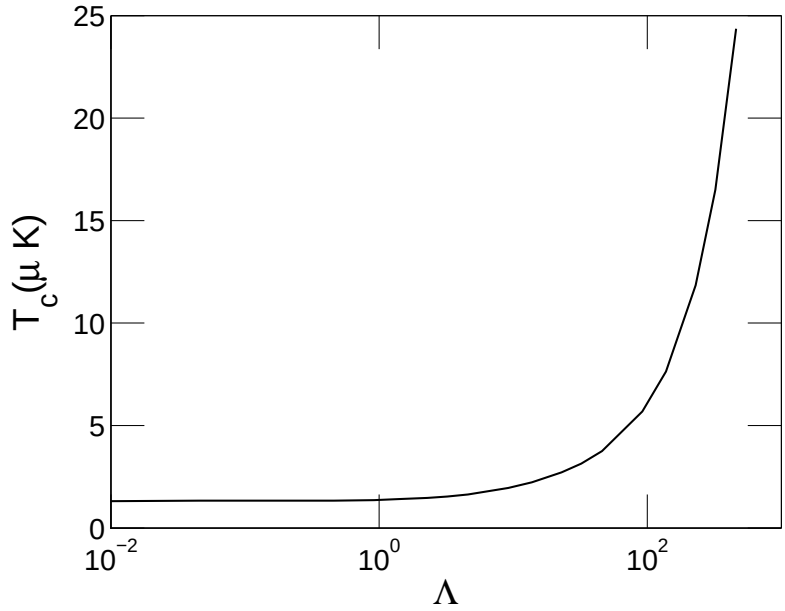

Figure 5.5. The critical temperature T_c vs. Λ for $N = 10^4$.

$1\,\mu$m to $100\,\mu$m. We define a dimensionless parameter in terms of σ as:

$$\Lambda = \sigma\sqrt{\frac{\hbar}{m\omega}}\ . \tag{5.8}$$

If $10^8\,1/\mathrm{m} \leq \sigma \leq 10^{10}\,1/\mathrm{m}$ then $460 \leq \Lambda \leq 46\,000$ for the experimental parameters m= 23 amu (^{23}Na), $\omega = 2\,\pi \times 21$ Hz [92] and $230 \leq \Lambda \leq 23\,000$ for the experimental parameters m= 133 amu (^{133}Cs), $\omega = 2\,\pi \times 14$ Hz [55]. In this work, we show that, even for smaller Λ values, condensate fraction and critical temperature change considerably.

The critical temperature (T_c) is obtained by taking the chemical potential equal to the ground state energy ($\mu = E_g = E_0$) and

$$N \approx \sum_{i=1}^{\infty} \frac{1}{e^{\beta_c \varepsilon_i} - 1}\ , \tag{5.9}$$

at $T = T_c$, where $\beta_c = 1/(k_B T_c)$. For finite N value, we define T_c^0 as the solution of the Equation (5.9) for $\Lambda = 0$ (only the harmonic trap).

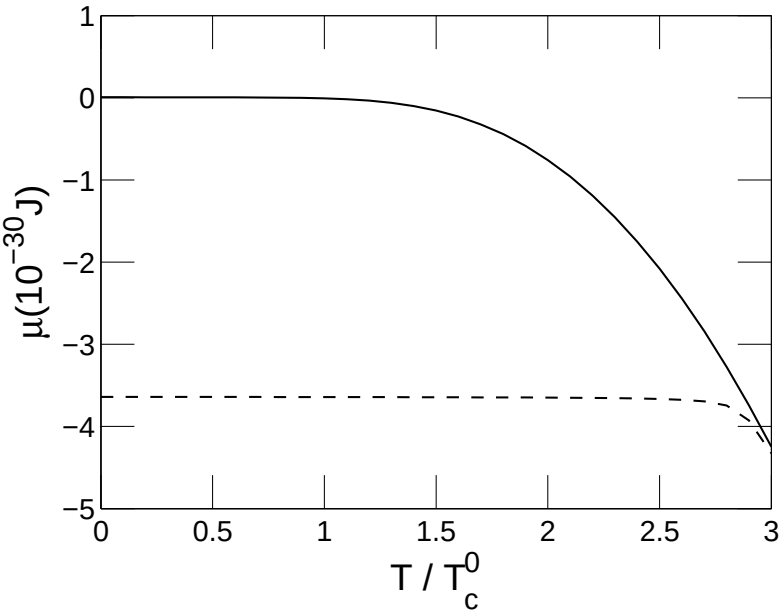

Figure 5.6. The chemical potential μ vs temperature T/T_c^0 for $N = 10^4$.

In the Equation (5.9), ε_i's are the eigenvalues for the potential given in the Equation (3.37). The energies of the odd states are unchanged and equal to $(2n + 1 + 1/2)\hbar\omega$. The energies of even states are found by solving the Equation (3.40) numerically. Then, these values are substituted into the Equation (5.9); and finally this equation is solved numerically to find T_c. We obtain T_c for different Λ and show our results in the Figure (5.5). In this figure, logarithmic scale is used for Λ axis. As Λ increases, the critical temperature increases very rapidly when $\Lambda > 1$. Here we take $N = 10^4$ and use experimental parameters m= 23 amu (^{23}Na) and $\omega = 2\pi \times 21$ Hz [92].

For a gas of N identical bosons, the chemical potential μ is obtained by solving

$$N = \sum_{i=0}^{\infty} \frac{1}{e^{\beta(\varepsilon_i - \mu)} - 1} = N_0 + \sum_{i=1}^{\infty} \frac{1}{e^{\beta(\varepsilon_i - \mu)} - 1} \, , \tag{5.10}$$

at constant temperature and for given N, where ε_i is the energy of state i. We present the change of μ as a function of T/T_c^0 in the Figure (5.6) for $N = 10^4$; $\Lambda = 0$ and

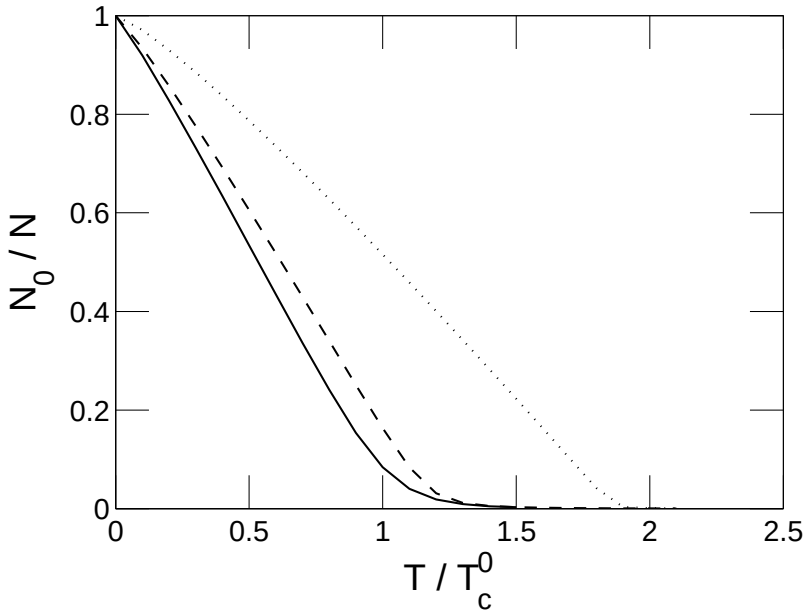

Figure 5.7. N_0/N vs T/T_c^0 for $N = 10^6$ and $\Lambda = 0, 4.6, 46$.

$\Lambda = 46$. By inserting μ values into the equation

$$N_0 = \frac{1}{e^{\beta(\varepsilon_0 - \mu)} - 1} \, , \tag{5.11}$$

we find the average number of particle in the ground state. N_0/N versus T/T_c^0 for $N = 10^6$ and $\Lambda = 0, 4.6, 46$ are shown in the Figure (5.7). In this figure the solid, dashed an dotted lines show N_0/N for $\Lambda = 0, 4.6, 46$, respectively. In this figure, the result for $\Lambda = 0$ is the same as the result obtained by Ketterle et.al. [74]. As mentioned in Ref. [74], the phase transitions due to a discontinuity in an observable macro parameter occurs only in thermodynamic limit, where $N \to \infty$. However, we make our calculations for a realistic system with a finite number of particles. Thus, N_0/N is a finite, non-zero quantity for $T < T_c$ without having any discontinuity at $T = T_c$.

It is useful to know the behavior of the condensate fraction as a function of the temperature for a fixed value of Λ. We present the condensate fraction for $N = 10^4, 10^6, 10^8$ when $\Lambda = 46$ in the Figure (5.8). All condensate fractions for different N values are drawn by using their corresponding T_c^0 values. These T_c^0 values are $13\,\mu$K

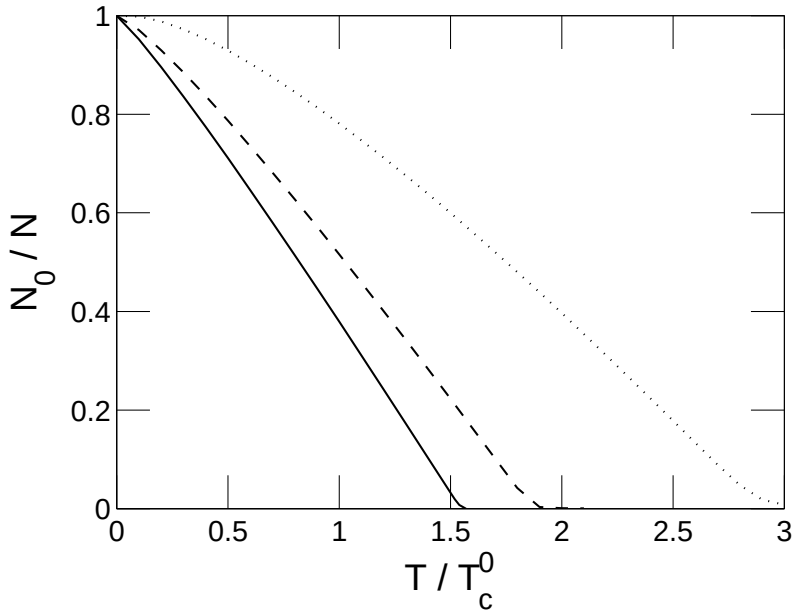

Figure 5.8. Condensate fraction N_0/N vs Temperature T/T_c^0 for $\Lambda = 46$ and $N = 10^4, 10^6, 10^8$.

for $N = 10^4$, 85 μK for $N = 10^6$ and 6 200 μK for $N = 10^8$. In this figure the solid, dashed an dotted lines show N_0/N for $N = 10^4, 10^6, 10^8$, respectively.

We also find the condensate fraction as a function of Λ at a constant $T = T_c^0$. These results for $N = 10^4$ are shown in the Figure (5.9). In the following section we show that the condensate fraction changes exponentially for large Λ. Thus, large Λ values ($\Lambda > 1$) induce sharp increase in the condensate fraction.

Finally, we compare the density profiles of condensates for a harmonic trap and a harmonic trap decorated with a delta function ($\Lambda = 4.6$) in Figure 5.10. Since the ground state wave functions can be calculated analytically for both cases, we find the density profiles by taking the absolute square of the ground state wave functions. In the Figure 5.10, the solid curve is the density profile of the BEC in the decorated potential. The dashed curve is the density profile of the one-dimensional harmonic trap $\Lambda = 0$. The parameter z is dimensionless length defined after the Equation (3.28).

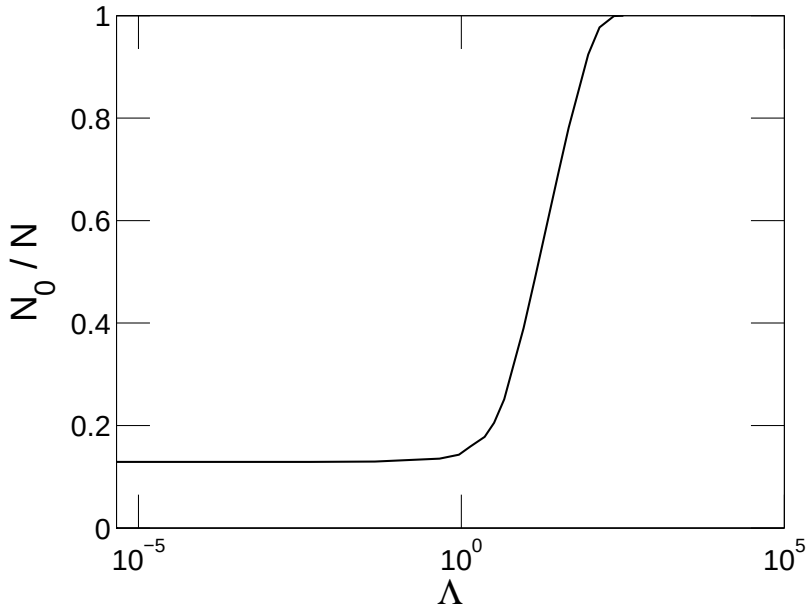

Figure 5.9. Condensate fraction N_0/N vs the strength of the Dirac delta potential Λ when $N = 10^4$.

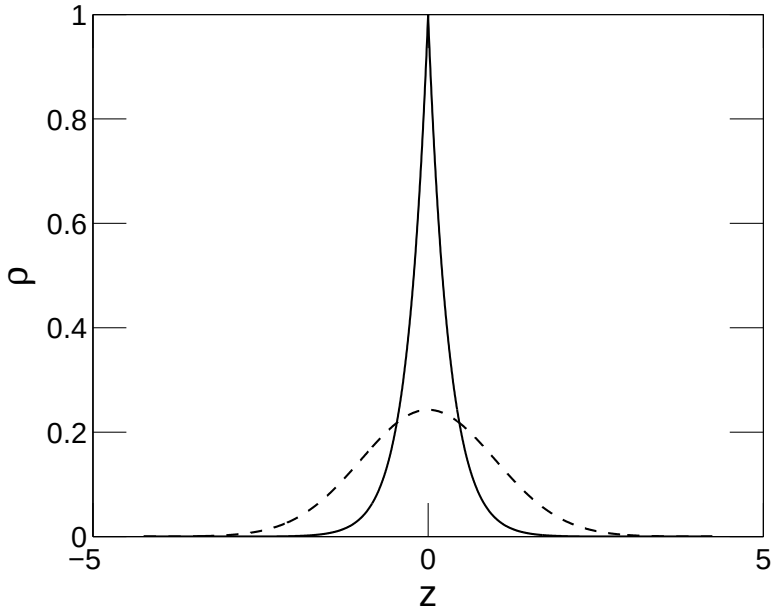

Figure 5.10. Comparison of density profiles.

5.3.2. Approximate Solutions of Critical Temperature and Condensate Fraction for Large σ

If we apply a deep dimple potential ($\sigma \to \infty$) to the atomic condensate in a harmonic trap, the problem can be solved analytically by approximating the summation

for N with an integral. As $T \to T_c$, $\mu \to \varepsilon_0 \approx E_\delta$, where

$$E_\delta = -\frac{\hbar^2}{2m}(\frac{\sigma}{2})^2 \tag{5.12}$$

and it is the bound state energy of a Dirac delta potential [20]. By using density of states $\rho(\varepsilon)$ and utilizing $E_{2n+2} \to E_{2n+1}$ (odd state energies) as $\sigma \to \infty$, the summation in the Equation (5.10) is converted to the following integral,

$$N = \frac{1}{\hbar\omega}\int_{(3/2)\hbar\omega}^{\infty} \frac{d\varepsilon}{e^{\beta_c\varepsilon+\alpha}-1} \tag{5.13}$$

where $\alpha = \beta_c(\hbar^2/(2m))(\sigma/2)^2$ and $\beta_c = 1/k_BT_c$. After calculating the integral, we get

$$N = -\frac{k_BT_c}{\hbar\omega}\ln\left\{1-\exp\left[-\beta_c\left(\frac{3\hbar\omega}{2}-\frac{\hbar^2}{2m}(\frac{\sigma}{2})^2\right)\right]\right\}. \tag{5.14}$$

Defining $A = |E_\delta|/\hbar\omega$, we have $A \gg 1$ and $\exp((-\beta_c\hbar\omega A)) \ll 1$ for very large σ. Then,

$$N \approx \frac{k_BT_c}{\hbar\omega}e^{-\beta_c\hbar\omega A} \tag{5.15}$$

for this case and we get for the critical temperature

$$k_BT_c \approx \frac{A}{\ln(\frac{A/N}{\ln(A/N)})}\hbar\omega\ , \tag{5.16}$$

for large A/N value. For one-dimensional experimental systems, $N \approx 10^3 - 10^6$ atoms. For a specific case $A/N \approx 10^4 \approx e^9$, one gets

$$k_BT_c \approx \frac{|E_\delta|}{7}\ , \tag{5.17}$$

which shows that the critical temperature increases linearly with the increasing bound state energy for the dimple potential.

By using the Equation (5.15), the condensate fraction can be written as

$$\frac{N_0}{N} = 1 - \frac{T}{T_c} e^{-\beta\beta_c k_B (T_c - T)\hbar\omega A} \tag{5.18}$$

for $T < T_c$. This result indicates an exponential increase of N_0 as a function of T for $T < T_c$. Thus, the number of atoms in the Bose-Einstein condensate will rise drastically when a very strong, very short-range (point) interaction is added to a harmonic confining potential. However, we ignore the interactions between the atoms and neglect non-linear term in the Gross-Pitaevski Equation which will modify these results.

6. CONCLUSION

We studied bound state solutions of the Schrödinger equation for solvable potential with a finite number of Dirac delta functions for one- and n-dimensional systems. We first introduced a general method to obtain bound state solutions of the Schrödinger equation for these potentials and proved that a central potential with P Dirac delta functions $U(r) = V(r) - \hbar^2/(2m)\sum_i^P \sigma_i \delta(r - r_i)$ can have at most P bound states with energy values less than the absolute minimum of the potential $V(r)$, if the expectation value of $V(r)$ is finite. Then, we applied the methodology to some specific potentials.

We first presented the solution of the Schrödinger equation for a constant potential with a finite number of Dirac delta functions. We have obtained the energy eigenvalue equation for bound states. Then, we investigated "Dirac delta well" (the potential with two Dirac delta functions) and showed that this potential has at most two and at least one bound state. Moreover, we obtained the bound state solutions and energy eigenvalue equation of the Schrödinger equation for the harmonic potential with a finite number of Dirac delta functions.

Then, we have studied bound states of the Schrödinger equation for the linear potential with a finite number of Dirac delta functions. We have obtained transfer matrices and eigenvalue equation. We have presented the wave functions in terms of Airy functions Ai and Bi. For one Dirac delta function, we have obtained a transcendental equation for the bound state energies and calculated the change of the energies for the low-lying bound states ($n = 1 - 10$) for a linear potential with attractive or repulsive Dirac delta functions. By solving the eigenvalue equations for one, two, four and eight Dirac delta functions, we investigated the change in the ground and first excited state energies for different strengths and positions of Dirac delta functions. We obtained that the attractive Dirac delta functions (positive σ_i) change the energy eigenvalues than repulsive ones (negative σ_i). Finally, we studied the change in the ground state energy for linear potential with Dirac delta functions at random locations.

We also investigated $\mathcal{PT}$-symmetric potential with Dirac delta function in one-dimension. We gave a general method to find the energy eigenvalues of the bound states and presented these equations for two and four $\mathcal{PT}$-symmetric Dirac delta functions. Solving the energy eigenvalue equations numerically, we found the energy eigenvalues of bound states of two (and four) $\mathcal{PT}$-symmetric Dirac delta functions for different σ_1 (and σ_2) values, where σ_1 (and σ_2) is the strength of Dirac delta functions located at $x = x_1$ (and $x = x_2$).

For complex eigenvalue equation, we utilized the argument principle and Rouche's theorem to find the number of the bound states and the dependence of $\mathcal{PT}$-symmetry of the bound states on the strengths and locations of Dirac delta functions for two $\mathcal{PT}$-symmetric Dirac delta functions. Resultantly, we found the following results for the bound sates of a potential consisting of two $\mathcal{PT}$-symmetric Dirac delta functions:

a) No bound states if
   i) $\frac{\mathbf{Re}(\sigma_1)}{|\sigma_1|^2 x_1} = 1$ and $|\sigma_1| x_1 \leq \frac{\sqrt{2}}{2}$.
   or,
   ii) $\frac{\mathbf{Re}(\sigma_1)}{|\sigma_1|^2 x_1} < 1$ and $|\sigma_1| x_1 < \frac{\sqrt{2}}{2}$.

b) Only one bound state with a real eigenvalue if
   i) $\frac{\mathbf{Re}(\sigma_1)}{|\sigma_1|^2 x_1} > 1$,
   or,
   ii) $\frac{\mathbf{Re}(\sigma_1)}{|\sigma_1|^2 x_1} = 1$ and $\frac{\sqrt{2}}{2} < |\sigma_1| x_1$.

c) Two bound states if $\frac{\mathbf{Re}(\sigma_1)}{|\sigma_1|^2 x_1} < 1$ and $|\mathbf{Im}(\sigma_1)| \leq \mathbf{Re}(\sigma_1)$. Moreover, the eigenvalues of these bound states are
   i) real if $\frac{(\mathbf{Im}(\sigma_1))^2}{|\sigma_1|^2} \leq e^{-2\mathbf{Re}(\sigma_1) x_1}$
   ii) complex conjugates if $\frac{(\mathbf{Im}(\sigma_1))^2}{|\sigma_1|^2} > e^{-2\mathbf{Re}(\sigma_1) x_1}$.

d) If σ_1 is a purely imaginary number, the number of roots is determined by the formula

$$\begin{aligned} &\text{No root if} && |\sigma_{1i}| \cdot x_1 \leq \tfrac{\sqrt{2}\pi}{4} \\ &\text{2n roots if} && (2n-1)\tfrac{\sqrt{2}\pi}{4} < |\sigma_{1i}| \cdot x_1 \leq (2n+1)\tfrac{\sqrt{2}\pi}{4} \ . \end{aligned}$$

In addition to these results, we found that $\mathcal{PT}$-symmetry breaks down for sufficiently large x_1 and $|\mathbf{Im}(\sigma_1)|$ values such that $x_1|\mathbf{Im}(\sigma_1)| > \frac{1}{2}$.

Then, we solved the Schrödinger equation for the potential $U(x) = \{(1/2)m^2\omega^3x^4/\hbar - (\hbar^2/2m)\sigma\,\delta(x)\}$, numerically. We have presented the change of the ground state with respect to σ and compared the ground state wave functions of the potentials with $\sigma = 0, \sqrt{\frac{m\omega}{\hbar}}$ and $2\sqrt{\frac{m\omega}{\hbar}}$.

Finally, we applied the solutions of the Schrödinger equation for potentials with Dirac delta functions at the center of the potential to some physical systems. First, we have applied the solution of the linear potential with a Dirac delta function to the charmonium. By taking the confining potential as a combination of linear and Dirac delta potentials, we obtain a mass spectrum for n=1, 2, ..., 10 levels. We have also presented the mass spectrum with relativistic corrections. Moreover, we used this potential to calculate the shift of the Fermi energy of an electron gas in GaAs/GaAlAs junction containing an impurity.

In addition, we used harmonic potential with a Dirac delta function at the center to model BEC in a harmonic trap with a dimple potential. Modelling the dimple potential with the Dirac delta function allows for analytical expressions for the eigenfunctions of the system and a simple eigenvalue equation greatly simplifying numerical treatment. Pure analytical results are obtained in the limit of infinitely deep dimple potential case.

We have calculated the critical temperature, chemical potential and condensate fraction of a BEC in harmonic trap with a dimple potential, to demonstrate the effect of the dimple potential. We have found that critical temperature can be enhanced by an order of magnitude for experimentally accessible dimple potential parameters. In general, T_c increases with the relative strength of the dimple potential with respect to the harmonic trap. In our model system, the increase in the strength of the Dirac delta function can be interpreted as increasing the depth of a dimple potential.

The change of the condensate fraction with respect to the strength of the Dirac delta function has been analyzed at a constant temperature ($T = T_c^0$), and with respect to temperature at a constant strength. It has been shown that the condensate fraction can be increased considerably and large condensates can be achieved at higher temperatures due to the strong localization effect of the dimple potential. Analytical expressions are given to clarify the relation of the condensate fraction and the critical temperature to the strength of deep dimple potential.

Finally, we have determined and compared the density profiles of the harmonic trap and the decorated harmonic trap with the Dirac delta function at the equilibrium point using analytical solutions of the model system. Comparing the graphics of density profiles, we see that a dimple potential maintain a considerably higher density at the center of the harmonic trap.

The presented results are obtained for the case of noninteracting condensate for simplicity. This treatment should be extended for the case of interacting condensates in order to make the results more relevant to experimental investigations.

We conclude that the addition of point interactions which can be modelled by Dirac delta functions change the properties of the physical systems considerably.

APPENDIX A: The Fortran Code for Bound State Solutions of the Schrödinger Equation for The Potential $\mathbf{U(x) = ((1/2)m\omega^3/\hbar)x^4 - (\hbar^2/2m)\sigma\,\delta(x)}$

We use the Runge Kutta Method to calculate the second derivative [93]. The fortran code for the computer program is as follows:

```
      **************************
**This program is a numerical solution for the potential
**U(x) = ((1/2)mω^3/ħ)x^4 - (ħ^2/2m)σ δ(x)
**************************

subroutine diff(u,du,psi,dpsi,eps,u1,alpha,i1)
* ——— This subroutine solves 2. order differential Equation
*——— Using Runge Kutta Method——
Real*8 psi(0:10000)
Real*8 dpsi(0:10000)
Real*8 u,du,u1,alpha,eps
Real*8 a1,b1,a2,b2,a3,b3,a4,b4
SECD(x,y,z)=(y**4-2*x)*z
i1=0
15 continue
If((u1.gt.u-du/2).and.(u1.lt.u+du/2))
dpsi(i1)=dpsi(i1)-(alpha/2)*psi(i1)
a1= du*dpsi(i1)
b1= du*SECD(eps,u,psi(i1))
a2= du*(dpsi(i1)+ .5*b1)
b2= du*SECD(eps,u,psi(i1)+ .5*a1)
a3= du*(dpsi(i1)+ .5*b2)
b3= du*SECD(eps,u,psi(i1)+ .5*a2)
```

```
a4= du*(dpsi(i1)+ .5*b3)
b4= du*SECD(eps,u,psi(i1)+ .5*a3)
psi(i1+1)=psi(i1) + (1.0/6.0)*(a1+2*a2+2*a3+a4)
dpsi(i1+1)=dpsi(i1)+(1.0/6.0)*(b1+2*b2+2*b3+b4)
u=u+du
if(Abs(psi(i1+1)).lt.10000) then
* uses the ultimate divergence of the algorithm to return to the main program

i1=i1+1
go to 15
end if

return
end

subroutine yaz(psi,du,l,eps,alpha)

*—This subroutine writes the wave function values for positive u to the file DDPout.dat–



Real*8 psi(0:10000)
Real*8 du,eps,alpha
open(30,file='DD4Pout.dat')
u=0.0
write(30,40) ' ground state energy = ', eps, 'alpha=',alpha
40 format(1x,a,f7.5,1x,a,f7.5)
do i=0,2000
write(30,*) u,psi(i)
u=u+du
end do
l=2001
50 continue
```

```
if(Abs(psi(l+1)).lt.Abs(psi(l))) then
write(30,*) u,psi(l)
u=u+du
l=l+1
go to 50
end if
close(30)
return
end


subroutine nyaz(psi,du,l,eps,alpha)

* ——-Using symmetry, this subroutine writes the values of the wave function for
*—negative u to the file DD4Nout.dat ——-

Real*8 psi(0:10000)
Real*8 du,eps,alpha
open(30,file='DD4Nout.dat')  u=-l*du
write(30,40) ' ground state energy = ', eps, 'alpha=',alpha
40 format(1x,a,f7.5,1x,a,f7.5)
do i=-l,0
write(30,*) u,psi(-i)
u=u+du
end do
close(30)
return
end


**********************************
**********************************
```

```
**********MAIN PROGRAM**********
**********
**********

Real*8 psi(0:10000)
Real*8 dpsi(0:10000)
Real*8 u,du,u1,alpha,pl,eps,den1,den2

***************Constants*********

du= 1.0/1000.0
*** discretization of position coordinate

u1=0.0
***The position of Dirac delta function

alpha=1.0
***The strength of the Dirac delta Function
TOL=0.0000001

*** Adjusts the precision***********

***End of Constants*****************



**********
pl=0.1
eps=0.53 **********Initial guess of energy****

psi(0)=1.0 *****Using linerity one can choose Psi(0)=1.0

dpsi(0)=0.0
```

*****Symmetry of x^4 requires dpsi(0)=0****

```
u=0.0
call diff(u,du,psi,dpsi,eps,u1,alpha,i1)
den1=psi(i1+1)
20 continue
eps=eps-pl
if(eps.lt.-20.0) go to 95
***prevents the infinite iteration****
psi(0)=1.0
dpsi(0)=0.0
u=0.0
call diff(u,du,psi,dpsi,eps,u1,alpha,i1)
den2=psi(i1+1)
if ((den2*den1.lt.0)) then
eps=eps+pl
pl=pl/10
if((pl.lt.TOL)) go to 70
go to 20
end if
den1=den2
go to 20


70 continue
call yaz(psi,du,l,eps,alpha)
**calls subprogram to collect the data of the wave function for positive u

call nyaz(psi,du,l,eps,alpha)
**calls subprogram to collect the data of the wave function for negative u

go to 90
```

```
95 print*, 'no result'
**Informs if the program does not find a result for a given lower limit
90 continue

stop
end
```

In this program the arrays psi and dpsi are used to collect the data for the wave function and its derivative of with respect to u, respectively. We choose the first guess of ϵ as 0.53. This guess is obtained by running the program for $\alpha = 0$ with a first guess 0.55 for ϵ. This guess is obtained using WKB approximation (See [4] pp. 294). The ground state energy of the potential $U(x) = \frac{1}{2}\frac{m^2\omega^3}{\hbar}x^4 - \frac{\hbar^2}{2m}\sigma\delta(x)$ is found as $E_0 = 0.157\,\hbar\omega$ when $\alpha = \sqrt{\frac{\hbar}{m\omega}}\sigma = 1$.

REFERENCES

1. Albeverio, S., L. Dąbrowski and P. Kurasov, 1998, "Symmetries of Schrödinger Operators with Point Interactions", *Lett. Math. Phys.*, vol. 45, pp. 33-47.

2. Albeverio, S., F. Gesztey, P. Hoegh-Krohn and H.Holden, 1988, *Solvable Models in Quantum Mechanics*, Springer-Verlag, New-York.

3. Cohen-Tannoudji, C., B. Diu and F. Laloë, 1977, *Quantum Mechanics Vol. II*, Hermann, Paris.

4. Griffiths, D.J., 1995, *Introduction to Quantum Mechanics*, Prentice Hall Inc., New Jersey.

5. Kittel C., 1996, *Introduction to Solid State Physics*, John Wiley & Sons, New-York.

6. Sànchez, A., E. Maàcia and F. Domìnguez-Adame, 1994, "Suppression of localization in Kronig-Penney models with correlated disorder", *Phys. Rev. B*, vol. 49, pp. 147-157.

7. Mèndez, B., F. Domìnguez-Adame and E. Maàcia, 1993, "A transfer matrix method for the determination of one-dimensional band structures", *J. Phys A: Math. Gen.*, vol. 26, pp. 171-177.

8. Ashour, H.S., A.I. Ass'ad, M.M. Shabat and M.S. Hamada, 2006, "Electronic conductance in binomially tailored quantum wire", *Microelectronics Journal*, vol. 37, pp. 79-83

9. Maksymowicz, A.Z. and M. Wołoszyn, 2006, "Density of states in structurally disordered 1D chains of atoms", *Journal of Non-Crystalline Solids*, vol. 352, pp. 4200-4205.

10. Barker, J.R., 1986, *The physics and fabrication of microstructures and microde-*

vices. Proceedings in Physics Kelly, M.S.Weisbuch, C. (eds.), Springer, Berlin.

11. Ellberfeld, W. and M. Kleber, 1988, "Tunneling from an ultrathin quantum well in a strong electrostaic field: A comparison of different methods" *Zeitschrift für Physik B*, vol. 73, pp. 23-32.

12. Ludviksson, A., 1987, "A simple model of a decaying quantum mechanical state", *J. Phys. A: Math. Gen.*, vol. 20, pp. 4733-4738.

13. Baltenkov, A.S., 1999, "Resonances in photoionization cross sections of inner subshells of atoms inside the fullerene cage", *J. Phys. B: At. Mol. Opt. Phys.*, vol. 32, pp. 2745-2751.

14. Korsch, H. J. and S. Mossmann, 2003, "Stark resonances for a double δ quantum well: crossing scenarios, exceptional points and geometric phases", *J. Phys. A: Math. Gen.*, vol. 36, pp. 2139-2153.

15. Àlvarez, G. and B. Sundaram, 2004, *J. Phys. A: Math. Gen.*, "Perturbation theory for the Stark effect in a double δ quantum well", vol. 37, pp. 9735-9748.

16. Avdonin, S.A, L.A. Dmitrieva, Y. A. Kuperin and V. V. Sartan, 2005, "Solvable model of a spin-dependent transport through a finite array of quantum dots.", *J. Phys. A: Math Gen*, vol. 38, pp. 4825-4833

17. Cox, B. J., N. Thamwattana and J. M. Hill, 2006, "Mechanics of atoms and fullerenes in single-walled carbon nanotubes. II. Oscillatory behaviour", *Proc. R. Soc. A*, vol. 463, pp. 477-494.

18. Demiralp, E., 2005, "Properties of a Bose-Einstein Condensate in a Harmonic Trap Decorated with Dirac Delta Functions", *Talk Given at Albert Einstein Century International Conference*, Paris.

19. Atkinson, A.D., W.H. Crater, 1975, "An exact treatment of the Dirac delta function potential in the Schrödinger equation", *Am. J. Phys*, Vol.43, pp. 301-304.

20. Avakian, M.P., A.N. Pogosyan, A.N. Sissakian and V.M. Ter-Antonyan, 1987, "Spectroscopy of a Singular Linear Oscillator", *Phys. Lett. A*, vol 124, pp. 233-236.

21. Manoukian, E.B., 1989, "Explicit derivation of the propagator for a Dirac delta Potential", *J. Phys. A: Math. Gen.*, vol. 22, pp. 67-70.

22. Demiralp, E. and H. Beker, 2003, "Properties of bound states of the Schrödinger Equation with attractive Dirac delta potentials", *J. Phys. A: Math. Gen.*, vol. 36, pp. 7449-7459.

23. Demiralp, E., 2005, " Bound states of n-dimensional harmonic oscillator decorated with Dirac delta functions", *J. Phys. A: Math. Gen.*, vol.22, pp. 4783-4793

24. Erkol, H. and E. Demiralp, 2007, "The WoodsSaxon potential with point interactions", *Phys. Lett. A*, vol. 365, pp. 55-63

25. Altunkaynak, B. İ., 2005, "Spectral and Scattering Properties of Point Interactions", M.S. Thesis, Boğaziçi University.

26. Altunkaynak, B. İ., F. Erman and O. T. Turgut, 2006, "Finitely Many Dirac-Delta Interactions on Riemannian Manifolds", *J. Math. Phys.*, vol. 47, pp. 082110-1-082110-23.

27. Witten, E., 1981, "Dynamical Breaking of Supersymmetry", *Nucl. Phys. B*, vol. 188, pp. 513-554.

28. Bender, C.M. and S. Boettcher, 1998, "Real Spectra in Non-Hermitian Hamiltonians Having $\mathcal{PT}$-Symmetry, *Phys. Rev. Lett.*, vol. 80, pp. 5243-5246.

29. Uchino, T. and I. Tsutsui, 2003, "Super Symmetric quantum mechanics under point singularities", *J. Phys A: Math. Gen.*, vol.36, pp. 6821-6846.

30. Goldstein, J., C. Lebiedzik and R.W. Robinett, 1993, "Super Symmetric quantum

mechanics: Examples with Dirac δ functions", *Am. J. Phys*, vol 62, pp.612-618.

31. Znojil, M. and V . Jakubsky, 2005, "Solvability and $\mathcal{PT}$-symmentry in a double-well model with point interactions", *J. Phys. A: Math. Gen.*, vol. 38, pp. 5041-5046.

32. Jakubsky, V. and M. Znojil, 2005, "An explicitly solvable model of the spontaneous $\mathcal{PT}$-symmetry breaking", *Czech J. Phys.*, vol. 55, pp. 1113-1116.

33. Albeverio, S., S.M. Fei and P. Kurasov, 2002, "Point interactions: $\mathcal{PT}$-Hermiticity and reality of the spectrum", *Lett. Math. Phys.*, vol. 59, pp. 227-242.

34. Weigert, S., 2004, "The physical interpretation of $\mathcal{PT}$-invariant potentials", *Czech J. Phys.*, vol. 54, pp. 1139-1142.

35. Demiralp E., 2005, "Properties of a pseudo-Hermitian Hamiltonian for harmonic oscillator decorated with Dirac delta interactions", *Czech J. Phys.* vol. 55, pp. 1081-1084.

36. Cerveró, J.M., 2003, "$\mathcal{PT}$-symmetry in one-dimensional quantum periodic potentials ", *Phys. Lett. A*, vol. 317, pp. 26-31.

37. Cerveró and J.M., A. Rodríguez, 2004, "The band spectrum of periodic potentials with $\mathcal{PT}$-symmetry", *J. Phys. A: Math. Gen.*, vol. 37, pp. 10167-10177.

38. Ahmed, Z., 2001, "Energy band structure due to a complex, periodic, $\mathcal{PT}$-invariant potential", *Phys. Lett. A*, vol. 286, pp. 231-235.

39. Albeverio, S. and S. Kuzhel, 2005, "One-dimensional Schrödinger operators with $\mathcal{P}$-symmetric zero-range potentials", *J. Phys. A: Math. Gen.*, vol. 38, pp. 4975-4988.

40. Muga, J.G., J.P. Palaob, B. Navarroa and I.L. Egusquizac, 2004,"Complex absorbing potentials", *Physics Reports*, vol. 395, pp. 357-426.

41. Deb, R.N., A. Khare and B.D. Roy, 2003, "Complex optical potentials and pseudo-Hermitian Hamiltonians", *Phys. Lett. A*, vol. 307, pp. 215-221.

42. Fei, S.M., 2003, "Integrability and $\mathcal{PT}$-symmetry of N-body systems with spin-coupling δ-interactions", *Czech J. Phys.*, vol. 53, pp. 1027-1033.

43. Fei, S.M., 2004, "Exactly solvable many-body systems and pseudo-Hermitian point interactions", *Czech J. Phys.*, vol. 54, pp. 43-49.

44. Znojil, M., 2004, "Fragile $\mathcal{PT}$-symmetry in a solvable model", *J. Math. Phys.*, vol. 45, pp. 4418-4430.

45. Coutinho, F.A.B., Y. Nogami, L. Tomio and F.M. Toyama, 2005, "$\mathcal{PT}$-invariant point interactions in one dimension", *J.Phys.A: Math. Gen.*, vol. 38, pp. L519-L522.

46. Uncu, H., H. Erkol, E. Demiralp and H. Beker, 2005, "Solutions of the Schrödinger equation for Dirac Delta Decorated Linear Potential", *CESJ*, vol. 1, pp. 1-19.

47. Uncu, H. and E. Demiralp, 2006, "Bound state solutions of the Schrödinger equation for a $\mathcal{PT}$-symmetric potential with Dirac delta functions.", *Phys. Lett. A*, vol. 359, pp. 190-198.

48. Greiner W. and B. Müller, 1994, *Quantum Mechanics: symmetries* 2^{nd} *revised Ed.*, Springer-Verlag, Berlin.

49. A. Einstein's letter to P. Ehrenfest in A. Pais, 2005, " *Subtle is The Lord*", Oxford University Press, New York.

50. Anderson, M. H., J. R. Ensher, M. R. Matthews, C. E. Wieman and E. A. Cornell, 1995, "Observation of Bose-Einstein Condensation in a Dilute Atomic Vapor", *Science*, vol. 269, pp. 198-200.

51. Bradley, C. C., C. A. Sackett, J. J. Tollett and R. G. Hulet, 1995, "Evidence

of Bose-Einstein Condensation in An Atomic Gas with Attractive Interactions", *Phys. Rev. Lett.*, vol. 75, pp. 1687-1690.

52. Davis, K. B., M.-O. Mewes, M. R. Andrews, N. J. van Druten, D. S. Durfee, D. M. Kurn and W. Ketterle, 1995, "Bose-Einstein Condensation in a Gas of Sodium Atoms", *Phys. Rev. Lett.*, vol. 75, 3969-3972 .

53. Pinkse, P. W. H., A. Mosk, M. Weidemüller, M. W. Reynolds, T. W. Hijmans and J. T. M. Walraven, 1993, "Adiabatically Changing the Phase-Space Density of a Trapped Gas", *Phys. Rev. Lett.*, vol. 78, 990-993.

54. Stamper-Kurn, D. M., H.J. Miesner, A. P. Chikkatur, S. Inouye, J. Stenger and W. Ketterle, 1998, "Reversible Formation of a Bose-Einstein Condensate", *Phys. Rev. Lett.*, vol. 81, pp. 2194-2197.

55. Weber, T., J. Herbig, M. Mark, H.-C. Nägerl and R. Grimm, 2003, "Bose-Einstein Condensation of Cesium", *Science*, vol. 299, pp. 232-235.

56. Ma, Z.Y., C. J. Foot and S. L. Cornish, 2004, "Optimized evaporative cooling using a dimple potential: an efficient route to BoseEinstein condensation", *J. Phys. B: At. Mol.Opt. Phys.*, vol. 37, pp. 3187-3195.

57. Uncu, H., D. Tarhan, E. Demiralp and Ö. Müstecaplıoğlu, "Bose-Einstein Condensate in a Harmonic Trap Decorated with Dirac Delta Functions", to be published in *Phys. Rev. A*.

58. Beker, H., 2006, *Fen ve Mühendislikte Matematik Metotlar*, Boğaziçi Üniversitesi Yayınevi, İstanbul.

59. Müller, C., 1966 *Spherical Harmonics Lecture Notes in Mathematics* Springer Verlag, New-York.

60. Courant, R. and D. Hilbert, 1989, *Method of Mathematical Physics Vol. I*, Wiley, New-York.

61. Lebedev, N. N., 1972, *Special Functions and Their Applications*, Dover Pub. Inc., New York.

62. Demiralp, E., "Properties of One-Dimensional Harmonic Oscillator with the Dirac delta Functions", *Unpublished Notes.*

63. Bender, C.M., Brody C.D. and Hugh F.J., 2003, "Must Hamiltonian be Hermitian" *Am. J. Phys.*, vol. 71, pp. 1095-1102

64. Mostafazadeh, A., 2003, "Exact $\mathcal{PT}$-symmetry is equivalent to Hermiticity ", *J. Phys. A: Math. Gen.*, vol 36, pp. 7081-7091.

65. Brown, J.D. and R.V. Churchill, 1996, *Complex Variables and Applications*, Mc. Graw Hill, Inc., New-York.

66. Particle Data Group, 2002, "Particles and Fields Part 1", *Phys. Rev. D*, vol. 66, pp. 719.

67. Weisbuch, C. and B. Vinter, 1996, *Quantum Semiconductor Structures*, Academic Press Inc., San-Diego.

68. Monozon, S.B., V. M. Ivanov and P. Schmelcher, 2004, "Impurity center in a semiconductor quantum ring in the presence of a radial electric field", *Phys. Rev. B*, vol. 70, pp. 205336-1-205336-12.

69. Einstein, A., "Quantentheorie des einatomigen idealen gases", 1924, Sitzber. Pr. Akad. Wiss. pp. 261-267.

70. Bose S. N., 1924, "Plancks gesetz und lichtquantenhypothese.", *Z. Phys.*, vol. 26, pp. 178-181.

71. Eisberg, R. and Resnick, R., 2003, *Quantum Physics of Atoms, Molecules, Solids, Nuclei, and Particles*, New-York, Wiley.

72. Petchick, C.J. and Smith H, 2002, *Bose Einsten Condensation in Dilute Gases*, Cambridge University Press, Cambridge.

73. F. London, 1938, "On the Bose-Einstein Condensation", *Phys. Rev.*, vol. 54, pp. 947-954.

74. Ketterle, W. and N. J. van Druten, 1996, "Bose-Einstein Condensation of a finite number of particles trapped in one or three dimensions", *Phys. Rev. A*, vol. 54, pp. 656-660.

75. Van Druten, N.J. and W. Ketterle, 1997, "Two Step Condensation of the Ideal Bose Gas in Highly Anisotropic Traps", *Phys. Rev. Lett.*, vol. 79, 549-552.

76. Al Khawaja, U., J. O. Andersen, N. P. Proukakis, and H. T. C. Stoof, "Low Dimensional Bose Gas", *Phys. Rev. A*, vol. 66, pp. 013615-1-013615-14.

77. Petrov, D. S., G. V. Shlyapnikov and J. T. M. Walraven, 2000, "Regions of Quantum Degeneracy in Trapped 1D Gases", *Phys. Rev. Lett.*, vol. 85, pp. 3745-3749.

78. de Groot, S.E., G. J. Hooyman, and C. A. ten Seldam, 1950, "On the Bose-Einstein Condensation", *Proc. R. London Ser. A*, vol. 203, pp. 266-286.

79. Mermin, N. D. and H. Wagner, 1966, "Absence Of Ferromagnetism Or Antiferromagnetism in One- or Two- Dimensional Isotropic Heisenberg Models", *Phys. Rev. Lett.*, vol. 17, pp. 113-116.

80. Hohenberg, P. C., 1967, "Existence of Long-Range Order in One and Two Dimensions", *Phys. Rev.*, vol. 158, pp. 383-386.

81. Görlitz, A., J. M. Vogels, A. E. Leanhardt, C. Raman, T. L. Gustavson, J. R. Abo-Shaeer, A. P. Chikkatur, S. Gupta, S. Inouye, T. Rosenband and W. Ketterle, 2001, "Realization of Bose-Einstein Condensates in Lower Dimensions", *Phys. Rev. Lett.*, vol. 87, pp. 130402-1-130402-4.

82. Ott, H., J. Fortagh, G. Schlotterbeck, A. Grossmann and C. Zimmermann, 2001, "Bose-Einstein Condensation in a Surface Microtrap", *Phys. Rev. Lett.*, vol. 87, pp. 230401-1-230401-4 .

83. Hänsel, W., P. Hommelhoff, T. W. Hänsch and J. Reichel, 2001, "Bose-Einstein condensation on a microelectronic chip", *Nature*, vol. 413, pp. 498-501.

84. Schreck, F., L. Khaykovich, K. L. Corwin, G. Ferrari, T. Bourdel, J. Cubizolles and C. Salomon, 2001, "Quasipure Bose-Einstein condensate immersed in a Fermi sea", *Phys. Rev. Lett.*, vol. 87, pp. 080403-1-080403-4.

85. Comparat, D., A. Fioretti, G. Stern, E. Dimova, B. Laburthe Tolra and P. Pillet, 2006, "Optimized production of large Bose-Einstein condensates ", *Phys. Rev. A*, vol.73, pp. 043410-1-043410-14.

86. Parker, N. G., N. P. Proukakis, M. Leadbeater and C. S. Adams, 2003, "Deformation of dark solitons in inhomogeneous Bose-Einstein condensates", *Phys. Rev. Lett.*, vol. 36, pp. 2891-2910.

87. Jaksch, D. and P. Zoller, 2005, "The cold atom Hubbard Toolbox", *Annals of Physics* vol. 315, pp. 52-79.

88. Diener, R. B., B. Wu, M. G. Raizen, and Q. Niu, 2002, "Quantum Tweezer for Atoms", *Phys. Rev. Lett.*, vol. 89, pp. 070401-1-070401-4.

89. Griffin, P. F., K. J. Weatherill, S. G. Macleod, R. M. Potvliege, and C. S. Adams, 2006, "Spatially selective loading of an optical lattice by light-shift engineering using an auxiliary laser field", *New Journal of Physics*, vol. 8, pp. 11-20.

90. Proukakis, N. P., J. Schmiedmayer, and H. T. C. Stoof, 2006, "Quasicondensate growth on an atom chip", *Phys. Rev. A*, vol. 73, pp. 053603-1-053603-11.

91. Anglin, J., 1996, "Cold, Dilute, Trapped Bosons, as an Open System", *Phys. Rev. Lett.*, vol. 79, pp. 6-9.

92. Hau, L.V., S.E. Harris, Z. Dutton and C.H. Behroozi, 1999, "Light speed reduction of 17 metres per second in ultracold atoms", *Nature*, vol. 397, pp.594-598.

93. Scheid, F., 1989, *Numerical Analysis, Schaum's Outline Series*, Mc Graw Hill, New-York.